Stony Brook University

The role of the Meiosis II Outer Plaque in membrane formation in *Saccharomyces cerevisiae*

A Dissertation Presented

by

Erin Marie Mathieson

to

The Graduate School

in Partial Fulfillment of the

Requirements for the Degree of

Doctor of Philosophy

in

Molecular and Cellular Biology

Stony Brook University

August 2009

Stony Brook University

The Graduate School

Erin Marie Mathieson

We, the dissertation committee for the above candidate for the

Doctor of Philosophy degree, hereby recommend

acceptance of this dissertation.

Dr. Aaron Neiman – Dissertation Advisor
Associate Professor, Department of Biochemistry

Dr. Deborah Brown – Chairperson of Defense
Professor, Department of Biochemistry

Dr. James Konopka
Professor, Department of Molecular Genetics and Microbiology

Dr. Rolf Sternglanz
Professor, Department of Biochemistry

Dr. Linda Huang
Assistant Professor, Department of Biology
University of Massachusetts Boston

This dissertation is accepted by the Graduate School.

Lawrence Martin
Dean of the Graduate School

The role of the Meiosis II Outer Plaque in membrane formation in *Saccharomyces cerevisiae*

by

Erin Marie Mathieson

Doctor of Philosophy

in

Molecular and Cellular Biology

Stony Brook University

2009

Diploid budding yeast cultured in the absence of nitrogen and the presence of a nonfermentable carbon source undergo sporulation, which is linked to meiosis. During Meiosis II, the cytoplasmic face of the spindle pole body, referred to as the Meiosis II Outer Plaque (MOP), is modified in both composition and structure and gains a new function as the initiation site for the de novo formation of a membrane, called the prospore membrane. Early in prospore membrane formation, the MOP serves as a docking complex for precursor vesicles that are targeted to its surface. The MOP is composed of the meiotically-induced proteins Mpc54p, Spo74p, Spo21p, and Ady4p as well as two constitutive components, Cnm67p and Nud1p. Using FRET analysis, I have determined the orientation of these proteins within the MOP structure and have thus found that the N-terminus of Mpc54p is proximal to the outer surface of the plaque. Interestingly, the N-terminus of Mpc54p also contains several regions of conservation. By targeting mutations to these conserved residues and characterizing the resulting phenotypes, I determined that Mpc54p plays a role in docking vesicles to the surface of the MOP and that the docking of vesicles to the MOP is essential for the subsequent fusion of these vesicles. Additionally, I have found that the coalescence of vesicles into a prospore membrane stabilizes the MOP structure, and that the connection between the MOP and the prospore membrane is maintained by Ady4p, an auxiliary stabilizing factor. Our findings suggest that MOP proteins are critical both for vesicle docking and for stabilizing the MOP structure during prospore membrane elongation.

Table of Contents

Acknowledgements……...v

I. Introduction……1

Figures…….....10

II. Mpc54p is involved in vesicle docking at the Meiosis II Outer Plaque ……14

Introduction……....14

Materials and Methods……..….16

Results……..…..23

Discussion…….……34

Figures…….…..…..37

Tables…….……46

III. Membrane Assembly Modulates the Stability of the Meiotic

Spindle Pole Body…….……74

Introduction…….……..74

Materials and Methods…….…….76

Results…….……..80

Discussion…….……86

Figures……..……..90

Tables…….……97

IV. Conclusions……..100

Bibliography……...…..…108

Appendix I Strains……...……...118

Appendix II Oliognucleotides……..132

Appendix III Plasmids……...……139

Appendix IV Screens……...……..141

Appendix V Transmission Electron Microscopy…… 143

Acknowledgements

Members of the Neiman Laboratory and my advisor, Aaron Neiman, were a constant source of support and new ideas and were a wonderful group to work with. My committee members, Deborah Brown, James Konopka, Rolf Sternglanz, Linda Huang, and Neta Dean provided excellent advice throughout my graduate career at Stony Brook University. My fellow graduate students provided a home away from home and a supportive and engaging environment throughout our time together in Stony Brook. The Royal Flush helped me to believe in myself and to find my potential by being truly fabulous women and friends. Amir supported and encouraged me throughout our time together in Stony Brook and was a great conspirator for planning getaways. My parents, Robert and Diane Mathieson believed in me and helped me to find the strength to maintain my southern sensibilities while battling the struggles and difficult personal growth of my graduate career. They always gave me a reason to smile. My brother, Mike, and his wife, Heather, and daughter, Terra, provided me with a much–needed California get-away where I could collect my thoughts and find inspiration to continue on towards my degree. And finally my grandmothers, Bertha Mathieson and Frances Esmacher, imparted in me a love of science and a drive for success through their contagious love of nature, their continuous curiosity about the world, and their example of achievement both at work and at home. Thank you all.

Chapter 1: Introduction

Vesicle Trafficking

Eukaryotic cells contain multiple membrane compartments within a plasma membrane. These membranes are composed of lipids and proteins which are directed to each membrane through vesicle trafficking (Palade, 1975). The cell's ability to identify and target discrete sites on its surface for the delivery of proteins and lipids is a requirement for many cellular processes, including asymmetric growth, differentiation, intracellular communication, and physiology (reviewed in (Bonifacino and Glick, 2004; Brennwald and Rossi, 2007; Verhage and Sorensen, 2008)). The targeting of proteins and lipids to a specific membrane is regulated by the delivery, docking, and fusion of a vesicle to its specific target membrane (Palade, 1975). These events are tightly regulated to ensure that vesicles fuse only with their appropriate target membrane (Bonifacino and Glick, 2004; Brennwald and Rossi, 2007). For example, vesicle fusion at specific sites in the plasma membrane of neuron cells is a tightly regulated process which ensures delivery of neurotransmitters to the synapses between two neurons (reviewed in (Brennwald and Rossi, 2007)). This polarized trafficking of vesicles is critical to the propagation of a nerve impulse and, therefore, to the intracellular communication between nerve cells. Additionally, the regulation of the polarity of cells, such as epithelial cells, is required for the delivery of vesicles to the appropriate region within a membrane (reviewed in (Brennwald and Rossi, 2007)). In epithelial cells, the delivery of vesicles to either the basolateral or apical plasma membrane is critical to targeting proteins to their proper location in the cell, thereby propagating both the morphology and the physiology of these cells.

Yeast Life Cycle

Yeast provide an excellent model for the study of vesicle trafficking and differentiation (Novick *et al.*, 1980; Herskowitz, 1988; Rothman, 1994). In rich media, budding yeast undergo mitotic division either as haploid cells or as diploid cells (Herskowitz, 1988) (Figure 1-1). Yeast have two mating types, **a** and α, and **a** and α haploid cells actively transcribe haploid-specific genes to produce the appropriate

receptors and signaling molecules for initiating mating between cells of opposite mating types (Herskowitz, 1988). During mating, **a** and α haploid cells fuse together to form an **a**/α diploid cell (Herskowitz, 1988). Haploid-specific genes are repressed in **a**/α diploid cells, and this repression is critical for the initiation of meiosis (Herskowitz, 1988).

Diploid cells grow mitotically as long as nutrients are present. However, **a**/α diploid cells that are cultured in the absence of nitrogen and the presence of a non-fermentable carbon source will exit the mitotic cycle and undergo sporulation (Herskowitz, 1988) (Figure 1-1). The sporulation process coordinates meiosis with spore formation so that a diploid cell produces four haploid spores contained within an ascus (Herskowitz, 1988). In meiosis, one round of DNA synthesis and two rounds of chromosomal segregation occur before cell division (Esposito, 1981). During sporulation, cell division occurs by the capture of daughter nuclei within new membranes, termed the prospore membranes, which are discontinuous from the mother cell plasma membrane (Moens and Rapport, 1971; Neiman, 1998). As spores mature, spore walls are formed, which protect the dormant spores until rich nutrient conditions return, prompting the spores to germinate (Herskowitz, 1988) (Figure 1-1).

Each different stage of the yeast life cycle involves a unique transcriptional program that promotes differentiation into a new cellular state (Herskowitz, 1988). A series of studies have defined changes in the expression of over 1,000 genes during sporulation (Percival-Smith and Segall, 1984; Holaway *et al.*, 1985; Briza *et al.*, 1990; Chu *et al.*, 1998; Primig *et al.*, 2000; Vershon and Pierce, 2000; Pak and Segall, 2002). Based on the timing of their expression, sporulation-induced genes are defined as early, early-middle, middle, mid-late or late sporulation genes (Percival-Smith and Segall, 1984; Briza *et al.*, 1990; Chu *et al.*, 1998; Pak and Segall, 2002). The majority of early genes are involved in meiotic chromosome metabolism. The transcription factor *NDT80*, an early-middle gene, is a master regulator of sporulation that drives the induction of the largest group of meiotically-induced genes, the middle genes (Chu *et al.*, 1998; Chu and Herskowitz, 1998). This group includes over 250 genes, many of which are not expresssed during the rest of the yeast life cycle (Chu and Herskowitz, 1998; Primig *et al.*, 2000). Middle genes are involved in progression through meiotic divisions as well as prospore membrane formation and spore construction (Chu *et al.*, 1998; Primig *et al.*,

2000). Mid-late and late genes are involved in spore wall assembly, stress response, and restoration of the haploid cell gene program (i.e. induction of haploid-specific genes) (Primig *et al.*, 2000). This temporal regulation of transcription during meiosis allows the cell to perform a critical task: coordinating the timing of meiosis with the formation of the prospore membranes. In this way, these two events are completed simultaneously, thereby ensuring that the correct nuclear contents are packaged into spores.

Prospore membrane formation

During vesicle trafficking in eukaryotic cells, vesicles bud from one membrane compartment, travel through the cytosol and then fuse with a different membrane compartment. The proper delivery, docking, and fusion of vesicles is critical for the proper targeting of essential cellular components to their required location (reviewed (Bonifacino and Glick, 2004; Brennwald and Rossi, 2007)). The specificity of vesicle fusion is conferred partially through the vesicle docking complex and partially through the action of the fusion machinery (Bonifacino and Glick, 2004).

The formation of the prospore membrane is an interesting model for studying the docking and fusion of vesicles. Spore formation begins at the onset of Meiosis II when four prospore membranes are formed (Moens and Rapport, 1971; Neiman, 1998). The formation of prospore membranes is a *de novo* process as prospore membranes are not produced from a pre-existing membrane structure (Neiman, 1998). Prospore membrane formation can be divided into three stages: initiation (which includes vesicle tethering, docking, and fusion), elongation, and closure (Moens and Rapport, 1971; Byers, 1981; Neiman, 2005) (Figure 1-2). The genes critical to each stage of prospore membrane formation are depicted in Figure 1-3.

Initiaton. Prospore membrane formation is initiated by the fusion of post-Golgi-derived vesicles that are targeted to the cytoplasmic face of the spindle pole body by a developmentally controlled rearrangement of the secretory pathway (Neiman, 1998). The mechanism through which these precursor vesicles are delivered to the spindle pole bodies remains unknown. Early in Meiosis II, precursor vesicles accumulate at the spindle pole body. Docking of precursor vesicles to the spindle pole body requires modification of the cytoplasmic face of this structure (this modification is described in

detail below) (Knop and Strasser, 2000; Bajgier *et al.*, 2001; Nickas *et al.*, 2003). Docked vesicles fuse together to form a flattened membrane sac which is attached to the spindle pole body (Davidow *et al.*, 1980; Knop and Strasser, 2000; Bajgier *et al.*, 2001). Interestingly, unlike typical vesicle fusion events, vesicles do not fuse with a pre-existing membrane at the onset of prospore membrane formation (Moens and Rapport, 1971; Bonifacino and Glick, 2004). Instead, vesicles fuse with each other to form a new membrane. After the initial vesicle-to-vesicle fusion which forms a small membrane, vesicles then fuse with the new membrane structure for the duration of prospore membrane growth. During the earliest stage of membrane growth, the prospore membrane appears as a small arc.

Soluble NSF attachment protein receptors (SNAREs) are required for vesicles fusion with pre-existing membranes throughout the secretory pathway (Bennett and Scheller, 1993; Weimbs *et al.*, 1998; Chen and Scheller, 2001). The SNARE hypothesis proposes that proper trafficking relies on the specificity between SNAREs associated with the vesicle (v-SNAREs) and SNAREs associated with the appropriate target membrane (t-SNAREs) (Sollner *et al.*, 1993; Rothman, 1994). Interestingly, the SNARE machinery that is required to target post-Golgi vesicles for fusion with the plasma membrane is also the SNARE machinery required for the fusion of post-Golgi-derived vesicles at the MOP, with a few modifications (Neiman, 1998; Nakanishi *et al.*, 2006). The differences between the two SNARE complexes are: 1) The addition of a meiotically-induced t-SNARE, Spo20p, that shares partially redundant function with its mitotic counterpart, Sec9p (Neiman, 1998; Yang *et al.*, 2008), and 2) The loss of the requirement for the t-SNARE Sso2p as Sso1p becomes an essential component of the SNARE complex during Meiosis II (Jantti *et al.*, 2002; Nakanishi *et al.*, 2006). In *spo20*Δ strains, precursor vesicles do not fuse at the prospore membrane as efficiently and the prospore membrane eventually loses its connection with the MOP (Neiman et al., 2000). In *sso1*Δ cells, vesicles dock to the spindle pole body but do not fuse (Nakanishi *et al.*, 2006).

The fusion of precursor vesicles at the MOP also depends on the activity and localization of Spo14p, a phospholipase D (PLD) enzyme that localizes to prospore membrane precursor vesicles and to the elongating prospore membrane (Rose *et al.*,

1995; Rudge *et al.*, 2001; Riedel *et al.*, 2005; Nakanishi *et al.*, 2006). PLD enzymes hydrolyze phosphatidyl choline (PC) to produce phosphatidic acid (PA) and choline. Since Spo20p preferentially localizes to PA-rich membranes, proper localization of Spo20p to the precursor vesicles and to the prospore membrane requires the localization and activation of Spo14p at these membranes (Rudge *et al.*, 1998; Nakanishi *et al.*, 2006; Liu *et al.*, 2007). However, in the absence of *SPO14*, vesicles do not fuse at the spindle pole body (a more severe phenotype than the *spo20*Δ mutant) (Nakanishi *et al.*, 2006). Additionally, recruitment of Spo20p to the MOP independently of Spo14p does not rescue prospore membrane formation in a *spo14*Δ mutant (Nakanishi *et al.*, 2006). Therefore, Spo14p has a larger role in prospore membrane initiation than simply the recruitment of Spo20p.

Elongation. As Meiosis II progresses, chromosomes segregate into four lobes of the nucleus and each prospore membrane elongates towards the center of the spindle, engulfing the adjacent nuclear lobe as well as cytoplasm and organelles (Moens and Rapport, 1971; Nickas *et al.*, 2003; Suda *et al.*, 2007). The morphology of the prospore membrane undergoes sequential changes during this process: from a small horseshoe shape, to a tubular shape, and finally an elliptical shape. The leading edge protein complex (composed of Ady3p, Don1p, and Ssp1p) is located at the actively growing lip of the prospore membrane (Moreno-Borchart *et al.*, 2001; Nickas and Neiman, 2002). Ssp1 is required for spore formation, and the presence of a competent leading edge protein complex ensures the proper shaping and direction of prospore membrane growth (Moreno-Borchart *et al.*, 2001).

Closure. At the completion of Meiosis II and nuclear division, the open end of each of the four prospore membranes closes to form four immature spores (Moens and Rapport, 1971; Neiman, 1998). This process requires the degradation of the leading edge protein complex protein Ssp1p (Maier *et al.*, 2007; Diamond *et al.*, 2009). After prospore membrane closure, spore wall material is deposited into the lumen of the prospore membrane (Lynn and Magee, 1970). Thus, the inner lipid bilayer of the prospore membrane, which is closest to the nucleus, becomes the new plasma membrane while the outer lipid bilayer of the prospore membrane is degraded during spore wall assembly. At

the end of sporulation, four autonomous haploid spores are contained within an ascus (Herskowitz, 1988).

The spindle pole body

The spindle pole body is the functional analogue of the centrosome in higher eukaryotes, in that it serves as a microtubule organizing center for both cytoplasmic and spindle microtubules (Robinow and Marak, 1966; Moens and Rapport, 1971; Byers and Goetsch, 1974). Cytological examination of spindle pole bodies by transmission electron microscopy has shown that spindle pole bodies are cylindrical, multi-layered complexes embedded in the nuclear envelope (Figure 1-4) (Moens and Rapport, 1971; Byers and Goetsch, 1975). Each layer of the spindle pole body structure is composed of multiple copies of a single protein or a small number of proteins (Rout and Kilmartin, 1990; Kilmartin *et al.*, 1993; Geissler *et al.*, 1996; Kilmartin and Goh, 1996; Bullitt *et al.*, 1997). The initial studies which characterized the gross spindle pole body structure were completed using electron microscopy, so descriptions of this structure frequently follow the terminology of this field. Thus, the spindle pole body is said to be composed of a series of electron-dense regions referred to as plaques (Robinow and Marak, 1966; Moens and Rapport, 1971; Byers and Goetsch, 1975; O'Toole *et al.*, 1999). Later studies which detailed the identity of proteins composing these plaques have been quite diverse in nature. Biochemistry, electron microscopy, yeast genetics, tomography and, most recently fluorescence techniques have all been employed with the goal of describing the components that define the spindle pole body structure (conclusions reviewed in (Helfant, 2002; Jaspersen and Winey, 2004)). A number of proteins are involved in orchestrating the changes in the morphology of the spindle pole body at various points in the cell cycle, but here I am restricting my description of the spindle pole body structure to those proteins that are central to its vertical architecture during vegetative growth and meiosis (Figure 1-4A).

The central plaque. The central plaque lies in the plane of the nuclear envelope and is composed primarily of Spc42p (Moens and Rapport, 1971; Byers and Goetsch, 1975; Rout and Kilmartin, 1990; Donaldson and Kilmartin, 1996). Spc29p, Cmd1p, and a small portion of Spc110p also localize to the central plaque (Sun *et al.*, 1992; Kilmartin

et al., 1993; Wigge *et al.*, 1998; Adams and Kilmartin, 1999; Elliott *et al.*, 1999). The central plaque serves as the core of the spindle pole body and is required for the assembly of other subunits of the spindle pole body (Bullitt *et al.*, 1997). FRET (fluorescence resonance energy transfer) analysis of the core of the spindle pole body has produced a detailed model of the arrangement of the core spindle pole body components within this structure (Muller *et al.*, 2005).

The inner plaque. The inner plaque resides within the nucleus and contains a microtubule nucleating complex composed of Tub4p, Spc98p, and Spc97p (Rout and Kilmartin, 1990; Sobel and Snyder, 1995; Geissler *et al.*, 1996; Knop *et al.*, 1997; Knop and Schiebel, 1997). A portion of Spc110p anchors Tub4p to the inner plaque, but the majority of Spc110p serves as a spacer protein connecting the central and inner plaques (Rout and Kilmartin, 1990; Kilmartin *et al.*, 1993; Geissler *et al.*, 1996).

The outer plaque. The outer plaque lies in the cytoplasm (Moens and Rapport, 1971). During mitosis and Meiosis I, the outer plaque is composed of Cnm67p, Nud1p, Spc72p, and a microtubule nucleating complex similar to that found at the inner plaque (Brachat *et al.*, 1998; Chen *et al.*, 1998; Knop and Schiebel, 1998; Soues and Adams, 1998; Wigge *et al.*, 1998; Adams and Kilmartin, 1999). Cnm67p connects the central and outer plaques (Adams and Kilmartin, 1999). Nud1p anchors Spc72p to the outer plaque (Gruneberg *et al.*, 2000). Spc72p docks the microtubule organizing complex composed of Tub4p, Spc98p, and Spc97p to the spindle pole body (Chen *et al.*, 1998; Knop and Schiebel, 1998; Soues and Adams, 1998). Therefore, during mitosis and Meiosis I, both the inner and the outer plaques of the spindle pole body organize microtubules.

The Meiosis II Outer Plaque

At the onset of Meiosis II, the two spindle pole bodies of the Meiosis I spindle are duplicated to form four spindle pole bodies which localize to the poles of the two Meiosis II spindles. At this stage Spc72p is removed from the cytoplasmic surface of the outer plaques to be replaced by meiotically-induced proteins (Knop and Strasser, 2000; Bajgier *et al.*, 2001). This change in composition of the outer plaque, now referred to as the Meiosis II outer plaque (MOP), leads to a change in structure and function (Figure 1-4B).

The MOP is larger and more electron-dense than its mitotic counterpart (Moens and Rapport, 1971; Knop and Strasser, 2000). No longer flat, the MOP has a domed and layered structure (Moens and Rapport, 1971).

The new, outer layer of the MOP is composed primarily of three meiosis-specific proteins: Spo21p, Spo74p, and Mpc54p (Knop and Strasser, 2000; Bajgier *et al.*, 2001; Nickas *et al.*, 2003). Deletion of the gene encoding any one of these components leads to the absence of the MOP structure and a complete block to prospore membrane formation, indicating that this structure is necessary to promote the initiation of prospore membrane growth. Spo21p and Spo74p are interdependent for localization to the MOP, and heterozygosity of either of these components also leads to a reduction of the number of spores formed (Bajgier *et al.*, 2001; Nickas *et al.*, 2003).

Besides Mpc54p, Spo21p, and Spo74p, the constitutive spindle pole body proteins Cnm67p and Nud1p are also found in the outer plaque during Meiosis II (Bullitt *et al.*, 1997; Adams and Kilmartin, 1999; Schaerer *et al.*, 2001). During sporulation, Cnm67p is proposed to maintain its role as the connection between the central and the outer plaques (Bajgier *et al.*, 2001). However, the role of Nud1p remains unclear. Additionally, Ady4p is a minor MOP component that promotes wild-type MOP assembly and prospore membrane formation, but is not required for either process. In an *ady4*Δ, cells contain variable numbers of prospore membranes and heterogeneous MOP morphologies (Nickas *et al.*, 2003).

While meiosis progresses to completion even in the absence of the MOP, prospore membrane formation requires the presence of the MOP (Knop and Strasser, 2000; Bajgier *et al.*, 2001). Each of the newly modified MOPs serves as the initiation site of the *de novo* formation of one prospore membrane (Moens and Rapport, 1971). Vesicles dock at the cytoplasmic surface of the MOP, and their subsequent fusion to form the prospore membrane is mediated by the meiotic SNARE machinery discussed earlier (Neiman, 1998; Neiman *et al.*, 2000; Nakanishi *et al.*, 2006). Since the docking of vesicles to the MOP is upstream of vesicle fusion by the SNAREs, this suggests that the MOP is similar to other vesicle docking complexes (Sollner *et al.*, 1993; Rothman, 1994; Sogaard *et al.*, 1994; Wickner and Schekman, 2008).

Docking complexes are diverse in nature, and can be single proteins or multi-subunit complexes (Rossi *et al.*, 1995; Jiang *et al.*, 1998; Lowe, 2000). Examples of vesicle docking complexes include the exocyst, which is a multi-subunit complex involved in docking post-Golgi vesicles to the plasma membrane during exocytosis (TerBush *et al.*, 1996; Guo *et al.*, 1999), and the TRAPP (transport protein particle) complex, which promotes docking specificity at the Golgi (Barrowman *et al.*, 2000; Lowe, 2000). By comparing these docking complexes with the MOP complex, we may be able to identify common features and requirements which promote the function of a docking complex.

The docking of vesicles to a membrane is required for subsequent fusion events to occur (Bonifacino and Glick, 2004). Therefore, understanding docking complexes is critical to understanding vesicle trafficking and membrane formation. In this light, analyzing the MOP components may provide insight not only into the role of the MOP during prospore membrane initiation, but also into function of vesicle tethering and docking complexes in general.

In this dissertation, I have examined the role of the MOP during prospore membrane formation. Mpc54p is shown to play a role in vesicle docking at the MOP. I propose that proper docking is required for the subsequent fusion of the docked vesicles. Additionally, the presence of the growing prospore membrane has a stabilizing effect on the MOP structure. Ady4p also acts as a stabilizing factor and maintains the connection between the MOP and the prospore membrane. This suggests that the stability of the MOP structure is regulated by multiple sources during Meiosis II. This work is a critical first step towards understanding the distinct functions of the MOP components during prospore membrane formation.

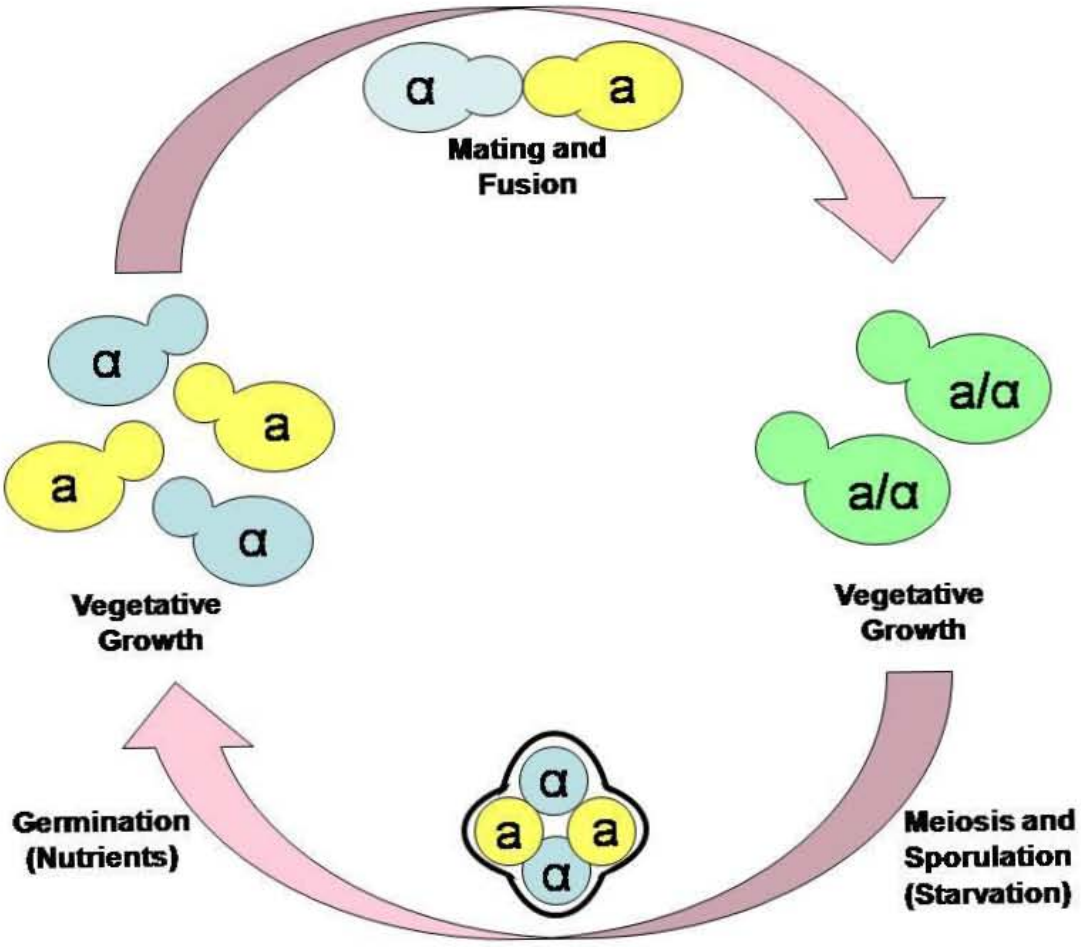

Figure 1-1: Yeast Life Cycle

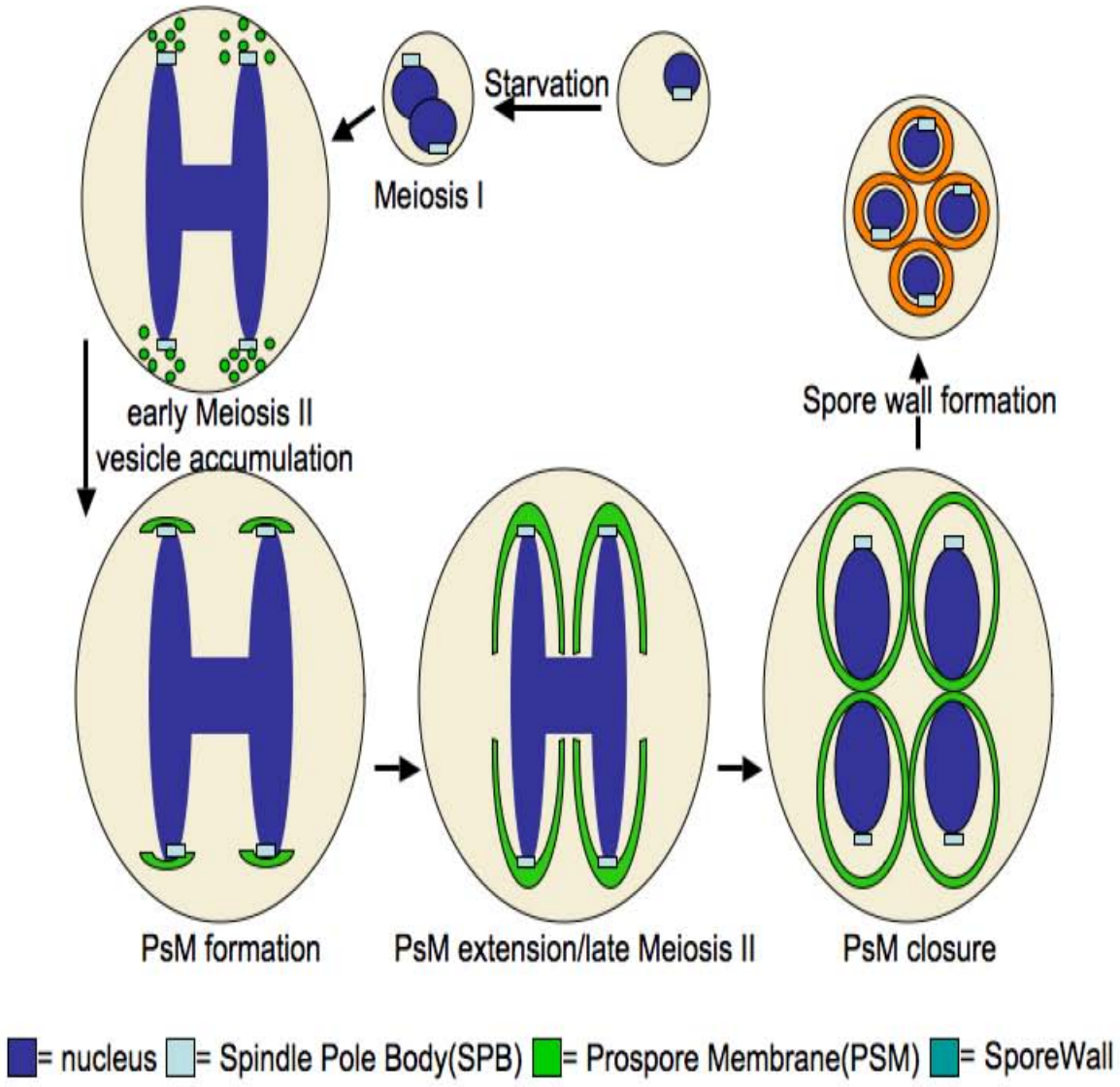

Figure 1-2: Prospore Membrane Formation

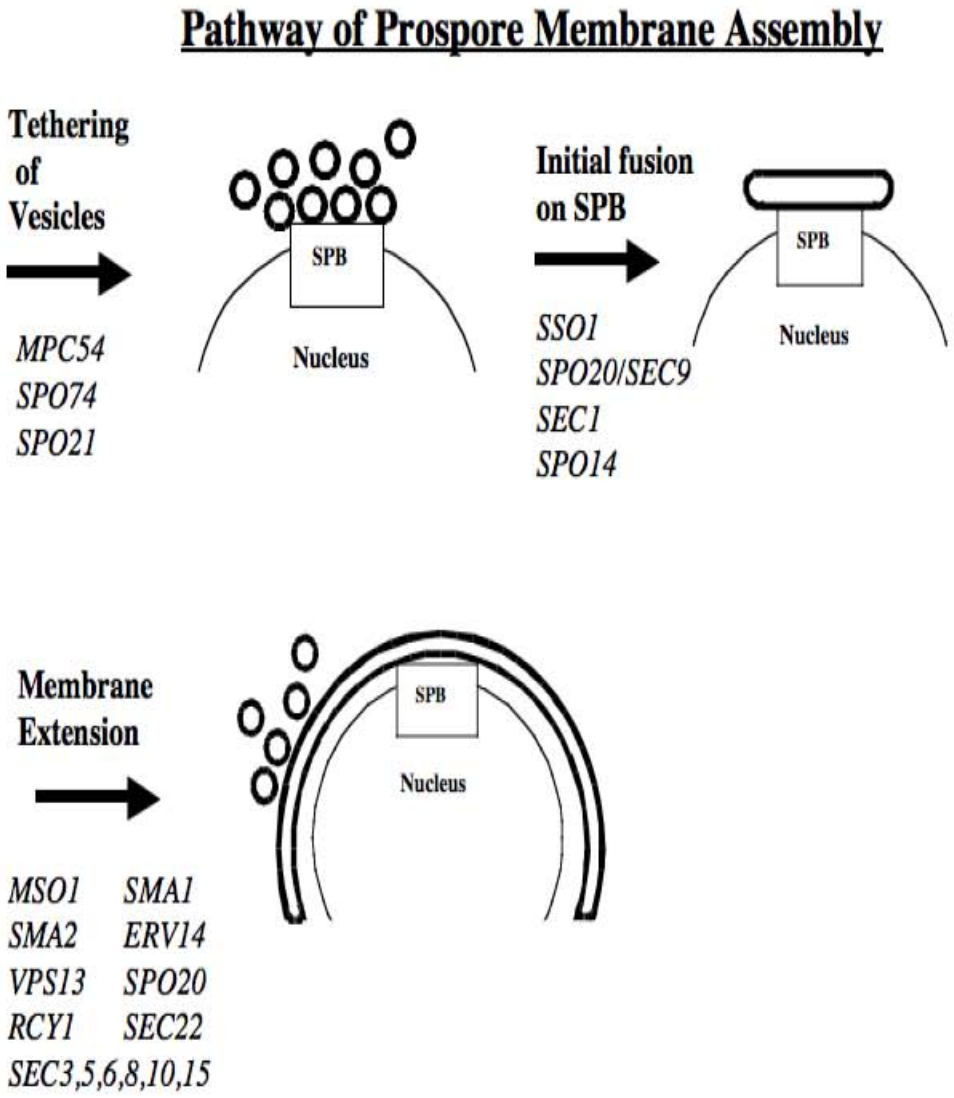

Figure 1-3: Genes Critical for Prospore Membrane Formation

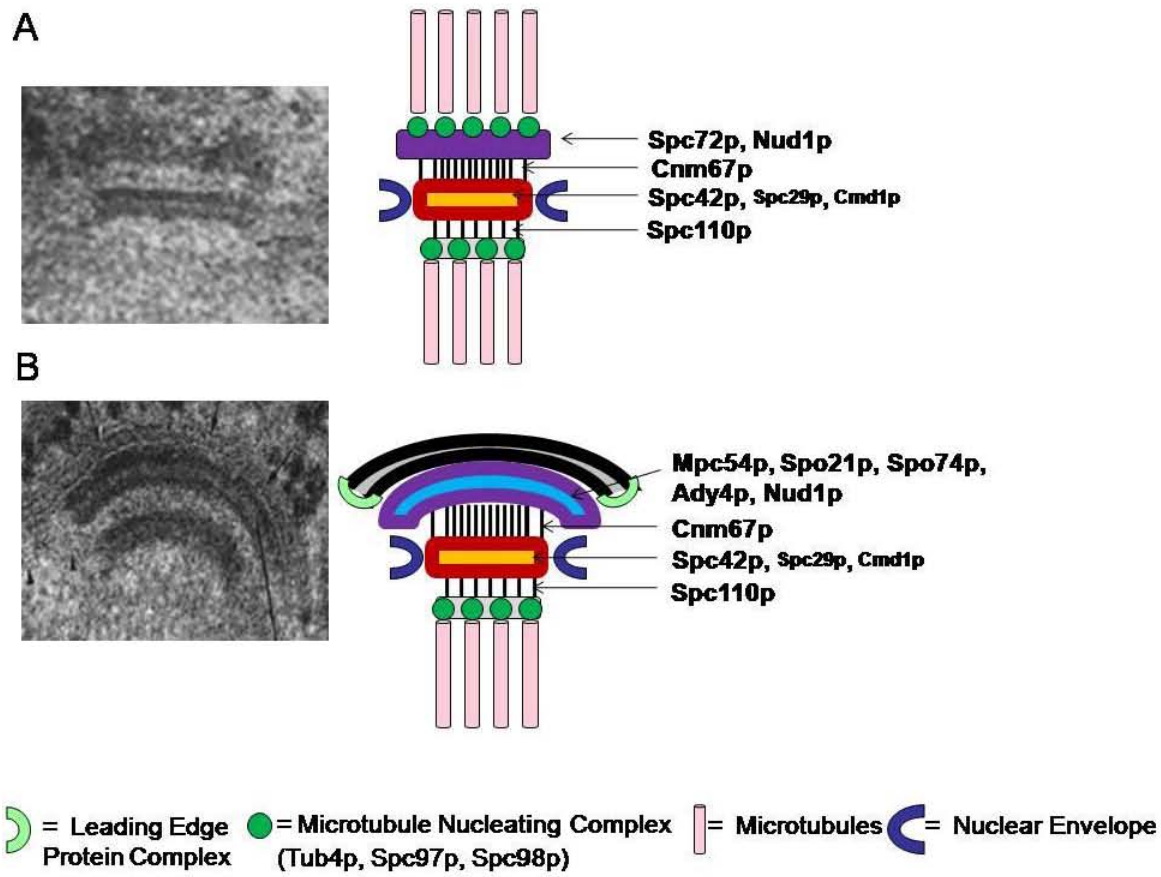

Figure 1-4: The spindle pole body structure
(A) A Mitotic spindle pole body (B) A Meiotic spindle pole body. TEM images are from Moens et al, 1971

Chapter 2: Mpc54p is involved in vesicle docking at the Meiosis II Outer Plaque

Introduction

In *Saccharomyces cerevisiae* meiosis and sporulation are induced when diploid cells are cultured in the absence of nitrogen and the presence of a nonfermentable carbon source (Esposito, 1981). During spore formation, cell division occurs by capturing daughter nuclei within new membranes, termed the prospore membranes, which are discontinuous from the mother cell plasma membrane (Moens and Rapport, 1971; Neiman, 1998). Prospore membrane formation is initiated by the fusion of post-Golgi vesicles that are targeted to the cytoplasmic face of the spindle pole body by a developmentally controlled rearrangement of the secretory pathway (Neiman, 1998). As Meiosis II progresses, chromosomes segregate into four lobes of the nucleus and each prospore membrane elongates towards the center of the spindle, engulfing the adjacent nuclear lobe as well as cytoplasm and organelles (Moens and Rapport, 1971; Nickas *et al.*, 2003; Suda *et al.*, 2007). At the completion of Meiosis II and nuclear division, each of the four prospore membranes closes to form four immature spores (Neiman, 1998).

During Meiosis II, each prospore membrane is attached to a spindle pole body, which is embedded in the nuclear envelope and serves as the microtubule organizing center of the cell, analogous to the centrosome in higher eukaryotes (Moens and Rapport, 1971; Rout and Kilmartin, 1990). During mitosis and Meiosis I, the cytoplasmic face, or outer plaque, of the spindle pole body nucleates cytoplasmic microtubules. At the onset of Meiosis II, the composition of the outer plaques, now called the Meiosis II Outer Plaque (MOP), change so that the cytoplasmic face of the spindle pole bodies serve as sites for prospore membrane nucleation (Moens and Rapport, 1971; Knop and Strasser, 2000).

The MOP is composed primarily of Cnm67p, Nud1p, Spo21p, Spo74p, and Mpc54p (Bullitt *et al.*, 1997; Adams and Kilmartin, 1999; Knop and Strasser, 2000; Bajgier *et al.*, 2001; Schaerer *et al.*, 2001; Nickas *et al.*, 2003). Cnm67p is a constitutive protein that serves to connect the MOP to the core of the spindle pole body, which is composed of Spc42p (Bullitt *et al.*, 1997; Adams and Kilmartin, 1999; Schaerer *et al.*, 2001). Expression of Spo21p, Spo74p, and Mpc54p is meiotically-induced, and deletion

of the genes encoding any one of these components leads to the absence of the MOP structure and a complete block to prospore membrane formation. This requirement of the MOP to initiate prospore membrane formation indicates that interaction between vesicles and the MOP is a necessary step for membrane formation.

During prospore membrane initiation, vesicles dock onto the surface of the MOP. The subsequent fusion of these vesicles to form the prospore membrane is mediated by a SNARE complex that includes Spo20p (Neiman, 1998; Neiman *et al.*, 2000; Nakanishi *et al.*, 2006). A portion of the Spo20p protein (amino acids 51-91) preferentially binds to membranes that are rich in negative phospholipids in vitro and partitions to phosphatidic acid rich membranes in vivo (Nakanishi et al., 2004). Spo14p is a phospholipase D enzyme that hydrolyzes phosphatidyl choline (PC) into phosphatidic acid (PA) and choline in precursor vesicles and the prospore membrane, thereby increasing the pool of negatively charged lipids in these membranes (Rose *et al.*, 1995). Since Spo20p preferentially localizes to PA-rich membranes, Spo14p localization and activity is required for proper localization of Spo20p (Rudge *et al.*, 1998; Nakanishi *et al.*, 2006).

In an earlier study, fluorescence resonance energy transfer (FRET) was used to define the relative positions of the central core proteins of the spindle pole body (Muller *et al.*, 2005). Using these findings, I have expanded upon this survey to include the MOP components. This new FRET data has provided us with a wealth of information, including the orientation of Mpc54p within the MOP. The N-terminus of Mpc54p is positioned at the cytoplasmic face of the MOP, which is the site of vesicle docking during prospore membrane initiation. Phylogenetically conserved residues within Spo74p and the N-terminus of Mpc54p were mutated and the phenotypes of the resulting alleles were characterized. I find that Mpc54p plays a role in vesicle docking at the MOP. Additionally, this docking function of Mpc54p promotes Spo14p activation. Thus the proper docking of vesicles to the MOP promotes vesicle fusion and the initiation of prospore membrane growth.

Materials and Methods

Yeast strains and media

Standard *S. cerevisiae* genetic methods and media were used (Rose, 1990). The strains used in this study are listed in Table 2-4. All strains used were in the fast-sporulating SK-1 strain background (Kane and Roth, 1974). Gene insertions and replacements were performed using cassettes amplified by PCR (Longtine *et al.*, 1998) and verified by PCR or phenotype.

FRET strains were constructed by crossing two haploid strains, one containing a CFP-tagged MOP component (CFP-A) and one containing a YFP-tagged MOP component (YFP-B). These strains were sporulated, tetrads were dissected, and two of the CFP-A / YFP-B segregants were mated. The required haploid strains were constructed as follows. For N-terminal CFP tags: *TRP1-*P_{CNM67}*-CFP* was inserted at the 5' end of the ORF of *CNM67* and *NUD1* in AN117-16D. *TRP1-*P_{MPC54}*-CFP* was inserted at the 5' end of the ORF of *MPC54*, *SPO21*, and *SPO74* AN117-16D. For C-terminal CFP tags: *CFP-TRP1* was inserted at the 3' end of the ORF of *CNM67* and *MPC54* in AN117-16D. *CFP-HIS3* was inserted at the 3' end of the ORF of *NUD1* and *SPO21* in AN117-16D. *CFP-TRP1* was inserted at the 3' end of the ORF of *MPC54* in AN117-4B. *CFP-HIS3* was inserted at the 3' end of the ORF of *SPO21* in AN117-4B. For N-terminal YFP tags: *URA-*P_{CNM67}*-YFP* was inserted at the 5' end of the ORF of *CNM67, MPC54* and *NUD1* in AN117-4B. *URA-*P_{MPC54}*-YFP* was inserted at the 5' end of the ORF of *MPC54, SPO21,* and *SPO74* in AN117-4B. For C-terminal YFP tags: *YFP-HIS3* was inserted at the 3' end of the ORF of *NUD1* and *SPO74* in AN117-16D. *YFP-HIS3* was inserted at the 3' end of the ORF of *NUD1* in AN117-4B.

To construct EMD71 (*ylr301w*Δ / *ylr301w*Δ), *TRP1* was inserted into the YLR301W ORF in AN117-16D and AN117-4B. The resulting haploids were mated. To construct a diploid strain with YLR301W-GFP, YLR301W-GFP (*MAT* **a**) was mated with AN117-4B.

To construct EMD26 (*MPC54*^{WT}*-RFP / MPC54*^{WT}*-RFP*), EMD27 (*mpc54-40-RFP / mpc54-40-RFP*), EMD28 (*mpc54-47-RFP / mpc54-47-RFP*), EMD29 (*mpc54-118-RFP / mpc54-118-RFP*), and EMD31 (*mpc54-145-RFP / mpc54-145-RFP*), the mpc54-

RFP allele of interest was inserted into the *TRP1* locus of NY51 (*MAT* **a**, *mpc54*Δ) and NY50 (*MAT* α, *mpc54*Δ) using an integrating plasmid containing the *mpc54-RFP* allele of interest. The resulting haploids were mated. To construct EMD112 (*mpc54-119*-RFP / mpc54Δ), *mpc54-119*-RFP was inserted into the *TRP1* locus of NY50 using an integrating plasmid containing the *mpc54-119*-RFP allele. The resulting haploid was mated with NY51.

To construct EMD50 (*SPO74 / SPO74*), EMD51 (*spo74-145 / spo74-145*), EMD56 (*spo74-180 / spo74-180*), and EMD57 (*spo74-243 / spo74-243*), the *spo74* allele of interest was inserted into the *TRP1* locus of AN1120 and MND39 using an integrating plasmid containing the *spo74* allele of interest. The resulting haploids were mated.

Plasmids

The plasmids used in this study are listed in Table 2-5. Construction of pFA6a-CFP(YFP)-CgTRP1(KlURA3) was as follows: pFA6a-yEGFP-HIS3MX6 was constructed by PCR amplifying yEGFP (including the linker region) from pYM12 (Knop et al., 1999) with primers MNO155 and MNO156. The PCR product was digested with PacI and AscI, and the digested fragment was ligated into the similarly digested pFA6a-GFP(S65T)-HIS3MX6 plasmid (Wach et al., 1997). The yEGFP was replaced with CFP or YFP by digesting pDH3 or pDH5 (Yeast Resource Center) with MscI and AscI. These digested fragments were subcloned into the pFA6a-yEGFP-HIS3MX6 backbone which was similarly digested with MscI and AscI to make pFA6a-CFP-HIS3MX6 and pFA6a-YFP-HIS3MX6. pFA6a-CgTRP1 was constructed by amplifying CgTRP1 from pCgW (gift from L. Huang) with the primers MNO162 and MNO163, digesting the PCR product with BglII and PmeI, and subcloning the fragment into a similarly digested pFA6a-TRP1. pFA6a-KlURA3 was constructed by amplifying KlURA3 from pKlU (gift from L. Huang) with the primers MNO162 and MNO163, digesting the PCR product with BglII and PmeI, and subcloning the fragment into a similarly digested pFA6a-TRP1. pFA6a-CFP(YFP)-CgTRP1(KlURA3) was constructed by subcloning the PacI-BglII fragment from pFA6a-CgTRP1 or pFA6a-KlURA3 into similarly digested pFA6-CFP-HIS3MX6 or pFA6a-YFP-HIS3MX6 to replace HIS3MX6 with CgTRP1 or KlURA3, respectively.

pMN101 was constructed by PCR amplifying CgTRP1 from pFA6a-CgTRP1 using primers MNO146 and MNO147. The PCR product was cut with PmeI-BglII and replaced the PmeI-BglII fragment of pFA6a-TRP1-PGAL1-GFP(S65T) (Longtine et al., 1998), making pFA6a-CgTRP1-PGAL-GFP(S65T). pMN102 was constructed by PCR amplifying KlURA3 from pFA6a-KlURA3 using primers MNO146 and MNO147. The PCR product was cut with PmeI-BglII and replaced the PmeI-BglII fragment of pFA6a-TRP1-PGAL1-GFP(S65T) , making pFA6a-CgTRP1-PGAL-GFP(S65T).

pMN103, pMN104, pMN105, and pMN106 were constructed by PCR amplifying the promoters of CNM67 or MPC54 from genomic DNA derived from AN117-4B using the primers MNO226 and MNO227 or MNO228 and MNO229, respectively. PCR products were digested with BglII-PacI and replaced the BglII-PacI fragments of pMN101 and pMN102.

pMN107, pMN108, pMN109, and pMN110 were constructed by PCR amplifying CFP or YFP from pFA6a-CFP-CgTRP1 or pFA6a-YFP-KlURA3, respectively, using the primers MNO224 and MNO225. PCR products were digested with PacI-AscI and replaced the PacI-AscII fragment of pMN103, pMN104, pMN105, or pMN106.

pRS424SPO74 was constructed by cloning a NotI-SacII fragment carrying SPO74 from pRS424-SPO21-SPO74 (gift from M. Nickas) into similary digested pRS424. pRS316-SPO74 was constructed by cloning a NotI-SacII fragment from pRS424SPO74 carrying SPO74 into a similarly digested pRS316. Quickchange mutagenesis (Stratagene) was targeted against the pRS316-SPO74 plasmid to construct the *spo74* mutant alleles (primers used for each mutation are listed in Table 2-7). The pRS426-SPO74^{X} plasmids (wild-type and mutant alleles) were constructed by cloning a NotI-SacII fragment from pRS316-SPO74^{X} carrying the appropriate *spo74* allele into a similarly digested pRS426. The pRS304-SPO74^{X} plasmids (wild-type and mutant alleles) were constructed by subcloning a XhoI-SacII fragment from pRS316-SPO74^{X} carrying the appropriate *spo74* allele into a similarly digested pRS304.

pRS314MPC54-RFP was constructed by cloning a SpeI-XhoI fragment carrying MPC54-RFP from pRS423-MPC54-RFP (gift from H. Nakanishi) into similarly digested pRS314. pRS316MPC54-RFP was constructed by cloning a SpeI-XhoI fragment carrying MPC54-RFP from pRS314MPC54-RFP into similary digested pRS316. Quickchange

mutagenesis was targeted against the pRS316-MPC54-RFP plasmid to construct the *mpc54* mutant alleles (primers used for each mutation are listed in Table 2-7). The pRS426-MPC54^{X} plasmids (wild-type and mutant alleles) were constructed by cloning a NotI-XhoI fragment from pRS316-MPC54^{X} carrying the appropriate *mpc54* allele into a similarly digested pRS426. The pR304-MPC54^{X} plasmids (wild-type and mutant alleles) were constructed by cloning a NotI-XhoI fragment from pRS316-MPC54^{X} carrying the appropriate *mpc54* allele into a similarly digested pRS304. The pSTT91-MPC54^{X}(1-200) plasmids (wild-type and mutant alleles) were constructed by PCR amplifying the N-terminus of the appropriate *mpc54* allele from pRS316-MPC54^{X} using the primers EMO64 and EMO75. The PCR product digested with BamHI-XhoI was subcloned into pSTT91 digested with BamHI-SalI.

QuickChange Site-Directed Mutagenesis

Mutagenic primers were designed based on the guidelines of the QuickChange Mutatgenesis Kit (Stratagene). Oligos are listed in Table 2-6. PCR using *PfuTurbo* DNA polymerase and the mutagenic oligos altered codons of phylogenetically conserved residues in plasmids containing *MPC54-RFP* or *SPO74*. Conserved residues were changed to alanines. PCR products were digested with *Dpn* I. The digestion product was analyzed by electrophoresis. Samples for which a band was visible after *Dpn* I digestion were transformed into BSJ72 *E. coli* cells. Samples for which no band was visible after *Dpn* I digestion were transformed into XL2-Blue MRF *E. coli*. Plasmids were recovered an mutations were confirmed by sequencing.

Sporulation assays

Cells were induced to sporulate in liquid medium essentially as described previously (Neiman, 1998). Briefly, cells were cultured to saturation in either rich medium or synthetic medium selective for plasmids, cultured overnight to mid-log phase in yeast extract-peptone-acetate medium, and transferred to 2% potassium acetate at a concentration of 3 X 10^{7} cells/ml.

Fluorescence microscopy

For direct detection of fluorescent proteins in fixed cells, cells were fixed with 3.7% formaldehyde for 5 min and mounted with mounting medium containing 4,6-diamidino-2-phenylindole (DAPI) (Vectashield; Vector Laboratories, United Kingdom). Images were acquired using a Zeiss Axioplan2 microscope (Carl Zeiss, Thornwood, NY) with a Zeiss mRM Axiocam and deconvolved using Zeiss Axiovision 4.6 software.

For the FRET studies, yeast strains containing spindle pole body proteins tagged with cyan fluorescent protein (CFP) and yellow fluorescent protein (YFP) were analyzed at approximately 4 hours after transfer to sporulation media. The progression through meiosis was asssessed by the status of the spindle pole bodies seen with CFP and YFP fluorescence. Cells that were in Meiosis II were analyzed.

Image acquisition for the FRET studies was conducted on microscopes at two sites: University of Washington, Seattle and Stony Brook University, Stony Brook. For the Seattle acquisitions, 200 ul of sporulating culture was spun down at 5K RPM. Cells were resuspended in 30ul of fresh 2% potassium acetate and sonicated to reduce flocculence. A 3 ul aliquot was mounted on a pad of 0.9% SeaKem LE agarose (FMC BioProducts, Rockland, ME) in SDC medium as described (Sundin *et al.*, 2004). Microscopy was performed on a DeltaVision system manufactured by Applied Precision (Issaquah, WA). The microscope was equipped with an Uplan Apo 100X oil objective (1.35 NA), a CoolSnap HQ digital camera from Roper Scientific (Tuscon, AZ), and optical filter sets from Omega Optical (Brattleboro, VT). For each strain 60-200 images were captured. Exposure times were 0.4 s with 2 X 2 binning and a final image size of 512 X 512. Using the DIC channel, fields were focused manually before an automated capture of a single focal plane in the order YFP, FRET, CFP, and DIC images. Because YFP photobleaches rapidly when exposed to CFP excitation light, the order of capture is critical (Hailey *et al.*, 2002).

For the Stony Brook acquisitions, 700 ul of sporulating culture was spun down at 5K RPM. Cells were resuspended in 70ul of fresh 2% potassium acetate and then sonicated. A 2 ul aliquot was mounted on a pad of 1% Agarose Low EEO (US Biologicals, Swampscott, MA) in S Media (0.17% yeast nitrogen base without amino acids (US Biologicals, Swampscoot, MA) and 0.5% ammonium sulfate) as described

(Sundin *et al.*, 2004). Microscopy was performed on a Zeiss Axioplan2 microscope (Carl Zeiss, Thornwood, NY) equipped with a 100X oil objective (Plan-Neofluar, numerical aperture 1.46) and a Zeiss mRM Axiocam. For each strain 100-300 images were captured. Exposure times were 0.8 s with 2 X 2 binning and a final image size of 650 X 514. Image acquisition was as described above.

FRET Analysis

For the Seattle aquisitions, the 12-bit images were converted into 16-bit Tiff format by the Java program R3DConverter (Ess, Riffle, and Muller, unpublished). For the Stony Brook aquisitions, the Zeiss-formatted images were converted to Tiffs using Image J (rsbweb.nih.gov/ij/). In both cases, these Tiff images were then analyzed by a custom Matlab program, FretSCal, that evaluates certain regions of the images based on user-defined criteria (Ess, Riffle, and Muller, unpublished). FRET values were expressed as a FRETR index, which measures the fold increase of fluorescence intensity in the FRET channel over a baseline determined from the fluorescence in the CFP and YFP channels (Muller *et al.*, 2005). Based on this index, the predicted value of FRETR is 1 if no energy is transferred. FRETR values above 1.2 were considered true.

Transmission electron microscopy

Sporulating cells were fixed for 1 h in 3% glutaraldehyde in cacodylate buffer (100 mM sodium cacodylate, 5 mM CaCl2, pH 6.8), washed once in cacodylate buffer, left overnight at 23°C, resuspended in 4% KMnO4 in distilled water, and incubated for 30 min at 23°C. The cells were then washed with distilled water until the supernatant was clear, resuspended in saturated uranyl acetate for 2 h, and then dehydrated by 10-minute incubations in a graded acetone series: two incubations each in 30%, 50%, 70%, and 95% acetone and four incubations in 100% acetone. For embedding, the cells were first incubated twice in acetonitrile for 10 min and then transferred to a 1:1 solution of acetonitrile Epon Mix (50% Epon 812, 15% dodecenyl succinic anhydride, 35% nadic methyl anhydride) for 4 h. The cells were then incubated in Epon Mix for 12 h with changes every 4 h, and finally, the catalyst 2,4,6-Tris(dimethylaminomethyl) phenol (DMP-30) was added and samples were placed into a vacuum oven at 60°C for 2 days to

harden. After the samples were sectioned, images were collected on an FEI BioTwin G2 microscope at 80 kV using an AMT XR-60 camera.

Galactosidase assays

Assays for two-hybrid interactions were performed in the strain L40. For the initial screen, L40 (Vojtek *et al.*, 1993) was cotransformed with pST119-LexA-MPC54$^{WT\ 1\text{-}67}$ (expressing the LexA DNA-binding domain) and the pACTII library (expressing yeast proteins fused with the Gal4 activation domain (GAD) (gift from N. Hollingsworth)). Transformants were cultured overnight at 30°C on a Whatman 50 filter on the surface of a plate of synthetic complete medium lacking His and Leu. The following day the filter was immersed in liquid N_2 for 10 s and then incubated at 30°C in Z buffer (Miller, 1972) containing 0.1% 5-bromo-4-chloro-3-indolyl-D-galactopyranoside (X-gal) and 0.027% β-mercaptoethanol.

Results

The organization of MOP components within the MOP structure

MOP proteins form the interface between the MOP and the prospore membrane, and are likely to be critical to the early stages of prospore membrane assembly. Therefore, it is important to determine the organization of the MOP proteins in order to predict which regions of the MOP components form the interface between the MOP and the prospore membrane. FRET analysis can be used to determine the proximity of two fluorescently-tagged molecules within the spindle pole body (Muller *et al.*, 2005). FRET ratio (FRETR) is a measurement of the transfer of energy from an excited donor fluorophore (e.g. CFP) to an adjacent acceptor fluorophore (e.g. YFP) (Muller *et al.*, 2005). Using FRET analysis, the relative positioning of the central core proteins of the mitotic spindle pole body has been determined (Muller *et al.*, 2005). Building on these results, I surveyed the orientation and position of spindle pole body components of the MOP (Figure 2-1).

The previous FRET study demonstrated that the C-terminus of Cnm67p was found to be proximal to the C-terminus of Spc42p, which is located at the outermost surface of the central plaque (Muller *et al.*, 2005). Like many proteins in the spindle pole body, Cnm67p contains a coiled-coil motif oriented vertically within the structure (Rout and Kilmartin, 1990; Kilmartin *et al.*, 1993; Donaldson and Kilmartin, 1996; Bullitt *et al.*, 1997; Adams and Kilmartin, 1999). This coiled-coil portion of Cnm67p was shown to comprise the intermediate layer which forms the space between the central and the outer plaques (Schaerer *et al.*, 2001). During Meiosis II, Cnm67p maintains its position within the spindle pole body (Bajgier *et al.*, 2001). Taken together, these characteristics of Cnm67p suggest that the N-terminus of Cnm67p is oriented towards the outer plaque. Therefore, determining the FRET interactions between the N-terminus of Cnm67p and the other MOP proteins would allow us to orient proteins within the MOP structure.

To complete FRET analysis of the MOP components, Cnm67p, Nud1p, Mpc54p, Spo21p, and Spo74p were tagged with CFP or YFP at either the N- or C-terminus. Different combinations of CFP- and YFP-tagged proteins were integrated into cells so that a single cell contained one CFP donor and one YFP acceptor. Each CFP/YFP

combination was constructed in two directions, so that the donor/acceptor combination in one strain would be reversed in another strain. In example, YFP-ProteinA and CFP-ProteinB in one strain would be considered one direction and CFP-ProteinA and YFP-ProteinB in another strain would be considered the opposite direction. This resulted in 100 possible combinations of FRET donor/acceptor pairs for the tagged MOP components (Figure 2-1). Fifty-eight of the possible combinations have been analyzed, so that analysis of the FRETR of almost every combination has been examined in at least one direction (Figure 2-1).

Like Cnm67p, Mpc54p and Spo21p are both coiled-coil proteins (Knop and Strasser, 2000). All other coiled-coil proteins in the spindle pole body are oriented vertically within the structure. Therefore, the alignment of Mpc54p and Spo21p within the MOP is likely to follow a similar vertical orientation (Rout and Kilmartin, 1990; Kilmartin *et al.*, 1993; Donaldson and Kilmartin, 1996; Bullitt *et al.*, 1997; Adams and Kilmartin, 1999). I examined the FRET between Mpc54p, Spo21p, and the outer N-terminus of Cnm67p to determine their orientation within the MOP structure. Our results show that the C-terminus, but not the N-terminus of both Mpc54p and Spo21p display a significant FRET with the N-terminus of Cnm67p. Therefore, the C-termini of these proteins are buried within the MOP, and the the N-termini may localize to the cytoplasmic surface of the MOP, making these proteins candidates for involvement in vesicle tethering or docking complexes.

Additionally, the C-termini of Spo21p and Mpc54p are both self-FRETing and FRET with each other, suggesting they may form tightly packed dimers near the N-terminus of Cnm67p. The C-terminus of Spo21p has stronger FRET with the N-terminus of Cnm67p than does Mpc54p, suggesting that the C-terminus of Mpc54p is slightly further from the N-terminus of Cnm67p. In contrast, the N-termini of Spo21p and Mpc54p do not FRET with each other, suggesting that these proteins are not in a parallel conformation, but may be splayed at their N-termini. This may account, in part, for the curving of the MOP structure during Meiosis II.

Both termini of Nud1p have FRET interactions with portions of proteins that are buried within the MOP (e.g. the N-terminus of Cnm67p and the C-terminus of Spo21p).

Therefore, Nud1p appears to be buried within the MOP structure near the N-terminus of Cnm67p.

Placing Spo74p within the MOP structure is more difficult. Previously, it was shown that Spo74p interacts with itself by two hybrid (Nickas *et al.*, 2003). FRETR data supports this finding in that the C-terminus of Spo74p displays a strong self-FRET. Interestingly, the C-terminus of Spo74p FRETs with proteins buried within the MOP (e.g. the N-terminus of Cnm67p and the C-terminus of Spo21p) and with proteins predicted to be at the surface of the MOP (e.g. the N-terminus of Spo21p and the N-terminus of Mpc54p). The N-terminus of Spo74p displays a similar FRET profile. Therefore I do not currently have a clear picture of how Spo74p fits into the organization of the MOP structure, but I propose that it forms oligomers composed of Spo74p dimers that are oriented in an antiparallel fashion within the MOP.

Identifying critical regions within Spo74p and Mpc54p

Position-specific iterated BLAST identified several regions of Mpc54p and Spo74p that were conserved between *Saccharomyces cerevisiae* and other yeasts (Figure 2). Significantly, the regions of conservation within Mpc54p were located in the N-terminus of the protein, which is predicted by FRET to be localized at the cytoplasmic face of the MOP. Therefore, these residues may be critical for its function during prospore membrane initiation. Since the structure of Spo74p is unknown, I are not ruling out the possibility that a portion of the globular Spo74p protein lies at the outer surface of the MOP structure. For both proteins, conserved residues were mutated and the mutations were verified by DNA sequencing and restriction analysis. Six *mpc54* mutant alleles and four *spo74* mutant alleles were constructed (Figure 2-2) and their sporulation phenotypes were characterized.

Conserved residues in Spo74p are critical for spore formation

To determine whether the conserved residues of Spo74p are critical for sporulation, their effect on spore formation was examined. *spo74-145*, *spo74-180*, *spo74-243*, or *spo74-267* under control of the *SPO74* promoter were transformed into a *spo74*Δ strain. Sporulation can be scored by the presence of asci by light microscopy

(Herskowitz, 1988). In wild-type cells, asci typically contain four spores called tetrads; however asci with three, two, or one spore are also produced and are called triads, dyads, or monads, respectively. It was observed that cells transformed with *SPO74*^{WT} and *spo74-267* sporulated with nearly the same efficiency (Table 2-1). In contrast, cells transformed with *spo74-243* produced half as many asci as *SPO74*^{WT} and displayed a greater percentage of dyads (Table 2-1). Cells transformed with *spo74-145* and *spo74-180* produced no spores (Table 2-1).

To ensure that the reduction in sporulation seen for the mutant alleles was due to the effects of the mutations, not to a reduction in their expression, *SPO74*^{WT}, *spo74-145*, *spo74-180*, and *spo74-243* were expressed from a high copy plasmid. While the sporulation efficiency of *SPO74*^{WT}, and and *spo74-243* improved slightly, in general the overexpression of these proteins did not significantly alter their sporulation efficiencies.

In the absence of *SPO74*, the MOP does not form and spores are not made (Nickas *et al.*, 2003). To ensure that Spo74p mutant proteins were stable, protein levels of the mutant alleles were determined by Western blot. A *spo74*Δ strain transformed with *SPO74*^{WT}, *spo74-145*, *spo74-180*, or *spo74-243* was sporulated and the progression of cells through meiosis was monitored by fluorescence microscopy of DAPI staining. Samples were collected when at least 15% of the cells were in Meiosis II, and cell lysates were analyzed by western blotting using antibodies that recognize Spo74p. Extracts of cells transformed with *SPO74*^{WT}, *spo74-145*, *spo74-243* all produced a strong signal for Spo74p (data not shown). Therefore, the phenotypes of *spo74*^{143}, and *spo74-243* are not due to the instability of Spo74p. The strain transformed with Spo74p^{180} grew poorly and extracts were not obtained.

Further examination of these alleles was not performed because the *mpc54* mutant alleles became the main focus of this project.

mpc54 mutant alleles disrupt spore formation

Mpc54p is essential for the formation of the prospore membrane and its N-terminus is localized at the region of the MOP associated with vesicle docking. Taken together, these observations suggest that Mpc54p may play a role in initiating prospore membrane formation. Although the information gained from analysis of the *mpc54* null

allele was critical to our understanding of the MOP, this allele is too blunt an instrument to determine the specific roles that Mpc54p may play in prospore membrane initiation beyond its requirement for MOP formation. Therefore, the *mpc54* mutant alleles were characterized and examined to find non-null alleles which disrupt prospore membrane initiation. These alleles were then be used as reagents to examine the role of Mpc54p during the earliest stages of prospore membrane formation.

To make the analysis of the stability of Mpc54p mutant proteins easier, mutations were directed against a functional RFP-tagged version of Mpc54p. The presence of RFP at the spindle pole bodies during Meiosis II indicates whether the Mpc54p alleles are stable and localize appropriately. Plasmids containing either *MPC54*^{WT}, *mpc54-40*, *mpc54-47*, *mpc54-118*, *mpc54-123*, *mpc54-119*, or *mpc54-145* under control of the *MPC54* promoter were transformed into an *mpc54Δ* strain and analyzed by fluorescence microscopy. Nearly all alleles (the exception being *mpc54-123*, which did not form RFP foci) were stable and localized to the spindle pole body (Table 2-2).

If the *mpc54* mutant alleles disrupt prospore membrane formation, then transforming these alleles into an *mpc54*Δ strain would not rescue sporulation. All strains expressing the Mpc54p mutant proteins displayed a dramatic reduction or a complete loss of sporulation compared to strains carrying wild-type Mpc54p-RFP (Table 2-2). The Mpc54p alleles were then integrated into the chromosome of cells lacking *MPC54* and the sporulation efficiency of these strains was determined. The efficiency of spore formation for the integrated strains followed the same trend but was slightly more robust for those strains which did sporulate (Table 2-2). However, in both cases, the asci that were formed in the mutant conditions were limited to monads or dyads suggesting that spore formation was deficient even in cells that were able to occasionally make spores.

Spore formation defects are not due to reduced expression

Mutations may cause defects in spore formation in two ways: Mpc54p mutant proteins may directly disrupt spore formation or the *mpc54* mutant alleles may lead to a reduction in the expression of the protein. This would disrupt the MOP structure since assembly of the structure is particularly susceptible to expression levels of the MOP components (Bajgier *et al.*, 2001; Nickas *et al.*, 2003). Therefore, to ensure that the

mutant phenotypes observed were not due to reduced expression levels, the mutant alleles were placed on high copy plasmids. The sporulation efficiency remained the same for each *mpc54* mutant (Table 2-2), suggesting that these phenotypes are not due to reduced expression.

mpc54 mutant alleles promote wild-type MOP composition

Examining the effect of each mutant allele on the composition of the MOP is critical to determining whether the phenotype of an allele is due to loss of a competent MOP structure. To examine if the mutations were causing defects in spore formation as a result of improperly formed MOPs, the recruitment of Spo21p and Spo74p to the MOP was analyzed (Figure 2-3A). Spo21-GFP or Spo74-GFP were co-transformed with the various Mpc54p alleles into an *mpc54* Δ mutant. Two hundred RFP dots were analyzed by fluorescence microscopy for colocalization with GFP dots under the assumption that the loss of plasmids containing the GFP-tagged MOP components would be equal between the samples. The recruitment of Spo21-GFP and Spo74-GFP in cells expressing *mpc54-47*, *mpc54-118*, *mpc54-119*, and *mpc54-145* was comparable to that of $MPC54^{WT}$ (Figure2-3B). *mpc54-40* displayed a modest reduction in the recruitment of Spo21-GFP and Spo74-GFP, suggesting that the MOPs formed in cells expressing *mpc54-40* may not be structurally normal (Figure 2-3B).

mpc54 mutant alleles disrupt early stages of prospore membrane formation

This analysis identified four alleles which do not compromise the composition of the MOP, yet disrupt spore formation: $Mpc54p^{47}$, $Mpc54p^{118}$, $Mpc54p^{119}$, and $Mpc54p^{145}$. To determine which stage of prospore membrane formation was disrupted for each of the *mpc54* mutant alleles, prospore membrane progression was analyzed by fluorescence microscopy. Dtr1-GFP and GFP-$Spo20^{51-91}$ are prospore membrane markers. Dtr1-GFP or GFP-$Spo20^{51-91}$ were co-transformed with the various *mpc54* alleles into an *mpc54* Δ mutant. For each *mpc54* allele, two hundred RFP dots were analyzed by fluorescence microscopy for colocalization with Dtr1-GFP or GFP-$Spo20^{51-91}$(Figure 2-4A) The GFP signal at the RFP-tagged spindle pole bodies was reduced for each of the *mpc54* mutant alleles, as compared to the wild-type allele (Figure 2-4B). This

suggests that the recruitment of precursor vesicles as well as prospore membrane formation is disrupted at the majority of mutant MOPs examined.

However, an examination of cells with both GFP and RFP signals revealed that for an individual mutant cell, Dtr1-GFP and Spo20$^{51-91}$ were recruited to a variable number of MOPs. In wild-type cells, Dtr1-GFP and Spo20$^{51-91}$ recruitment to the MOP was homogeneous, meaning that either all or none of the MOPs within a single cell had GFP-colocalization at the MOP (Figure 2-4C). In contrast, each mutant allele presented some degree of heterogeneity in the colocalization of GFP-tagged membrane markers with the RFP-tagged MOPs, meaning that within a single cell, some RFP dots were absent of GFP while others colocalized with GFP (Figure 2-4C). This suggests that the mutant MOPs are able to recruit precursor vesicles, but that the recruitment is not universal for all MOPs in a single cell.

mpc54 mutant alleles maintain proper MOP ultrastructure

Thin section TEM analysis was used to examine the structure of the MOP as well as the stages of prospore membrane formation in fine detail. Both cells expressing the mutant alleles from plasmids and cells in which the mutant alleles were integrated in the chromosome were examined. Analysis of cells expressing the *mpc54* mutants revealed that the morphology of their MOPs resembled the distinct, layered morphology of wild-type MOPs (Figure 2-5). This clearly defined MOP structure was absent in the *mpc54*Δ mutant (Figure 2-5). These results support our finding that *mpc54* mutant alleles maintain proper recruitment of Spo21p and Spo74p.

Mpc54p plays a role in vesicle docking

In order to identify the stage of prospore membrane formation that is disrupted by the *mpc54* mutant alleles, the progression of prospore membrane formation was assessed for each *mpc54* allele using TEM analysis. Mutant phenotypes were compared to wild-type, an *mpc54*Δ strain, and an *sso1*Δ strain (in which vesicles are able to dock to the MOP but do not fuse together (Nakanishi *et al.*, 2006)) (Figure 2-5).

For all of the *mpc54* mutant alleles and the *sso1*Δ mutant, the number of vesicles accumulating at a MOP was similar to wild type, suggesting that the mutant alleles did

not disrupt the targeting and delivery of vesicles to the region near the MOP (Figure 2-5, Table 2-3). Interestingly, vesicles docked to the MOP at a higher rate in the wild-type and the *sso1*Δ mutant than in the *mpc54* mutant alleles (Table 2-3). The disruption of vesicle docking in the *mpc54* mutant alleles suggests that Mpc54p plays a role in vesicle docking at the surface of the MOP. However, wild-type, Mpc54p^{118}, Mpc54p^{119}, and Mpc54p^{145} were able to form membranes adjacent to the MOP (Table 2-3), suggesting that these mutations in *MPC54* did not completely disrupt Mpc54p's role in vesicle docking.

Additionally, for the MOPs in cells expressing the *mpc54* mutant alleles, vesicles remained at a stereotypic distance from the MOP, as though they were associating with the MOP but could not dock to the MOP surface (Figure 2-5, Table 2-3). The distance between the center of these "associating" vesicles and the surface of the MOP consistently ranged between 36-60 nm, suggesting that, though unable to dock, these vesicles were maintained at a specific distance from the MOP. This could be the result of a loose tethering of the vesicle to the MOP.

Mpc54p interacts with YLR301Wp

The Mpc54p mutant proteins provide us with a new tool for examining the role of the MOP during prospore membrane initiation. Using the mutant proteins, I were able to determine that Mpc54p plays a role in vesicle docking. Identifying proteins which interact with Mpc54p would further define the mechanism through which Mpc5p4 promotes vesicle docking. Therefore, a two hybrid screen was undertaken to identify proteins that interact with the N-terminus of wild-type Mpc54p. Using pSTT91-LexA-MPC54^{WT}(1-200) as bait, I screened the ActII library. 422,000 transformants were screened, fifteen were found to be *HIS*+ and *LacZ*+. Twelve of these fifteen positives retested. Of those that retested, four were mitochondrial DNA, three were out of frame, and five were in frame (YLR301Wp$^{37\text{-STOP}}$, YLR301Wp$^{98\text{-STOP}}$, NUP159p$^{293\text{-}606}$, CRM1p$^{771\text{-}1069}$, PWP2p$^{711\text{-STOP}}$). NUP159p and CRM1p are associated with the nuclear pore complex and with nuclear export, respectively, and PWP2p plays a role in ribosome assembly (Jordan *et al.*, 1977; Shafaatian *et al.*, 1996; Stade *et al.*, 1997). Therefore, although these three proteins may interact with Mpc54p, it is unlikely that this interaction

is required for vesicle docking at the MOP. In contrast, YLR301Wp is an uncharacterized protein that was pulled out of the screen twice (Figure 2-6A). Previously YLR301Wp was shown by two-hybrid to interact with Mpc54p (unpublished data from the Yeast Resource Center at The University of Washington, Seattle). The YLR301Wp positives were retested against the N-termini of the Mpc54p mutant proteins to examine the specificity of the interaction and to determine if the mutations in Mpc54p disrupted this interaction. YLR301Wp$^{37\text{-STOP}}$ retested against Mpc54p^{WT}(1-200), Mpc54p^{40}(1-200), and Mpc54p^{47}(1-200), but not against Mpc54p^{118}(1-200), Mpc54p^{119}(1-200), or Mpc54p^{145}(1-200) (Figure 2-6B). Interestingly, YLR301Wp$^{98\text{-STOP}}$ retested against all of the Mpc54p mutant proteins, although the *LacZ* signal was low in Mpc54p^{118}(1-200), Mpc54p^{119}(1-200), or Mpc54p^{145}(1-200) (Figure 2-6B). Taken together, this data suggests that the interaction between YLR301Wp and Mpc54p is weakened or disrupted by mutations within the N-terminus of *MPC54*.

YLR301W is not essential for prospore membrane formation

Previously, no one had examined the *ylr301w* knock out during sporulation. Therefore, I created *ylr301wΔ/ ylr301wΔ* mutant an examined its sporulation efficiency. *ylr301wΔ* cells have no sporulation phenotype, suggesting that it is not essential for prospore membrane formation, and therefore is not essential for the function of Mpc54p during vesicle docking (Figure 2-6E). Additionally, YLR301W-GFP localization was diffuse in cytoplasm during Meiosis II (Figure 2-6D). Therefore, although Mpc54p and YLR301Wp may interact during Meiosis II, this interaction is not required for vesicle docking.

Mpc54p mutant proteins disrupt Spo14p activation

Spo14p is a phospholipase D enzyme whose activity is critical for vesicle fusion during prospore membrane formation (Nakanishi *et al.*, 2006). Spo14p localizes to the prospore membrane where it converts PC to PA, thereby increasing the population of negative phospholipids in this membrane. In vitro, GFP-Spo20$^{51\text{-}91}$ preferentially localizes to membranes rich in negative phospholipids (Nakanishi *et al.*, 2004). During Meiosis II, GFP-Spo20$^{51\text{-}91}$ relocates from the plasma membrane to the prospore

membrane, and this relocation requires the activation of Spo14p (Nakanishi *et al.*, 2004; Nakanishi *et al.*, 2006). It was observed that GFP-Spo20$^{51-91}$ frequently remained at the plasma membrane in cells expressing the Mpc54p mutant proteins (Figure 2-7A). This could be explained in several ways: 1) GFP-Spo20$^{51-91}$ remaining at the plasma membrane is an artifact of examining cells at different stages of prospore membrane growth. H. Nakanishi observed that GFP-Spo20$^{51-91}$ does not relocate completely to the prospore membrane until the prospore membrane is elongating. Since the Mpc54p mutant proteins frequently block prospore membrane growth, these cells may be stalled prior to the point when GFP-Spo20$^{51-91}$ relocalizes from the plasma membrane. 2) I have demonstrated that precursor vesicles are not recruited equally to all MOPs within a single cell expressing the Mpc54p mutant protein. If only a small group of precursor vesicles are getting modified by Spo14p, then the population of phospholipids in the membranes near the MOP may not be sufficient to recruit GFP-Spo20$^{51-91}$ from the plasma membrane to the prospore membrane at the appropriate levels. Therefore, some GFP-Spo20$^{51-91}$ would remain at the plasma membrane. 3) Mpc54p may play a role in Spo14p activation. Therefore, Mpc54p mutant proteins might disrupt Spo14p activation and therefore disrupt the recruitment of GFP-Spo20$^{51-91}$.

To examine this first possibility, GFP-Spo20$^{51-91}$ localization at the plasma membrane was analyzed in cells expressing Mpc54p^{WT} or Mpc54p^{118}. The stage of prospore membrane formation was determined by examining the GFP-Spo20$^{51-91}$ phenotype at the MOPs of a single cell. Cells with at least one GFP dot but no GFP lines (representing prospore membranes) were considered to be in an early stage of prospore membrane formation. Cells with at least one GFP line were considered to be in later stages of prospore membrane formation. This classification would ensure that the cells examined were all at the same stage of prospore membrane formation. After determining the state of prospore membrane growth for each cell, the retention of GFP-Spo20$^{51-91}$ at the plasma membrane was examined. As expected, GFP-Spo20$^{51-91}$ remains at the plasma membrane in cells at early stages of prospore membrane growth regardless of which Mpc54p protein was expressed (Figure 2-7B). In contrast, GFP-Spo20$^{51-91}$ was absent from the plasma membrane (suggesting it had completely relocalized to the prospore membrane) in 47% of the late-stage wild-type cells examine, but remained at

the plasma membrane in 96% of late-stage cells expressing Mpc54p^{118} (Figure 2-7B). This suggests that Mpc54p^{118} may disrupt Spo14p activation, thereby preventing GFP-Spo20$^{51-91}$ relocation to the prospore membranes at the MOP. Since the MOP is assembled properly for this mutant allele, Mpc54p must promote Spo14p activation through the docking of vesicles and not through the formation of the MOP structure.

Spo14p localizes properly in cells expressing Mpc54p mutant proteins

Proper localization of Spo14p during Meiosis II is required for its function during vesicle fusion (Rudge *et al.*, 1998). Therefore, GFP-Spo20$^{51-91}$ may remain at the plasma membrane in Mpc54p^{118} simply as a result of mislocalization of Spo14p. To examine whether Mpc54p^{118} had an effect on the recruitment of Spo14p to the MOP, Spo14-GFP localization was examined in Meiosis II cells expressing this RFP-tagged Mpc54p mutant protein. Two hundred RFP-tagged MOPs were analyzed for colocalization with Spo14-GFP. Spo14-GFP localization was not significantly inhibited in cells expressing Mpc54p^{118} (Figure 2-7C). Since Spo14-GFP localized properly yet Spo14p activity was disrupted in cells expressing Mpc54p^{118}, this may suggest that proper vesicle docking to the MOP through the action of Mpc54p is required for Spo14p activation but not for Spo14p localization.

Discussion: Mpc54p is involved in vesicle docking at the Meiosis II Outer Plaque

The organization of the MOP

FRET analysis of MOP proteins has provided a great deal of information about the organization of the MOP structure. Based on our FRETR data, I have constructed a model of the organization of the MOP structure (Figure 2-8). In the model, the N-termini of Spo21p and Mpc54p are proximal to the outer surface of the MOP, while the C-termini of these proteins are buried within the MOP near the Nud1p and the N-terminus of Cnm67p.

Determining the organization of Spo74p within the MOP structure is difficult since the structure of Spo74p has yet to be determined and its FRET profile is complicated. However, I propose two possibilities for its organization based on the FRETR data. 1) Spo74p forms a tetramer with one dimer oriented N-termini "in" and the other dimer oriented N-termini "out." 2) Spo74p may have multiple interactions with Spo21p, thereby forming two or more conformations as it arrives at the MOP prior to MOP assembly. In the model, I present the first of these two possibilities.

The orientation and arrangement of MOP proteins has shed light onto their possible functions during prospore membrane formation. For instance, I have found that the N-terminus of Mpc54p localizes to the surface of the MOP where vesicles dock and fuse at the onset of prospore membrane formation, and that this portion of Mpc54p is, in fact, important to vesicle docking.

Mutations of conserved residues of Spo74p and Mpc54 produce new alleles for examining the role of these proteins during prospore membrane formation

Previous studies of Mpc54p, Spo21p, and Spo74p characterized the function and interactions of these proteins in the MOP, but were inhibited by the sole availability of null alleles (Knop and Strasser, 2000; Bajgier *et al.*, 2001; Nickas *et al.*, 2003). Since the deletion of any one of these three proteins leads to the dramatic loss of the entire MOP structure, determining the roles of these proteins in processes downstream of MOP formation requires more subtle approaches. I report that the mutation of conserved

residues of Spo74p and Mpc54p produce new alleles for examining the specific roles of these proteins during prospore membrane formation.

Mpc54p is involved in vesicle docking

Examination of the Mpc54p mutant proteins demonstrated that Mpc54p^{47}, Mpc54p^{118}, Mpc54p^{119}, and Mpc54p^{145} allow the formation of a typical MOP structure, but inhibit prospore membrane initiation. TEM analysis determined that vesicle docking was frequently blocked in cells expressing these Mpc54p mutant proteins. Interestingly, Mpc54p^{118}, Mpc54p^{119}, and Mpc54p^{145}were able to form spores at a reduced rate, suggesting that although Mpc54p plays a role in vesicle docking, it may not be required for this process or the mutations may not completely block docking.

YLR301Wp serves an unknown function

YLR301Wp interacts with the N-terminus of Mpc54p in the two hybrid system and this interaction is disrupted by mutating residues in the N-terminus of Mpc54p which are critical for vesicle docking. However, the function of YLR301Wp has yet to be determined.

Vesicle docking promotes Spo14p activity

Proper localization of Spo14p is critical to its function during prospore membrane formation (Rudge *et al.*, 1998). I have observed that Spo14p localization was not disrupted at MOPs in cells expressing Mpc54p^{118}. Interestingly, Spo14p activity is nonetheless impaired in cells expressing Mpc54p^{118}. These findings suggest that vesicle docking is required for Spo14p activation. A further examination of the activation of Spo14p through a biochemical analysis of PA formation in cells expressing the Mpc54p mutant proteins would verify these cytological experiments. How do docking events at the MOP impact activation of an enzyme? I propose that vesicle docking may regulate Spo14p activity (Figure 2-9). Our model for Spo14p activation proposes that Spo14p arrives at the SPB in an inactive state. Vesicle docking then triggers the activation of Spo14p through an unknown molecular mechanism. Activated Spo14p converts PC to PA in the docked precursor vesicles, thereby recruiting Spo20p and promoting vesicle

fusion. Thus, vesicles only fuse after docking to the MOP. By restricting vesicle fusion events to vesicles docked at the MOP, cells ensure that each prospore membrane will be attached to a MOP and therefore to the nucleus. This model proposes that the cell regulates the location and timing of prospore membrane initiation based on the activation of Spo14p on vesicles that are docked to the MOP.

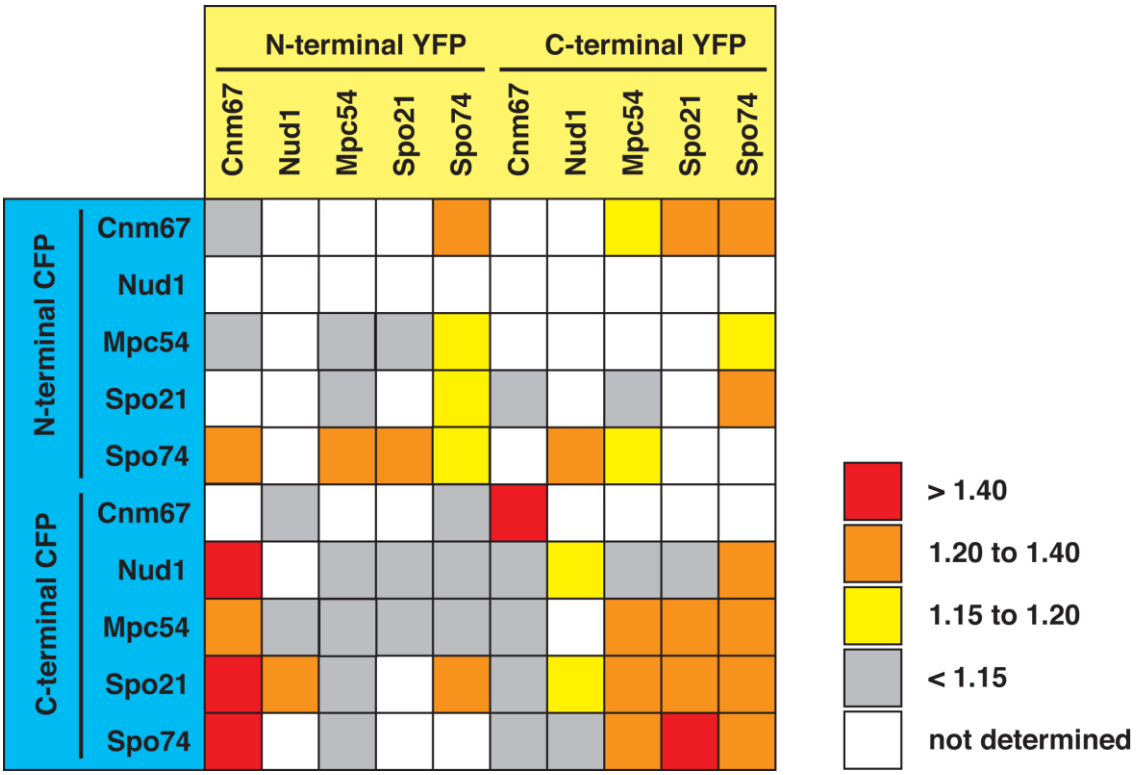

Figure 2-1: FRET interactions between the MOP components
(A) A compilation of completed FRETR measurements. The yellow box designates proteins tagged with YFP and the blue box designates proteins tagged with CFP. Each square represents one of the 100 possible FRET combinations between the five MOP proteins. The FRETR values have been grouped as the FRETR increases, which corresponds to an increase in energy transferred between the two fluores.

A

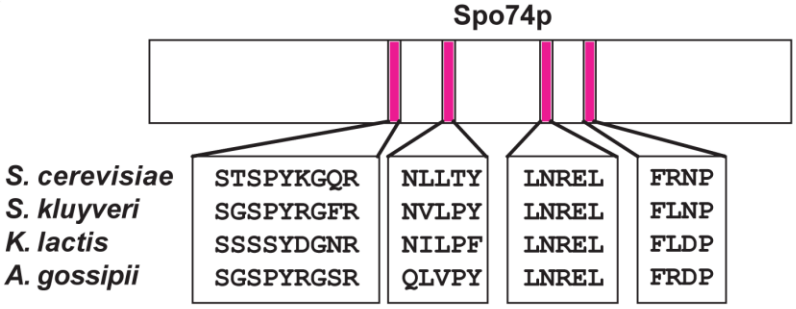

B

Name of allele	Amino Acids	Mutation
spo74 145	145-149	SxYxG : AxAxA
spo74 180	180-183	LLxY : AAxA
spo74 243	243-247	LNREL: LAAAL
spo74 267	267-270	FxxP :AxxA

C

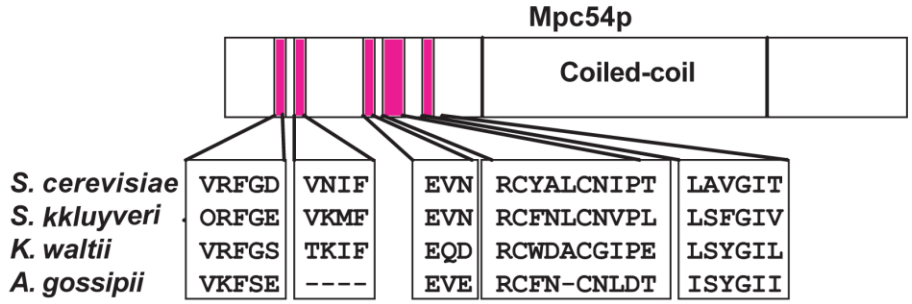

D

Name of allele	Amino Acids	Mutation
mpc54 40	40-42	RFG:AAA
mpc54 47	47-49	NIF:AAA
mpc54 118	118-120	RCY:AAA
mpc54 123	123-126	CNIP: AAAA
mpc54 119	119-124	CYxxCN:AAxxAA
mpc54 145	145-149	LxxGI:AxxAA

Figure 2-2: Construction of mutant alleles based on conservation of residues
(A) Conserved residue of Spo74p. The Spo74p schematic is oriented with the N-terminus to the left. Conserved regions are highlighted in pink and the protein sequence of those regions is shown below. (B) Conserved residues were mutated to alanines to construct *spo74* mutant alleles. (C) Conserved residue of Mpc54. The Mpc54p schematic is oriented with the N-terminus to the left. Conserved regions are highlighted in pink and the protein sequence of those regions is shown below. (D) Conserved residues were mutated to alanines to construct *mpc54* mutant alleles.

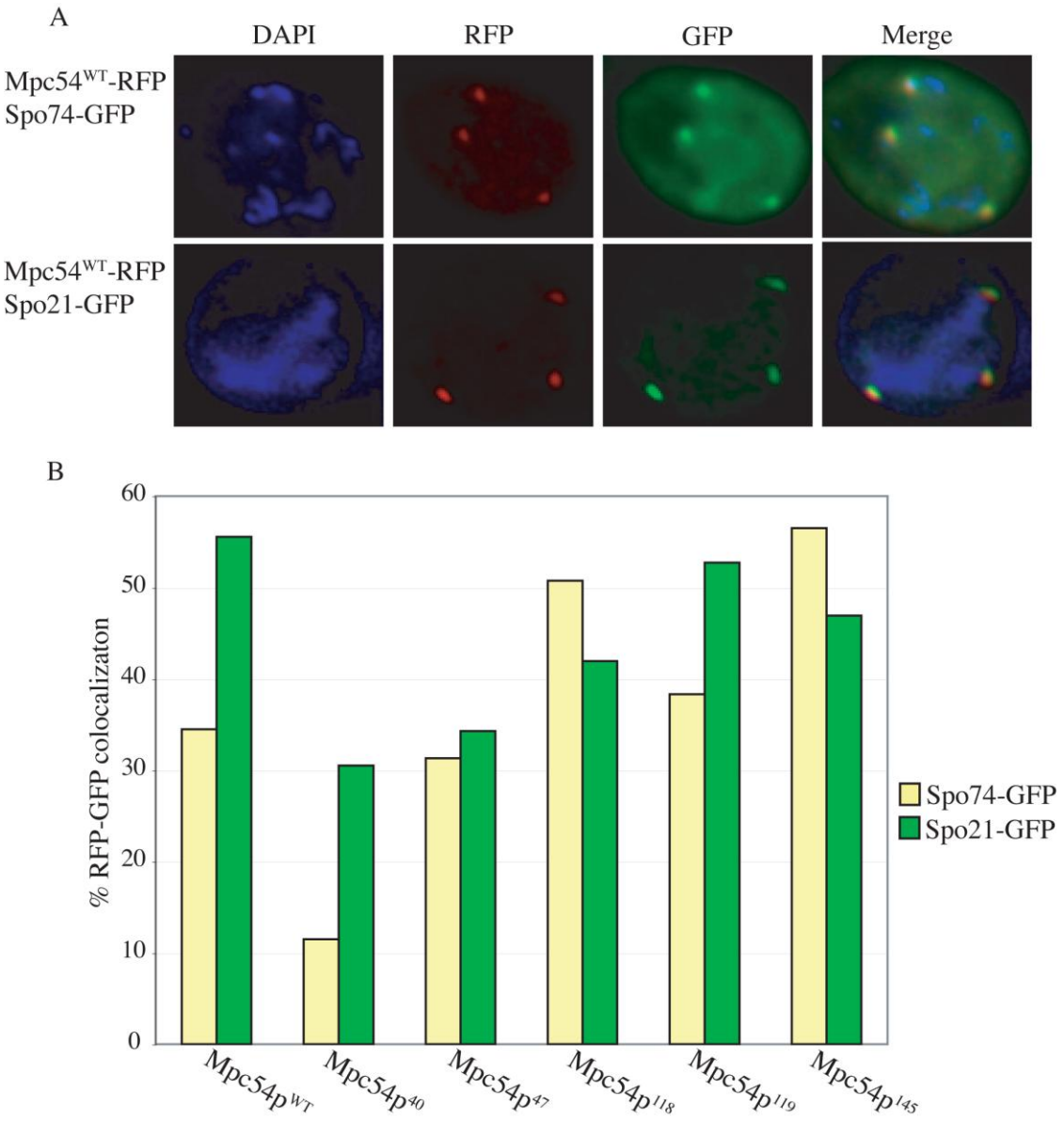

Figure 2-3: The effect of Mpc54p alleles on the composition of the MOP
(A) Representative examples of the colocalization between Mpc54^{WT}-RFP and Spo74-GFP (top panel) or Spo21-GFP (bottom panel) in Meiosis II cells. (B) Colocalization between RFP-tagged Mpc54p mutant proteins and Spo74-GFP (yellow bars) or Spo21-GFP (green bars) during Meiosis II. 200 RFP dots were analyzed for GFP colocalization for each
experiment.

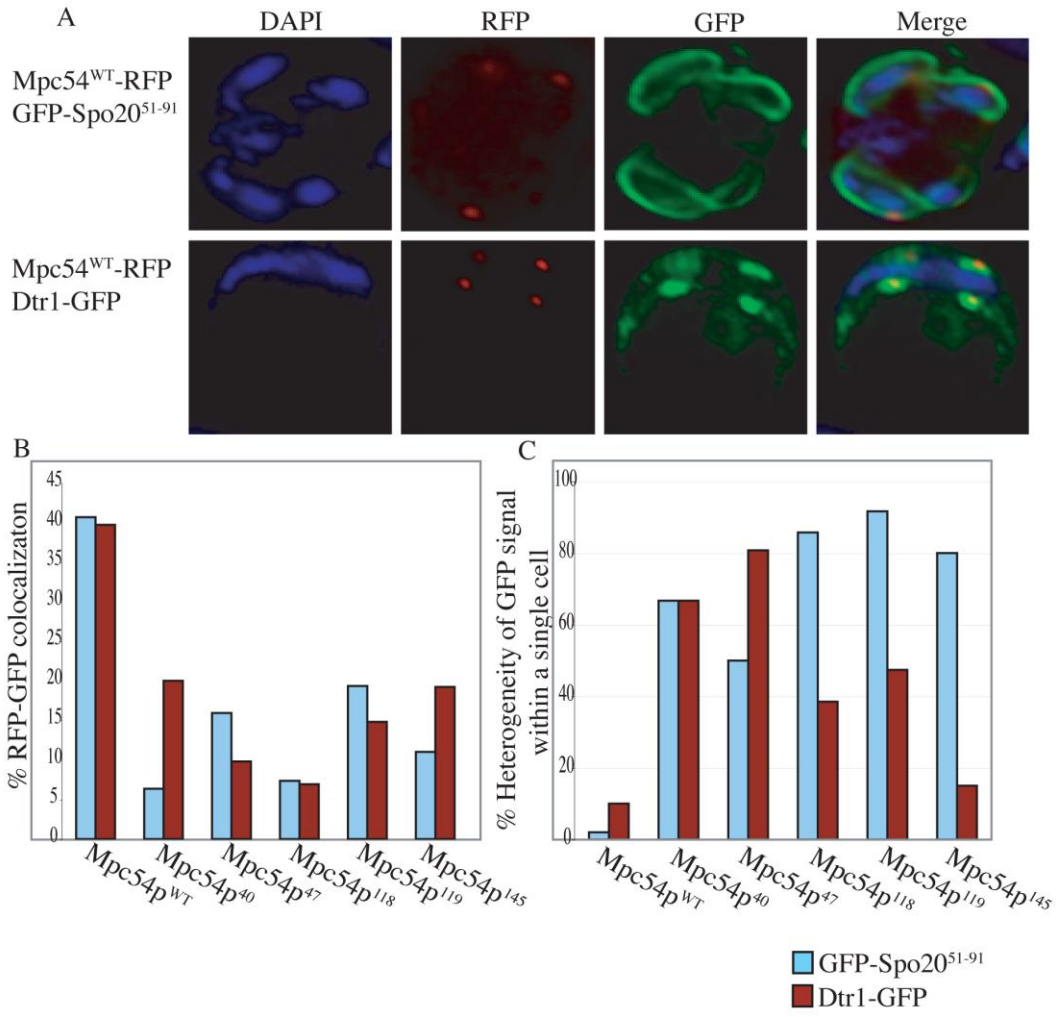

Figure 2-4: The effect of Mpc54p alleles on prospore membrane formation
(A) Representative examples of the colocalization between Mpc54^{WT}-RFP and GFP-Spo20$^{51-91}$ (top panel) or Dtr1-GFP (bottom panel) in Meiosis II cells. (B) Colocalization between RFP-tagged Mpc54p mutant proteins and GFP-Spo20$^{51-91}$ (blue bars) or Dtr1-GFP (red bars) during Meiosis II. 200 RFP dots were analyzed for GFP colocalization for each experiment. (C) The heterogeneity of the GFP signal of GFP-Spo20$^{51-91}$ (blue bars) or Dtr1-GFP (red bars) at the RFP dots within a single cell. Cells in which some RFP dots colocalized with GFP while others did not were considered heterogeneous. Cells in which all RFP colocalized with GFP or all RFP dots lacked a GFP signal were considered homogeneous. n>13.

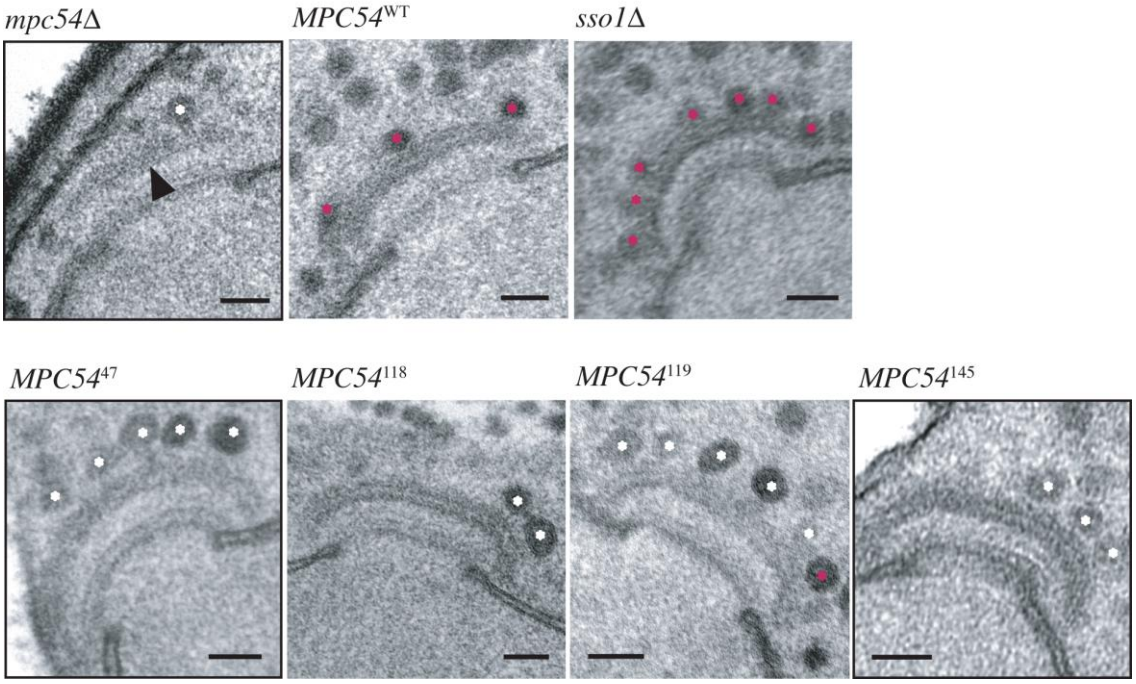

Figure 2-5: Characterizing the ultrastructure of the MOP and the progression of prospore membrane formation using TEM analysis

Single sections of Meiosis II spindle pole bodies. Vesicles sitting on the MOP's surface are indicated with a pink asterisk. Vesicles sitting a distance away from the MOP's surface are indicated with a white asterisk. The MOP structure in the *mpc54*Δ is truncated and lacks distinct layering (black arrow).

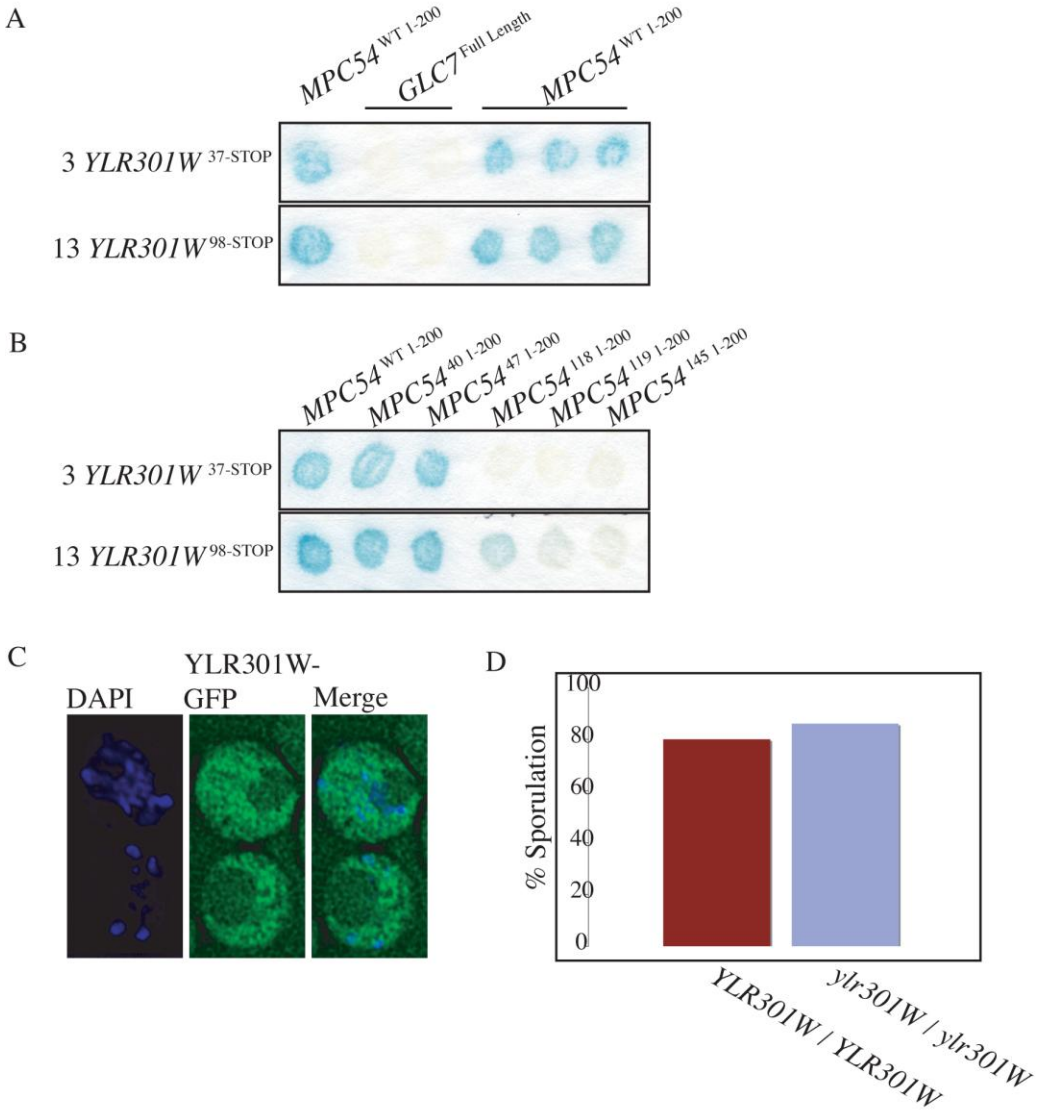

Figure 2-6: Characterizing YLR301W
(A) A LexA-Mpc54p^{WT}(1-200) fusion was tested for interactions with fusions of GAD to residues using a β-galactosidase filter lift assay as described in materials and methods. Two separate GAD-YLR301Wp fusions interacted with LexA-Mpc54p^{WT}(1-200). GAD-Glc7p$^{1-312}$ was used as a negative control. A blue signal indicates an interaction between the two proteins tested. (B) The interaction with GAD-YLR301Wp$^{37\text{-}STOP}$ and GAD-YLR301Wp$^{98\text{-}STOP}$ was retested against LexA-Mpc54p mutant proteins. (C) Localization of YLR301W-GFP during Meiosis II. (D) Comparing the sporulation efficiency of a *YLR301W* / *YLR301W* strain and a *ylr301w*Δ / *ylr301w*Δ mutant.

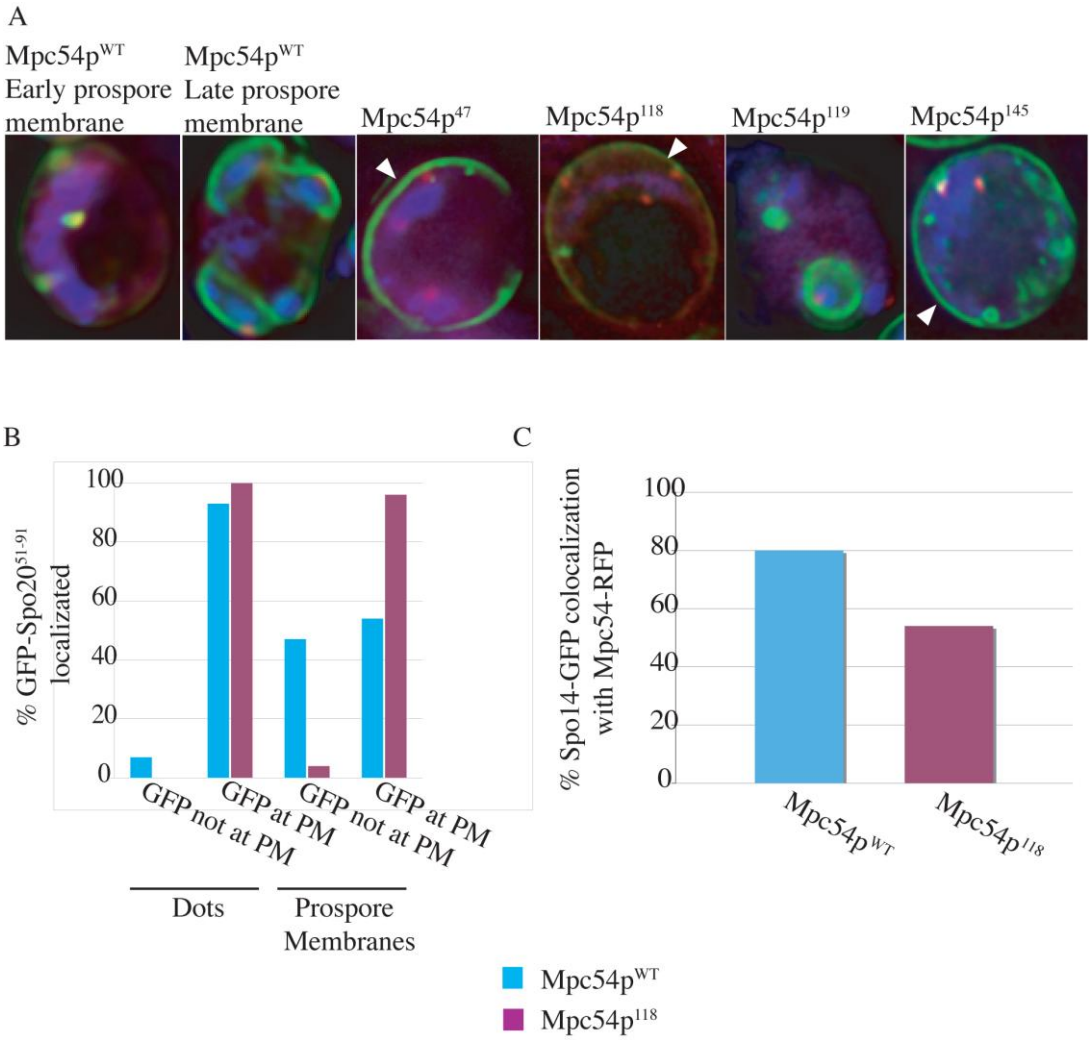

Figure 2-7: Spo14p activity in the *mpc54* mutant alleles
(A) Representative images of GFP-Spo20$^{51-91}$ localization in cells expressing Mpc54p-RFP mutant proteins. DAPI (blue), GFP-Spo20$^{51-91}$ (green), and Mpc54p-RFP mutant proteins (red) are shown in each image. GFP-Spo20$^{51-91}$ localization at the plasma membrane is indicated with a white arrow. (B) Quantification of GFP-Spo20$^{51-91}$ localization in cells expressing wild-type Mpc54-RFP or a mutant protein. (C) Spo14-GFP localization in cells expressing wild-type Mpc54-RFP or a mutant protein.

A

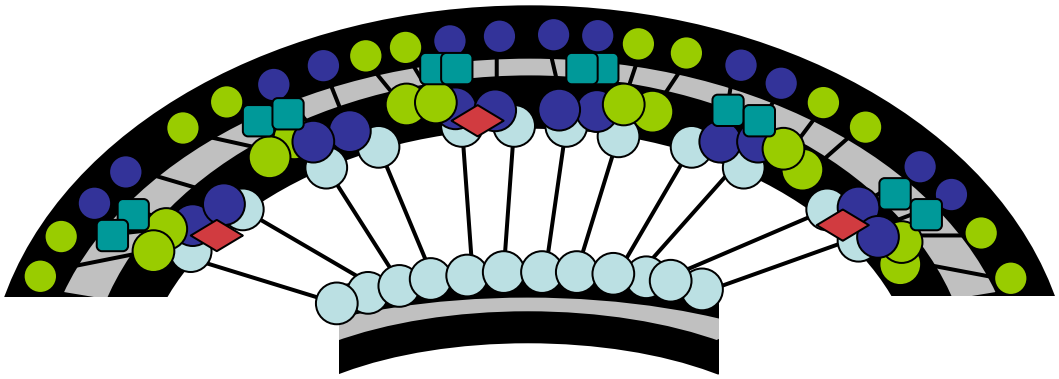

B

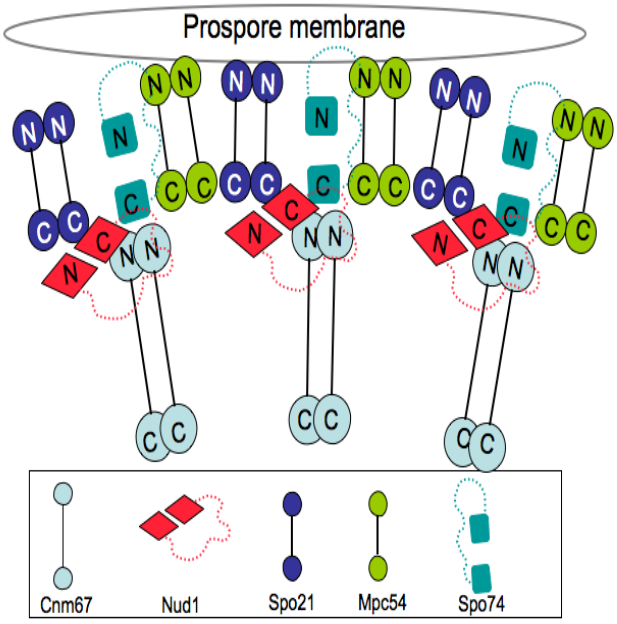

Figure 2-8: The organization of the MOP
(A) Positioning the MOP proteins within the MOP structure. (B) A model for the relative positions of the N- and C- termini of each MOP component. The protein designations are the same for both (A) and (B).

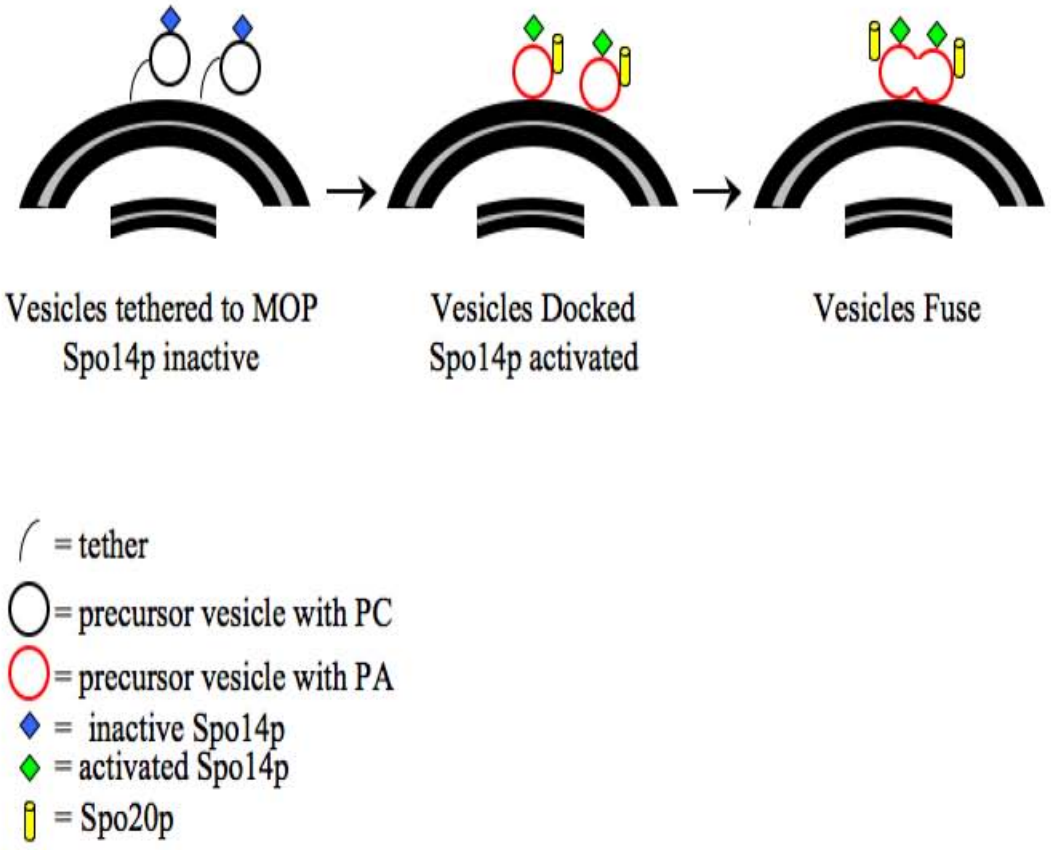

Figure 2-9: Model for Spo14p activation

Expression of *SPO74* Allele	% Sporulation	% Monads/Dyads	% Triads/Tetrads
CEN *SPO74*^{WT}	24	85	15
2µ *SPO74*^{WT}	75	29	71
SPO74^{WT} / *SPO74*^{WT}	89	99	1
CEN *spo74*^{145}	0	0	0
2µ *spo74*^{145}	0	0	0
spo74^{145} / *spo74*^{145}	0	0	0
CEN *SPO74*^{180}	0	0	0
2µ *spo74*^{180}	0	0	0
spo74^{180} / *spo74*^{180}	0	0	0
CEN *spo74*^{243}	12	84	7
2µ *spo74*^{243}	47	96	4
spo74^{243} / *spo74*^{243}	31	100	0
CEN *spo74*^{267}	22	68	29
spo74 / *spo74*	0	0	0

Table 2-1: The sporulation efficiency of the *spo74* mutant alleles
Sporulation was monitored using light microscopy. The equation used to determine the sporulation efficiency follows. Asci are described as monads (1 spore), dyads (2 spores), triads (3 spores), or tetrads (4 spores). I define these as the "spore type" in the equation that determines the percentage of spores in each category.

$$\% \text{ Sporulation} = 100 \times \frac{n_{Asci}}{n_{Cells}} \qquad \% \text{ Spore Type} = 100 \times \frac{n_{Spore\ Type}}{n_{Asci}}$$

Expression of *MPC54* Allele	% Sporulation	% Monads	% Dyads	% Triads	% Tetrads	RFP at SPB
CEN *MPC54*^{WT}	36	5	37	40	19	Y
2µ *MPC54*^{WT}	53	3	28	50	20	Y
MPC54^{WT} / *MPC54*^{WT}	67	2	12	42	44	Y
CEN *mpc54*^{40}	0	0	0	0	0	Y
2µ *mpc54*^{40}	0	0	0	0	0	Y
mpc54^{40} / *mpc54*^{40}	0	0	0	0	0	Y
CEN *mpc54*^{47}	0	0	0	0	0	Y
2µ *mpc54*^{47}	0	0	0	0	0	Y
mpc54^{47} / *mpc54*^{47}	0	0	0	0	0	Y
CEN *mpc54*^{118}	2	25	75	0	0	Y
2µ *mpc54*^{118}	16	60	40	0	0	Y
mpc54^{118} / *mpc54*^{118}	18	70	30	0	0	Y
CEN *mpc54*^{119}	6	57	43	0	0	Y
2µ *mpc54*^{119}	17	63	37	0	0	Y
mpc54^{119} / *mpc54*^{119}	0	0	0	0	0	Y
CEN *mpc54*^{145}	7	43	57	0	0	Y
2µ *mpc54*^{145}	12	70	30	0	0	Y
mpc54^{145} / *mpc54*^{145}	25	66	34	0	0	Y
CEN *mpc54*^{123}	0	0	0	0	0	N
mpc54 / mpc54	0	0	0	0	0	n/a

Table 2-2: The sporulation efficiency of the *mpc54* mutant alleles
Sporulation was monitored using light microscopy. The equation used to determine the sporulation efficiency follows. Asci are described as monads (1 spore), dyads (2 spores), triads (3 spores), or tetrads (4 spores). I define these as the "spore type" in the equation that determines the percentage of spores in each category.

$$\% \text{ Sporulation} = 100 \times \frac{n_{Asci}}{n_{Cells}} \qquad \% \text{ Spore Type} = 100 \times \frac{n_{Spore\ Type}}{n_{Asci}}$$

	Docked Vesicles 15-35nm	Tethered Vesicles 36-60nm	Accumulated Vesicles 61-300nm	Total Vesicles 15-300nm	Prospore membranes at MOPs
sso1Δ	5.6	1.4	11.9	19	N
mpc54Δ	0.5	1.5	4.0	6	N
MPC54^{WT}	3.0	2.3	7.3	13	Y
mpc54^{47}	0.2	1.8	5.5	8	N
mpc54^{118}	0.1	3.2	7.5	11	Y
mpc54^{119}	0.3	3.7	7.3	11	Y
mpc54^{145}	0.5	2.8	6.4	10	Y

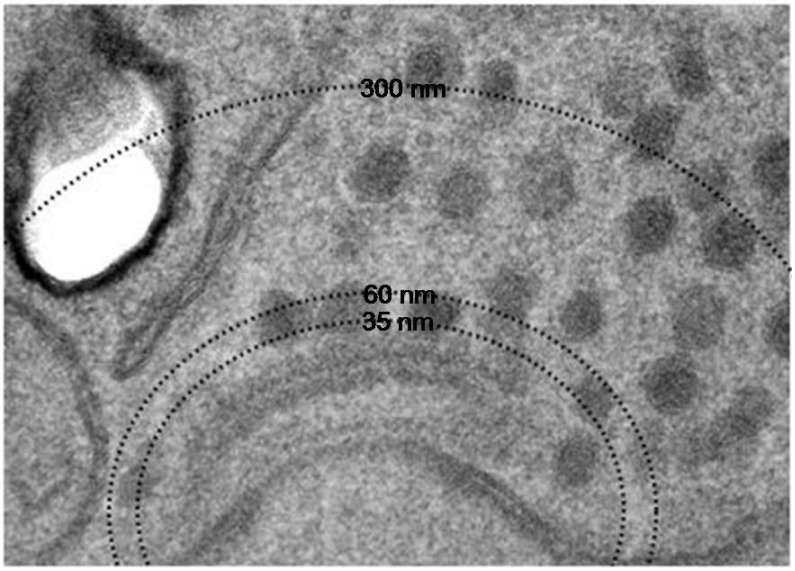

Table 2-3: The effect of the Mpc54p mutant proteins on vesicle docking at the MOP
For each data set, the distance between the MOP and the center of proximal vesicles was measured. Each vesicle was grouped according to its distance from the MOP. The numbers displayed were derived from averaging the number of vesicles in each category for each MOP analyzed. Only MOPs lacking prospore membranes were analyzed. The number of sections examined for each condition from top to bottom are as follows: 11, 33, 3, 22, 16, 12, 13. The image indicates the designations for the vesicle groupings.

Table 2-4. Strains used in this study.

Strain	Genotype	Source
AN117-4B	*MAT***α** *arg4-NspI his3SK ho::LYS2 leu2 lys2 rme1::LEU2 trp1::hisG ura3*	(Neiman et al., 2000)
AN117-16D	*MAT***a** *his3/SK ho::LYS2 leu2 lys2 trp1::hisG ura3*	(Neiman et al., 2000)
YLR301W-GFP	*MAT***a** *his3Δ1 leu2Δ0 met15Δ0 ura3Δ0 YLR301W-GFP*	(Huh *et al.*, 2003)
NY50	*MAT***α** *ura3 his3ΔSK trp1::hisG arg4-NspI lys2 ho::Lys2 rme1::LEU2 leu2 mpc54Δ::his5*	(Nickas *et al.*, 2003)
NY51	*MAT***a** *ura3 leu2 trp1-hisG his3ΔSK lys2 ho:: LYS2 mpc54Δ::his5*	(Nickas *et al.*, 2003)
MNH39	*MAT***α** *arg4 his3 ho::LYS2 leu2 lys2 rme1::LEU2 trp1 ura3 spo74Δ::HIS3MX6*	(Nickas *et al.*, 2003)
AN1120	*MAT***a** *ura3 leu2 trp1-hisG his3ΔSK ho:: LYS2 spo74Δ::HIS3MX6*	(Nickas *et al.*, 2003)
L40	*MAT***a** *leu2 ade2 his3 trp1 LYS2::lexAop-HIS3 URA3::lexAop-lacZ*	(Vojtek *et al.*, 1993)
NY541	*MAT***a**/*MAT*α *ARG4/arg4-NspI his3SK/his3SK ho::LYS2/ho::LYS2 leu2/leu2lys2/lys2 RME1/rme1::LEU2 trp1::hisG/trp1::hisG ura3/ura3 mpc54Δ::his5/ mpc54Δ::his5*	(Nickas *et al.*, 2003)
MND58	*MAT***α**/*MAT*α *ARG4/arg4-NspI his3SK/his3SK ho::LYS2/ho::LYS2 leu2/leu2lys2/lys2 RME1/rme1::LEU2 trp1::hisG/trp1::hisG ura3/ura3 spo74Δ::HIS3MX6/ spo74Δ::HIS3MX6*	(Nickas *et al.*, 2003)
EMD26	*MAT***a**/*MAT*α *ARG4/arg4-NspI his3SK/his3SK ho::LYS2/ho::LYS2 leu2/leu2lys2/lys2 RME1/rme1::LEU2 trp1::hisG/trp1::hisG ura3/ura3 mpc54Δ::his5/ mpc54Δ::his5 MPC54-RFP::TRP1/ MPC54-RFP::TRP1*	This study

Strain	Genotype	Source
EMD27	*MAT***a**/*MATα ARG4/arg4-NspI his3SK/his3SK ho::LYS2/ho::LYS2 leu2/leu2lys2/lys2 RME1/rme1::LEU2 trp1::hisG/trp1::hisG ura3/ura3 mpc54Δ::his5/ mpc54Δ::his5 mpc54-RFP^{40}::TRP1/ mpc54-RFP^{40}::TRP1*	This study
EMD28	*MAT***a**/*MATα ARG4/arg4-NspI his3SK/his3SK ho::LYS2/ho::LYS2 leu2/leu2lys2/lys2 RME1/rme1::LEU2 trp1::hisG/trp1::hisG ura3/ura3 mpc54Δ::his5/ mpc54Δ::his5 mpc54-RFP^{47}::TRP1/ mpc54-RFP^{47}::TRP1*	This study
EMD29	*MAT***a**/*MATα ARG4/arg4-NspI his3SK/his3SK ho::LYS2/ho::LYS2 leu2/leu2lys2/lys2 RME1/rme1::LEU2 trp1::hisG/trp1::hisG ura3/ura3 mpc54Δ::his5/ mpc54Δ::his5 mpc54-RFP^{118}::TRP1/ mpc54-RFP^{118}::TRP1*	This study
EMD112	*MAT***a**/*MATα ARG4/arg4-NspI his3SK/his3SK ho::LYS2/ho::LYS2 leu2/leu2lys2/lys2 RME1/rme1::LEU2 trp1::hisG/trp1::hisG ura3/ura3 mpc54Δ::his5/ mpc54-RFP^{119}::TRP1*	This study
EMD31	*MAT***a**/*MATα ARG4/arg4-NspI his3SK/his3SK ho::LYS2/ho::LYS2 leu2/leu2lys2/lys2 RME1/rme1::LEU2 trp1::hisG/trp1::hisG ura3/ura3 mpc54Δ::his5/ mpc54Δ::his5 mpc54-RFP^{145}::TRP1/ mpc54-RFP^{145}::TRP1*	This study
EMD50	*MAT***a**/*MATα ARG4/arg4-NspI his3SK/his3SK ho::LYS2/ho::LYS2 leu2/leu2lys2/lys2 RME1/rme1::LEU2 trp1::hisG/trp1::hisG ura3/ura3 spo74Δ::HIS3MX6/ spo74Δ::HIS3MX6 SPO74::TRP1/ SPO74::TRP1*	This study
EMD51	*MAT***a**/*MATα ARG4/arg4-NspI his3SK/his3SK ho::LYS2/ho::LYS2 leu2/leu2lys2/lys2 RME1/rme1::LEU2 trp1::hisG/trp1::hisG ura3/ura3 spo74Δ::HIS3MX6/ spo74Δ::HIS3MX6 spo74-243::TRP1/ spo74-243::TRP1*	This study

Strain	Genotype	Source
EMD56	*MAT***a**/*MATα ARG4/arg4-NspI his3SK/his3SK ho::LYS2/ho::LYS2 leu2/leu2lys2/lys2 RME1/rme1::LEU2 trp1::hisG/trp1::hisG ura3/ura3 spo74Δ::HIS3MX6/ spo74Δ::HIS3MX6 spo74-145::TRP1/ spo74-145::TRP1*	This study
EMD57	*MAT***a**/*MATα ARG4/arg4-NspI his3SK/his3SK ho::LYS2/ho::LYS2 leu2/leu2lys2/lys2 RME1/rme1::LEU2 trp1::hisG/trp1::hisG ura3/ura3 spo74Δ::HIS3MX6/ spo74Δ::HIS3MX6 spo74-180::TRP1/ spo74-180::TRP1*	This study
EMD71	*MAT***a**/*MATα ARG4/arg4-NspI his3SK/his3SK ho::LYS2/ho::LYS2 leu2/leu2lys2/lys2 RME1/rme1::LEU2 trp1::hisG/trp1::hisG ura3/ura3 ylr301wΔ:: TRP1/ ylr301wΔ::TRP1*	This study
YS148	*MAT***a** *his3/SK ho::LYS2 leu2 lys2 trp1::hisG ura3 CgTRP1-*P_{CNM67}*-CFP::CNM67*	This study
MNH53	*MAT***a** *his3/SK ho::LYS2 leu2 lys2 trp1::hisG ura3 CNM67::CFP-CgTRP1*	This study
AN1107	*MATα arg4-NspI his3SK ho::LYS2 leu2 lys2 rme1::LEU2 trp1::hisG ura3 CNM67-YFP::his5*	This study
YS200	*MAT***a** *his3/SK ho::LYS2 leu2 lys2 trp1::hisG ura3 mpc54::CgTRP1-* P_{MPC54}*-CFP::MPC54*	This study
YS91	*MATα arg4-NspI his3SK ho::LYS2 leu2 lys2 rme1::LEU2 trp1::hisG ura3 KlURA3-* P_{MPC54}*-YFP::MCP54*	This study
MNH51	*MAT***a** *his3/SK ho::LYS2 leu2 lys2 trp1::hisG ura3 MPC54::CFP-CgTRP1*	This study
YS115	*MATα arg4-NspI his3SK ho::LYS2 leu2 lys2 rme1::LEU2 trp1::hisG ura3 MPC54::CFP-CgTRP1*	This study
AN1108	*MATα arg4-NspI his3SK ho::LYS2 leu2 lys2 rme1::LEU2 trp1::hisG ura3 MPC54-YFP::his5*	This study
YS311	*MAT***a** *his3/SK ho::LYS2 leu2 lys2 trp1::hisG ura3 CgTRP1-*P_{CNM67}*-CFP::NUD1*	This study

Strain	Genotype	Source
YS149	*MAT***α** *arg4-NspI his3SK ho::LYS2 leu2 lys2 rme1::LEU2 trp1::hisG ura3 KlURA3-*P_{CNM67}*-YFP::NUD1*	This study
AN1116	*MAT***a** *his3/SK ho::LYS2 leu2 lys2 trp1::hisG ura3 NUD1-CFP::his5*	This study
AN1122	*MAT***a** *his3/SK ho::LYS2 leu2 lys2 trp1::hisG ura3 NUD1::YFP::his5*	This study
YS236	*MAT***a** *his3/SK ho::LYS2 leu2 lys2 trp1::hisG ura3 CgTRP1-*P_{MPC54}*-CFP::SPO21*	This study
YS92	*MAT***α** *arg4-NspI his3SK ho::LYS2 leu2 lys2 rme1::LEU2 trp1::hisG ura3 KlURA3-*P_{MPC54}*-YFP::SPO21*	This study
AN1117	*MAT***a** *his3/SK ho::LYS2 leu2 lys2 trp1::hisG ura3 SPO21-CFP::his5*	This study
MNH52	*MAT***α** *arg4-NspI his3SK ho::LYS2 leu2 lys2 rme1::LEU2 trp1::hisG ura3 SPO21::YFP-CgTRP1*	This study
YS235	*MAT***a** *his3/SK ho::LYS2 leu2 lys2 trp1::hisG ura3 CgTRP1-*P_{MPC54}*-CFP::SPO74*	This study
YS132	*MAT***α** *arg4-NspI his3SK ho::LYS2 leu2 lys2 rme1::LEU2 trp1::hisG ura3 KlURA3-*P_{MPC54}*-YFP::SPO74*	This study
YS114	*MAT***α** *arg4-NspI his3SK ho::LYS2 leu2 lys2 rme1::LEU2 trp1::hisG ura3 SPO74::linkerCFP ::his5+*	This study
AN1124	*MAT***a** *his3/SK ho::LYS2 leu2 lys2 trp1::hisG ura3 SPO74::YFP::his+*	This study
MNH50	*MAT***α** *arg4-NspI his3SK ho::LYS2 leu2 lys2 rme1::LEU2 trp1::hisG ura3 SPO74::*YFP-*HIS3MX6*	This study
MNH55	*MAT***α** *arg4-NspI his3SK ho::LYS2 leu2 lys2 rme1::LEU2 trp1::hisG ura3 KlURA3-* P_{CNM67}*-YFP::CNM67*	This study

Strain	Genotype	Source
YS312	*MAT***a** *his3/SK ho::LYS2 leu2 lys2 trp1::hisG ura3 CgTRP1-P_{MPC54}-CFP::MPC54*	This study
YS316	*MAT***a** *his3/SK ho::LYS2 leu2 lys2 trp1::hisG ura3 CgTRP1-P_{MPC54}-CFP::SPO21*	This study
YS323	*MAT***a** *his3/SK ho::LYS2 leu2 lys2 trp1::hisG ura3 CgTRP1- P_{MPC54}-CFP::SPO74*	This study
KBH1	*MAT***α** *arg4-NspI his3SK ho::LYS2 leu2 lys2 rme1::LEU2 trp1::hisG ura3 KlURA3- P_{CNM67}-YFP::MPC54*	This study
AN1121	*MAT***α** *arg4-NspI his3SK ho::LYS2 leu2 lys2 rme1::LEU2 trp1::hisG ura3 NUD1::YFP::his5*	This study
EMD95	*MAT***a**/*MAT*α *ARG4/arg4-NspI his3SK/his3SK ho::LYS2/ho::LYS2 leu2/leu2lys2/lys2 RME1/rme1::LEU2 trp1::hisG/trp1::hisG ura3/ura3 KlURA3- P_{CNM67}-YFP::CNM67/ CgTRP1-P_{CNM67}-CFP::CNM67*	This study
YS362	*MAT***a**/*MAT*α *ARG4/arg4-NspI his3SK/his3SK ho::LYS2/ho::LYS2 leu2/leu2lys2/lys2 RME1/rme1::LEU2 trp1::hisG/trp1::hisG ura3/ura3 KlURA3- P_{CNM67}-YFP::CNM67/ KlURA3- P_{CNM67}-YFP::CNM67 CgTRP1-P_{CNM67}-CFP::NUD1/ CgTRP1-P_{CNM67}-CFP::NUD1*	This study
YS335	*MAT***a**/*MAT*α *ARG4/arg4-NspI his3SK/his3SK ho::LYS2/ho::LYS2 leu2/leu2lys2/lys2 RME1/rme1::LEU2 trp1::hisG/trp1::hisG ura3/ura3 KlURA3- P_{CNM67}-YFP::CNM67/ KlURA3- P_{CNM67}-YFP::CNM67 CgTRP1-P_{MPC54}-CFP::MPC54/ CgTRP1-P_{MPC54}-CFP::MPC54*	This study

Strain	Genotype	Source
YS344	*MAT***a**/*MATα ARG4/arg4-NspI his3SK/his3SK ho::LYS2/ho::LYS2 leu2/leu2lys2/lys2 RME1/rme1::LEU2 trp1::hisG/trp1::hisG ura3/ura3 KlURA3- P_{CNM67}-YFP::CNM67/ KlURA3- P_{CNM67}-YFP::CNM67 CgTRP1-P_{MPC54}-CFP::SPO21/ CgTRP1-P_{MPC54}-CFP::SPO21*	This study
YS383	*MAT***a**/*MATα ARG4/arg4-NspI his3SK/his3SK ho::LYS2/ho::LYS2 leu2/leu2lys2/lys2 RME1/rme1::LEU2 trp1::hisG/trp1::hisG ura3/ura3 KlURA3- P_{CNM67}-YFP::CNM67/ KlURA3- P_{CNM67}-YFP::CNM67 CgTRP1- P_{MPC54}-CFP::SPO74/ CgTRP1- P_{MPC54}-CFP::SPO74*	This study
EMD96	*MAT***a**/*MATα ARG4/arg4-NspI his3SK/his3SK ho::LYS2/ho::LYS2 leu2/leu2lys2/lys2 RME1/rme1::LEU2 trp1::hisG/trp1::hisG ura3/ura3 KlURA3- P_{CNM67}-YFP::CNM67// CNM67::CFP-CgTRP1*	This study
MND102	*MAT***a**/*MATα ARG4/arg4-NspI his3SK/his3SK ho::LYS2/ho::LYS2 leu2/leu2lys2/lys2 RME1/rme1::LEU2 trp1::hisG/trp1::hisG ura3/ura3 KlURA3- P_{CNM67}-YFP::CNM67/ KlURA3- P_{CNM67}-YFP::CNM67 NUD1-CFP::his5/ NUD1-CFP::his5*	This study
MND101	*MAT***a**/*MATα ARG4/arg4-NspI his3SK/his3SK ho::LYS2/ho::LYS2 leu2/leu2lys2/lys2 RME1/rme1::LEU2 trp1::hisG/trp1::hisG ura3/ura3 KlURA3- P_{CNM67}-YFP::CNM67/ KlURA3- P_{CNM67}-YFP::CNM67 MPC54::CFP-CgTRP1 / MPC54::CFP-CgTRP1*	This study
MND103	*MAT***a**/*MATα ARG4/arg4-NspI his3SK/his3SK ho::LYS2/ho::LYS2 leu2/leu2lys2/lys2 RME1/rme1::LEU2 trp1::hisG/trp1::hisG ura3/ura3 KlURA3- P_{CNM67}-YFP::CNM67/ KlURA3- P_{CNM67}-YFP::CNM67 SPO21-CFP::his5/ SPO21-CFP::his5*	This study

Strain	Genotype	Source
MND104	*MAT***a**/*MATα ARG4/arg4-NspI his3SK/his3SK ho::LYS2/ho::LYS2 leu2/leu2lys2/lys2 RME1/rme1::LEU2 trp1::hisG/trp1::hisG ura3/ura3 KlURA3- P_{CNM67}-YFP::CNM67/ KlURA3- P_{CNM67}-YFP::CNM67 SPO74::linkerCFP ::his5+/SPO74::linkerCFP ::his5+*	This study
YS179	*MAT***a**/*MATα ARG4/arg4-NspI his3SK/his3SK ho::LYS2/ho::LYS2 leu2/leu2lys2/lys2 RME1/rme1::LEU2 trp1::hisG/trp1::hisG ura3/ura3 KlURA3-P_{CNM67}-YFP::NUD1/ KlURA3-P_{CNM67}-YFP::NUD1 CgTRP1-P_{CNM67}-CFP::CNM67/ CgTRP1-P_{CNM67}-CFP::CNM67*	This study
EMD91	*MAT***a**/*MATα ARG4/arg4-NspI his3SK/his3SK ho::LYS2/ho::LYS2 leu2/leu2lys2/lys2 RME1/rme1::LEU2 trp1::hisG/trp1::hisG ura3/ura3 KlURA3-P_{CNM67}-YFP::NUD1/ CgTRP1-P_{CNM67}-CFP::NUD1*	This study
YS152	*MAT***a**/*MATα ARG4/arg4-NspI his3SK/his3SK ho::LYS2/ho::LYS2 leu2/leu2lys2/lys2 RME1/rme1::LEU2 trp1::hisG/trp1::hisG ura3/ura3 KlURA3-P_{CNM67}-YFP::NUD1/ KlURA3-P_{CNM67}-YFP::NUD1 KlURA3- P_{CNM67}-YFP::CNM67/ KlURA3- P_{CNM67}-YFP::CNM67*	This study
EMD92	*MAT***a**/*MATα ARG4/arg4-NspI his3SK/his3SK ho::LYS2/ho::LYS2 leu2/leu2lys2/lys2 RME1/rme1::LEU2 trp1::hisG/trp1::hisG ura3/ura3 KlURA3-P_{CNM67}-YFP::NUD1/ NUD1-CFP::his5*	This study
YS155	*MAT***a**/*MATα ARG4/arg4-NspI his3SK/his3SK ho::LYS2/ho::LYS2 leu2/leu2lys2/lys2 RME1/rme1::LEU2 trp1::hisG/trp1::hisG ura3/ura3 KlURA3-P_{CNM67}-YFP::NUD1/ KlURA3-P_{CNM67}-YFP::NUD1 MPC54::CFP-CgTRP1 /MPC54::CFP-CgTRP1*	This study

Strain	Genotype	Source
YS158	*MAT***a**/*MATα ARG4/arg4-NspI his3SK/his3SK ho::LYS2/ho::LYS2 leu2/leu2lys2/lys2 RME1/rme1::LEU2 trp1::hisG/trp1::hisG ura3/ura3 KlURA3-P$_{CNM67}$-YFP::NUD1/ KlURA3-P$_{CNM67}$-YFP::NUD1 SPO21-CFP::his5/ SPO21-CFP::his5*	This study
YS161	*MAT***a**/*MATα ARG4/arg4-NspI his3SK/his3SK ho::LYS2/ho::LYS2 leu2/leu2lys2/lys2 RME1/rme1::LEU2 trp1::hisG/trp1::hisG ura3/ura3 KlURA3-P$_{CNM67}$-YFP::NUD1/ KlURA3-P$_{CNM67}$-YFP::NUD1 SPO74::linkerCFP ::his5+/ SPO74::linkerCFP ::his5+*	This study
YS176	*MAT***a**/*MATα ARG4/arg4-NspI his3SK/his3SK ho::LYS2/ho::LYS2 leu2/leu2lys2/lys2 RME1/rme1::LEU2 trp1::hisG/trp1::hisG ura3/ura3 MPC54::KlURA3-P$_{MPC54}$-YF/ MPC54::KlURA3-P$_{MPC54}$-YFP CgTRP1-P$_{CNM67}$-CFP::CNM67/ CgTRP1-P$_{CNM67}$-CFP::CNM67*	This study
EMD107	*MAT***a**/*MATα ARG4/arg4-NspI his3SK/his3SK ho::LYS2/ho::LYS2 leu2/leu2lys2/lys2 RME1/rme1::LEU2 trp1::hisG/trp1::hisG ura3/ura3 MPC54::KlURA3-P$_{MPC54}$-YFP/ CgTRP1-P$_{MPC54}$-CFP::MPC54*	This study
YS95	*MAT***a**/*MATα ARG4/arg4-NspI his3SK/his3SK ho::LYS2/ho::LYS2 leu2/leu2lys2/lys2 RME1/rme1::LEU2 trp1::hisG/trp1::hisG ura3/ura3 KlURA3-P$_{MPC54}$-YFP::MPC54/ KlURA3-P$_{MPC54}$-YFP::MPC54 CNM67::CFP-CgTRP1 /CNM67::CFP-CgTRP1*	This study
KBD2	*MAT***a**/*MATα ARG4/arg4-NspI his3SK/his3SK ho::LYS2/ho::LYS2 leu2/leu2lys2/lys2 RME1/rme1::LEU2 trp1::hisG/trp1::hisG ura3/ura3 KlURA3- P$_{CNM67}$-YFP::MPC54 / KlURA3- P$_{CNM67}$-YFP::MPC54 NUD1-CFP::his5/NUD1-CFP::his5*	This study

Strain	Genotype	Source
EMD105	*MAT***a**/*MATα ARG4/arg4-NspI his3SK/his3SK ho::LYS2/ho::LYS2 leu2/leu2lys2/lys2 RME1/rme1::LEU2 trp1::hisG/trp1::hisG ura3/ura3 MPC54::KlURA3-*P_{MPC54}*-YFP/MPC54::CFP-CgTRP1*	This study
KBD3	*MAT***a**/*MATα ARG4/arg4-NspI his3SK/his3SK ho::LYS2/ho::LYS2 leu2/leu2lys2/lys2 RME1/rme1::LEU2 trp1::hisG/trp1::hisG ura3/ura3 KlURA3-* P_{CNM67}*-YFP::MPC54 / KlURA3-* P_{CNM67}*-YFP::MPC54 SPO21-CFP::his5/ SPO21-CFP::his5*	This study
KBD4	*MAT***a**/*MATα ARG4/arg4-NspI his3SK/his3SK ho::LYS2/ho::LYS2 leu2/leu2lys2/lys2 RME1/rme1::LEU2 trp1::hisG/trp1::hisG ura3/ura3 KlURA3-* P_{CNM67}*-YFP::MPC54 / KlURA3-* P_{CNM67}*-YFP::MPC54 SPO74::linkerCFP ::his5+/ SPO74::linkerCFP ::his5+*	This study
YS182	*MAT***a**/*MATα ARG4/arg4-NspI his3SK/his3SK ho::LYS2/ho::LYS2 leu2/leu2lys2/lys2 RME1/rme1::LEU2 trp1::hisG/trp1::hisG ura3/ura3 KlURA3-*P_{MPC54}*-YFP::SPO21/ KlURA3-*P_{MPC54}*-YFP::SPO21 CgTRP1-*P_{CNM67}*-CFP::CNM67/ CgTRP1-*P_{CNM67}*-CFP::CNM67*	This study
YS368	*MAT***a**/*MATα ARG4/arg4-NspI his3SK/his3SK ho::LYS2/ho::LYS2 leu2/leu2lys2/lys2 RME1/rme1::LEU2 trp1::hisG/trp1::hisG ura3/ura3 KlURA3-*P_{MPC54}*-YFP::SPO21/ KlURA3-*P_{MPC54}*-YFP::SPO21 CgTRP1-*P_{CNM67}*-CFP::NUD1/ CgTRP1-*P_{CNM67}*-CFP::NUD1*	This study
EMD52	*MAT***a**/*MATα ARG4/arg4-NspI his3SK/his3SK ho::LYS2/ho::LYS2 leu2/leu2lys2/lys2 RME1/rme1::LEU2 trp1::hisG/trp1::hisG ura3/ura3 KlURA3-*P_{MPC54}*-YFP::SPO21/ KlURA3-*P_{MPC54}*-YFP::SPO21 CgTRP1-*P_{MPC54}*-CFP::MPC54/ CgTRP1-*P_{MPC54}*-CFP::MPC54*	This study

Strain	Genotype	Source
EMD99	*MAT***a**/*MATα ARG4/arg4-NspI his3SK/his3SK ho::LYS2/ho::LYS2 leu2/leu2lys2/lys2 RME1/rme1::LEU2 trp1::hisG/trp1::hisG ura3/ura3 KlURA3-*P_{MPC54}*-YFP::SPO21/ CgTRP1-*P_{MPC54}*-CFP::SPO21*	This study
YS392	*MAT***a**/*MATα ARG4/arg4-NspI his3SK/his3SK ho::LYS2/ho::LYS2 leu2/leu2lys2/lys2 RME1/rme1::LEU2 trp1::hisG/trp1::hisG ura3/ura3 KlURA3-*P_{MPC54}*-YFP::SPO21/ KlURA3-*P_{MPC54}*-YFP::SPO21 CgTRP1- P* $_{MPC54}$*-CFP::SPO74/ CgTRP1- P* $_{MPC54}$*-CFP::SPO74*	This study
YS104	*MAT***a**/*MATα ARG4/arg4-NspI his3SK/his3SK ho::LYS2/ho::LYS2 leu2/leu2lys2/lys2 RME1/rme1::LEU2 trp1::hisG/trp1::hisG ura3/ura3 KlURA3-*P_{MPC54}*-YFP::SPO21/ KlURA3-*P_{MPC54}*-YFP::SPO21 CNM67::CFP-CgTRP1 /CNM67::CFP-CgTRP1*	This study
YS107	*MAT***a**/*MATα ARG4/arg4-NspI his3SK/his3SK ho::LYS2/ho::LYS2 leu2/leu2lys2/lys2 RME1/rme1::LEU2 trp1::hisG/trp1::hisG ura3/ura3 KlURA3-*P_{MPC54}*-YFP::SPO21/ KlURA3-*P_{MPC54}*-YFP::SPO21 NUD1-CFP::his5/ NUD1-CFP::his5*	This study
YS118	*MAT***a**/*MATα ARG4/arg4-NspI his3SK/his3SK ho::LYS2/ho::LYS2 leu2/leu2lys2/lys2 RME1/rme1::LEU2 trp1::hisG/trp1::hisG ura3/ura3 KlURA3-*P_{MPC54}*-YFP::SPO21/ KlURA3-*P_{MPC54}*-YFP::SPO21 MPC54::CFP-CgTRP1 /MPC54::CFP-CgTRP1*	This study
EMD100	*MAT***a**/*MATα ARG4/arg4-NspI his3SK/his3SK ho::LYS2/ho::LYS2 leu2/leu2lys2/lys2 RME1/rme1::LEU2 trp1::hisG/trp1::hisG ura3/ura3 KlURA3-*P_{MPC54}*-YFP::SPO21/ SPO21-CFP::his5*	This study

Strain	Genotype	Source
YS113	*MAT***a**/*MATα ARG4/arg4-NspI his3SK/his3SK ho::LYS2/ho::LYS2 leu2/leu2lys2/lys2 RME1/rme1::LEU2 trp1::hisG/trp1::hisG ura3/ura3 KlURA3-P$_{MPC54}$-YFP::SPO21/ KlURA3-P$_{MPC54}$-YFP::SPO21 SPO74::linkerCFP ::his5+/SPO74::linkerCFP ::his5+*	This study
YS185	*MAT***a**/*MATα ARG4/arg4-NspI his3SK/his3SK ho::LYS2/ho::LYS2 leu2/leu2lys2/lys2 RME1/rme1::LEU2 trp1::hisG/trp1::hisG ura3/ura3 KlURA3-P$_{MPC54}$-YFP::SPO74/ KlURA3-P$_{MPC54}$-YFP::SPO74 CgTRP1-P$_{CNM67}$-CFP::CNM67/ CgTRP1-P$_{CNM67}$-CFP::CNM67*	This study
YS315	*MAT***a**/*MATα ARG4/arg4-NspI his3SK/his3SK ho::LYS2/ho::LYS2 leu2/leu2lys2/lys2 RME1/rme1::LEU2 trp1::hisG/trp1::hisG ura3/ura3 KlURA3-P$_{MPC54}$-YFP::SPO74/ KlURA3-P$_{MPC54}$-YFP::SPO74 CgTRP1-P$_{CNM67}$-CFP::NUD1/ CgTRP1-P$_{CNM67}$-CFP::NUD1*	This study
EMD53	*MAT***a**/*MATα ARG4/arg4-NspI his3SK/his3SK ho::LYS2/ho::LYS2 leu2/leu2lys2/lys2 RME1/rme1::LEU2 trp1::hisG/trp1::hisG ura3/ura3 KlURA3-P$_{MPC54}$-YFP::SPO74/ KlURA3-P$_{MPC54}$-YFP::SPO74 CgTRP1-P$_{MPC54}$-CFP::MPC54/ CgTRP1-P$_{MPC54}$-CFP::MPC54*	This study
YS347	*MAT***a**/*MATα ARG4/arg4-NspI his3SK/his3SK ho::LYS2/ho::LYS2 leu2/leu2lys2/lys2 RME1/rme1::LEU2 trp1::hisG/trp1::hisG ura3/ura3 KlURA3-P$_{MPC54}$-YFP::SPO74/ KlURA3-P$_{MPC54}$-YFP::SPO74 CgTRP1-P$_{MPC54}$-CFP::SPO21/ CgTRP1-P$_{MPC54}$-CFP::SPO21*	This study
EMD103	*MAT***a**/*MATα ARG4/arg4-NspI his3SK/his3SK ho::LYS2/ho::LYS2 leu2/leu2lys2/lys2 RME1/rme1::LEU2 trp1::hisG/trp1::hisG ura3/ura3 KlURA3-P$_{MPC54}$-YFP::SPO74/ CgTRP1-P$_{MPC54}$-CFP::SPO74*	This study

Strain	Genotype	Source
YS138	*MAT***a**/*MATα ARG4/arg4-NspI his3SK/his3SK ho::LYS2/ho::LYS2 leu2/leu2lys2/lys2 RME1/rme1::LEU2 trp1::hisG/trp1::hisG ura3/ura3 KlURA3-P$_{MPC54}$-YFP::SPO74/ KlURA3-P$_{MPC54}$-YFP::SPO74 CNM67::CFP-CgTRP1 /CNM67::CFP-CgTRP1*	This study
YS144	*MAT***a**/*MATα ARG4/arg4-NspI his3SK/his3SK ho::LYS2/ho::LYS2 leu2/leu2lys2/lys2 RME1/rme1::LEU2 trp1::hisG/trp1::hisG ura3/ura3 KlURA3-P$_{MPC54}$-YFP::SPO74/ KlURA3-P$_{MPC54}$-YFP::SPO74 NUD1-CFP::his5/ NUD1-CFP::his5*	This study
YS141	*MAT***a**/*MATα ARG4/arg4-NspI his3SK/his3SK ho::LYS2/ho::LYS2 leu2/leu2lys2/lys2 RME1/rme1::LEU2 trp1::hisG/trp1::hisG ura3/ura3 KlURA3-P$_{MPC54}$-YFP::SPO74/ KlURA3-P$_{MPC54}$-YFP::SPO74 MPC54::CFP-CgTRP1 /MPC54::CFP-CgTRP1*	This study
YS147	*MAT***a**/*MATα ARG4/arg4-NspI his3SK/his3SK ho::LYS2/ho::LYS2 leu2/leu2lys2/lys2 RME1/rme1::LEU2 trp1::hisG/trp1::hisG ura3/ura3 KlURA3-P$_{MPC54}$-YFP::SPO74/ KlURA3-P$_{MPC54}$-YFP::SPO74 SPO21-CFP::his5/ SPO21-CFP::his5*	This study
EMD97	*MAT***a**/*MATα ARG4/arg4-NspI his3SK/his3SK ho::LYS2/ho::LYS2 leu2/leu2lys2/lys2 RME1/rme1::LEU2 trp1::hisG/trp1::hisG ura3/ura3 CNM67-YFP::his5/ CgTRP1-P$_{CNM67}$-CFP::CNM67*	This study
YS374	*MAT***a**/*MATα ARG4/arg4-NspI his3SK/his3SK ho::LYS2/ho::LYS2 leu2/leu2lys2/lys2 RME1/rme1::LEU2 trp1::hisG/trp1::hisG ura3/ura3 CNM67-YFP::his5/ CNM67-YFP::his5 CgTRP1-P$_{CNM67}$-CFP::NUD1/ CgTRP1-P$_{CNM67}$-CFP::NUD1*	This study

Strain	Genotype	Source
YS326	*MAT***a**/*MATα ARG4/arg4-NspI his3SK/his3SK ho::LYS2/ho::LYS2 leu2/leu2lys2/lys2 RME1/rme1::LEU2 trp1::hisG/trp1::hisG ura3/ura3 CNM67-YFP::his5/ CNM67-YFP::his5 CgTRP1-P_{MPC54}-CFP::MPC54/ CgTRP1-P_{MPC54}-CFP::MPC54*	This study
YS353	*MAT***a**/*MATα ARG4/arg4-NspI his3SK/his3SK ho::LYS2/ho::LYS2 leu2/leu2lys2/lys2 RME1/rme1::LEU2 trp1::hisG/trp1::hisG ura3/ura3 CNM67-YFP::his5/ CNM67-YFP::his5 CgTRP1-P_{MPC54}-CFP::SPO21/ CgTRP1-P_{MPC54}-CFP::SPO21*	This study
YS395	*MAT***a**/*MATα ARG4/arg4-NspI his3SK/his3SK ho::LYS2/ho::LYS2 leu2/leu2lys2/lys2 RME1/rme1::LEU2 trp1::hisG/trp1::hisG ura3/ura3 CNM67-YFP::his5/ CNM67-YFP::his5 CgTRP1- P_{MPC54}-CFP::SPO74/ CgTRP1- P_{MPC54}-CFP::SPO74*	This study
EMD94	*MAT***a**/*MATα ARG4/arg4-NspI his3SK/his3SK ho::LYS2/ho::LYS2 leu2/leu2lys2/lys2 RME1/rme1::LEU2 trp1::hisG/trp1::hisG ura3/ura3 CNM67-YFP::his5/ CNM67::CFP-CgTRP1*	This study
MND84	*MAT***a**/*MATα ARG4/arg4-NspI his3SK/his3SK ho::LYS2/ho::LYS2 leu2/leu2lys2/lys2 RME1/rme1::LEU2 trp1::hisG/trp1::hisG ura3/ura3 CNM67-YFP::his5/ CNM67-YFP::his5 SPO74::linkerCFP ::his5+/ SPO74::linkerCFP ::his5+*	This study
MND88	*MAT***a**/*MATα ARG4/arg4-NspI his3SK/his3SK ho::LYS2/ho::LYS2 leu2/leu2lys2/lys2 RME1/rme1::LEU2 trp1::hisG/trp1::hisG ura3/ura3 CNM67-YFP::his5/ CNM67-YFP::his5 MPC54::CFP-CgTRP1 /MPC54::CFP-CgTRP1*	This study
AN317	*MAT***a**/*MATα ARG4/arg4-NspI his3SK/his3SK ho::LYS2/ho::LYS2 leu2/leu2lys2/lys2 RME1/rme1::LEU2 trp1::hisG/trp1::hisG ura3/ura3 CNM67-YFP::his5/CNM67-YFP::his5 SPO21-CFP::his5/ SPO21-CFP::his5*	This study

Strain	Genotype	Source
MND85	*MAT***a**/*MATα ARG4/arg4-NspI his3SK/his3SK ho::LYS2/ho::LYS2 leu2/leu2lys2/lys2 RME1/rme1::LEU2 trp1::hisG/trp1::hisG ura3/ura3 CNM67-YFP::his5/ CNM67-YFP::his5 NUD1-CFP::his5/ NUD1-CFP::his5*	This study
YS167	*MAT***a**/*MATα ARG4/arg4-NspI his3SK/his3SK ho::LYS2/ho::LYS2 leu2/leu2lys2/lys2 RME1/rme1::LEU2 trp1::hisG/trp1::hisG ura3/ura3 NUD1::YFP::his5/ NUD1::YFP::his5 CgTRP1-P_{CNM67}-CFP::CNM67/ CgTRP1-P_{CNM67}-CFP::CNM67*	This study
EMD93	*MAT***a**/*MATα ARG4/arg4-NspI his3SK/his3SK ho::LYS2/ho::LYS2 leu2/leu2lys2/lys2 RME1/rme1::LEU2 trp1::hisG/trp1::hisG ura3/ura3 NUD1::YFP::his5/ CgTRP1-P_{CNM67}-CFP::NUD1*	This study
YS319	*MAT***a**/*MATα ARG4/arg4-NspI his3SK/his3SK ho::LYS2/ho::LYS2 leu2/leu2lys2/lys2 RME1/rme1::LEU2 trp1::hisG/trp1::hisG ura3/ura3 NUD1::YFP::his5/ NUD1::YFP::his5 CgTRP1-P_{MPC54}-CFP::MPC54/ CgTRP1-P_{MPC54}-CFP::MPC54*	This study
YS356	*MAT***a**/*MATα ARG4/arg4-NspI his3SK/his3SK ho::LYS2/ho::LYS2 leu2/leu2lys2/lys2 RME1/rme1::LEU2 trp1::hisG/trp1::hisG ura3/ura3 NUD1::YFP::his5/ NUD1::YFP::his5 CgTRP1-P_{MPC54}-CFP::SPO21/ CgTRP1-P_{MPC54}-CFP::SPO21*	This study
YS398	*MAT***a**/*MATα ARG4/arg4-NspI his3SK/his3SK ho::LYS2/ho::LYS2 leu2/leu2lys2/lys2 RME1/rme1::LEU2 trp1::hisG/trp1::hisG ura3/ura3 NUD1::YFP::his5/ NUD1::YFP::his5 CgTRP1- P_{MPC54}-CFP::SPO74/ CgTRP1- P_{MPC54}-CFP::SPO74*	This study

Strain	Genotype	Source
EMD90	*MAT***a**/*MATα ARG4/arg4-NspI his3SK/his3SK ho::LYS2/ho::LYS2 leu2/leu2lys2/lys2 RME1/rme1::LEU2 trp1::hisG/trp1::hisG ura3/ura3 NUD1::YFP::his5+/ NUD1-CFP::his5+*	This study
MND86	*MAT***a**/*MATα ARG4/arg4-NspI his3SK/his3SK ho::LYS2/ho::LYS2 leu2/leu2lys2/lys2 RME1/rme1::LEU2 trp1::hisG/trp1::hisG ura3/ura3 NUD1::YFP::his5+/ NUD1::YFP::his5+ SPO21-CFP::his5+/ SPO21-CFP::his+5*	This study
AN330	*MAT***a**/*MATα ARG4/arg4-NspI his3SK/his3SK ho::LYS2/ho::LYS2 leu2/leu2lys2/lys2 RME1/rme1::LEU2 trp1::hisG/trp1::hisG ura3/ura3 NUD1::YFP::his5+/NUD1::YFP::his5+ SPO74::linkerCFP ::his5+/SPO74::linkerCFP ::his5+*	This study
YS164	*MAT***a**/*MATα ARG4/arg4-NspI his3SK/his3SK ho::LYS2/ho::LYS2 leu2/leu2lys2/lys2 RME1/rme1::LEU2 trp1::hisG/trp1::hisG ura3/ura3 MPC54-YFP::his5/MPC54-YFP::his5 CgTRP1-P_{CNM67}-CFP::CNM67/ CgTRP1-P_{CNM67}-CFP::CNM67*	This study
YS371	*MAT***a**/*MATα ARG4/arg4-NspI his3SK/his3SK ho::LYS2/ho::LYS2 leu2/leu2lys2/lys2 RME1/rme1::LEU2 trp1::hisG/trp1::hisG ura3/ura3 MPC54-YFP::his5/MPC54-YFP::his5 CgTRP1-P_{CNM67}-CFP::NUD1/ CgTRP1-P_{CNM67}-CFP::NUD1*	This study
YS359	*MAT***a**/*MATα ARG4/arg4-NspI his3SK/his3SK ho::LYS2/ho::LYS2 leu2/leu2lys2/lys2 RME1/rme1::LEU2 trp1::hisG/trp1::hisG ura3/ura3 MPC54-YFP::his5+/MPC54-YFP::his5+ CgTRP1-P_{MPC54}-CFP::SPO21/ CgTRP1-P_{MPC54}-CFP::SPO21*	This study
EMD104	*MAT***a**/*MATα ARG4/arg4-NspI his3SK/his3SK ho::LYS2/ho::LYS2 leu2/leu2lys2/lys2 RME1/rme1::LEU2 trp1::hisG/trp1::hisG ura3/ura3 MPC54-YFP::his5+/ MPC54::CFP-CgTRP1*	This study

Strain	Genotype	Source
YS401	*MAT***a**/*MAT*α *ARG4/arg4-NspI his3SK/his3SK ho::LYS2/ho::LYS2 leu2/leu2lys2/lys2 RME1/rme1::LEU2 trp1::hisG/trp1::hisG ura3/ura3 MPC54-YFP::his5+/ MPC54-YFP::his5+ CgTRP1- P $_{MPC54}$-CFP::SPO74/ CgTRP1- P $_{MPC54}$-CFP::SPO74*	This study
AN314	*MAT***a**/*MAT*α *ARG4/arg4-NspI his3SK/his3SK ho::LYS2/ho::LYS2 leu2/leu2lys2/lys2 RME1/rme1::LEU2 trp1::hisG/trp1::hisG ura3/ura3 MPC54-YFP::his5+/ MPC54-YFP::his5+ NUD1-CFP::his5+/ NUD1-CFP::his5+*	This study
AN310	*MAT***a**/*MAT*α *ARG4/arg4-NspI his3SK/his3SK ho::LYS2/ho::LYS2 leu2/leu2lys2/lys2 RME1/rme1::LEU2 trp1::hisG/trp1::hisG ura3/ura3 MPC54-YFP::his5+/ MPC54-YFP::his5+ SPO21-CFP::his5+/ SPO21-CFP::his5+*	This study
KBD5	*MAT***a**/*MAT*α *ARG4/arg4-NspI his3SK/his3SK ho::LYS2/ho::LYS2 leu2/leu2lys2/lys2 RME1/rme1::LEU2 trp1::hisG/trp1::hisG ura3/ura3 MPC54-YFP::his5+/ MPC54-YFP::his5+ SPO74::linkerCFP ::his5+/ SPO74::linkerCFP ::his5+*	This study
YS170	*MAT***a**/*MAT*α *ARG4/arg4-NspI his3SK/his3SK ho::LYS2/ho::LYS2 leu2/leu2lys2/lys2 RME1/rme1::LEU2 trp1::hisG/trp1::hisG ura3/ura3 SPO21::YFP-CgTRP/ SPO21::YFP-CgTRP1 CgTRP1-P$_{CNM67}$-CFP::CNM67/ CgTRP1-P$_{CNM67}$-CFP::CNM67*	This study
YS377	*MAT***a**/*MAT*α *ARG4/arg4-NspI his3SK/his3SK ho::LYS2/ho::LYS2 leu2/leu2lys2/lys2 RME1/rme1::LEU2 trp1::hisG/trp1::hisG ura3/ura3 SPO21::YFP-CgTRP/ SPO21::YFP-CgTRP1 CgTRP1-P$_{CNM67}$-CFP::NUD1/ CgTRP1-P$_{CNM67}$-CFP::NUD1*	This study

Strain	Genotype	Source
YS329	*MAT***a**/*MATα ARG4/arg4-NspI his3SK/his3SK ho::LYS2/ho::LYS2 leu2/leu2lys2/lys2 RME1/rme1::LEU2 trp1::hisG/trp1::hisG ura3/ura3 SPO21::YFP-CgTRP/ SPO21::YFP-CgTRP1 CgTRP1-P_{MPC54}-CFP::MPC54/ CgTRP1-P_{MPC54}-CFP::MPC54*	This study
EMD101	*MAT***a**/*MATα ARG4/arg4-NspI his3SK/his3SK ho::LYS2/ho::LYS2 leu2/leu2lys2/lys2 RME1/rme1::LEU2 trp1::hisG/trp1::hisG ura3/ura3 SPO21::YFP-CgTRP/ CgTRP1-P_{MPC54}-CFP::SPO21*	This study
YS404	*MAT***a**/*MATα ARG4/arg4-NspI his3SK/his3SK ho::LYS2/ho::LYS2 leu2/leu2lys2/lys2 RME1/rme1::LEU2 trp1::hisG/trp1::hisG ura3/ura3 SPO21::YFP-CgTRP/ SPO21::YFP-CgTRP1 CgTRP1- P_{MPC54}-CFP::SPO74/ CgTRP1- P_{MPC54}-CFP::SPO74*	This study
MND117	*MAT***a**/*MATα ARG4/arg4-NspI his3SK/his3SK ho::LYS2/ho::LYS2 leu2/leu2lys2/lys2 RME1/rme1::LEU2 trp1::hisG/trp1::hisG ura3/ura3 SPO21::YFP-CgTRP/ SPO21::YFP-CgTRP1 NUD1-CFP::his5/ NUD1-CFP::his5*	This study
MND116	*MAT***a**/*MATα ARG4/arg4-NspI his3SK/his3SK ho::LYS2/ho::LYS2 leu2/leu2lys2/lys2 RME1/rme1::LEU2 trp1::hisG/trp1::hisG ura3/ura3 SPO21::YFP-CgTRP/ SPO21::YFP-CgTRP1 MPC54::CFP-CgTRP1 /MPC54::CFP-CgTRP1*	This study
EMD98	*MAT***a**/*MATα ARG4/arg4-NspI his3SK/his3SK ho::LYS2/ho::LYS2 leu2/leu2lys2/lys2 RME1/rme1::LEU2 trp1::hisG/trp1::hisG ura3/ura3 SPO21::YFP-CgTRP/ SPO21-CFP::his5*	This study
MND120	*MAT***a**/*MATα ARG4/arg4-NspI his3SK/his3SK ho::LYS2/ho::LYS2 leu2/leu2lys2/lys2 RME1/rme1::LEU2 trp1::hisG/trp1::hisG ura3/ura3 SPO21::YFP-CgTRP/ SPO21::YFP-CgTRP1 SPO74::linkerCFP ::his5+/SPO74::linkerCFP ::his5+*	This study

Strain	Genotype	Source
YS173	*MAT***a**/*MATα ARG4/arg4-NspI his3SK/his3SK ho::LYS2/ho::LYS2 leu2/leu2lys2/lys2 RME1/rme1::LEU2 trp1::hisG/trp1::hisG ura3/ura3 SPO74::*YFP-*HIS3MX6 /SPO74::*YFP-*HIS3MX6 CgTRP1-*P_{CNM67}*-CFP::CNM67/ CgTRP1-*P_{CNM67}*-CFP::CNM67*	This study
YS380	*MAT***a**/*MATα ARG4/arg4-NspI his3SK/his3SK ho::LYS2/ho::LYS2 leu2/leu2lys2/lys2 RME1/rme1::LEU2 trp1::hisG/trp1::hisG ura3/ura3 SPO74::*YFP-*HIS3MX6 /SPO74::*YFP-*HIS3MX6 KlURA3-*P_{CNM67}*-YFP::NUD1/ KlURA3-*P_{CNM67}*-YFP::NUD1*	This study
YS322	*MAT***a**/*MATα ARG4/arg4-NspI his3SK/his3SK ho::LYS2/ho::LYS2 leu2/leu2lys2/lys2 RME1/rme1::LEU2 trp1::hisG/trp1::hisG ura3/ura3 SPO74::*YFP-*HIS3MX6 /SPO74::*YFP-*HIS3MX6 CgTRP1-*P_{MPC54}*-CFP::MPC54/ CgTRP1-*P_{MPC54}*-CFP::MPC54*	This study
YS350	*MAT***a**/*MATα ARG4/arg4-NspI his3SK/his3SK ho::LYS2/ho::LYS2 leu2/leu2lys2/lys2 RME1/rme1::LEU2 trp1::hisG/trp1::hisG ura3/ura3 SPO74::*YFP-*HIS3MX6 /SPO74::*YFP-*HIS3MX6 CgTRP1-*P_{MPC54}*-CFP::SPO21/ CgTRP1-*P_{MPC54}*-CFP::SPO21*	This study
EMD79	*MAT***a**/*MATα ARG4/arg4-NspI his3SK/his3SK ho::LYS2/ho::LYS2 leu2/leu2lys2/lys2 RME1/rme1::LEU2 trp1::hisG/trp1::hisG ura3/ura3 SPO74::*YFP-*HIS3MX6 / SPO74::CgTRP1-*P_{MPC54}*-CFP::SPO74*	This study
MND119	*MAT***a**/*MATα ARG4/arg4-NspI his3SK/his3SK ho::LYS2/ho::LYS2 leu2/leu2lys2/lys2 RME1/rme1::LEU2 trp1::hisG/trp1::hisG ura3/ura3 SPO74::*YFP-*HIS3MX6 / SPO74::*YFP-*HIS3MX6 NUD1-CFP::his5/NUD1-CFP::his5*	This study

Strain	Genotype	Source
MND118	*MAT***a**/*MATα ARG4/arg4-NspI his3SK/his3SK ho::LYS2/ho::LYS2 leu2/leu2lys2/lys2 RME1/rme1::LEU2 trp1::hisG/trp1::hisG ura3/ura3 SPO74::*YFP-*HIS3MX6* / *SPO74::*YFP-*HIS3MX6 MPC54::CFP-CgTRP1* / *MPC54::CFP-CgTRP1*	This study
MND83	*MAT***a**/*MATα ARG4/arg4-NspI his3SK/his3SK ho::LYS2/ho::LYS2 leu2/leu2lys2/lys2 RME1/rme1::LEU2 trp1::hisG/trp1::hisG ura3/ura3 SPO74::*YFP-*HIS3MX6* / *SPO74::*YFP-*HIS3MX6 SPO21-CFP::his5/ SPO21-CFP::his5*	This study
EMD102	*MAT***a**/*MATα ARG4/arg4-NspI his3SK/his3SK ho::LYS2/ho::LYS2 leu2/leu2lys2/lys2 RME1/rme1::LEU2 trp1::hisG/trp1::hisG ura3/ura3 SPO74::*YFP-*HIS3MX6* / *SPO74::linkerCFP ::his5+*	This study

Table 2-5. Plasmids used in this study

Plasmid	Relevant features	Source
pFA6a-GFP (S65T)-HIS3MX6	*GFP(S65T)-T_{ADH}-HIS3MX6*	(Wach et al., 1997)
pFA6a-yEGFP-HIS3MX6	*yEGFP-HIS3MX6*	(Nickas and Neiman, 2002)
pDH3	*CFP*	Yeast Resource Center
pDH5	*YFP*	Yeast Resource Center
pFA6a-CFP-HIS3MX6	*CFP- T_{ADH}-HIS3MX6*	(Nickas and Neiman, 2002)
pFA6a-YFP-HIS3MX6	*YFP- T_{ADH}-HIS3MX6*	This study
pFA6a-CgTRP1	*C.g.TRP1*	This study
pCgW	*C.g.TRP1*	Linda Huang
pFA6a-TRP1	*C.g.TRP1*	(Longtine et al., 1998)
pFA6a-KlURA3	*K.l.URA3*	This study
pKlU	*K.l.URA3*	M. Nickas
pFA6a-CFP-CgTRP1	*CFP- T_{ADH}-HIS3MX6*	This study
pFA6a-YFP-KlURA3	*YFP- T_{ADH}-HIS3MX6*	This study
pMN101	*C.g.TRP1-P_{GAL} –GFP(S65T)- T_{ADH}*	This study
pMN102	*K.l.URA3-P_{GAL} –GFP(S65T)- T_{ADH}*	This study
pMN103	*C.g.TRP1-P_{CNM67} –GFP(S65T)- T_{ADH}*	This study
pMN104	*K.l.URA3- P_{CNM67} –GFP(S65T)- T_{ADH}*	This study
pMN105	*C.g.TRP1-P_{MPC54} –GFP(S65T)- T_{ADH}*	This study
pMN106	*K.l.URA3- P_{MPC54} –GFP(S65T)- T_{ADH}*	This study
pMN107	*C.g.TRP1-P_{CNM67} –CFP- T_{ADH}*	This study
pMN108	*K.l.URA3- P_{CNM67} –YFP- T_{ADH}*	This study
pMN109	*C.g.TRP1-P_{MPC54} –CFP- T_{ADH}*	This study
pMN110	*K.l.URA3- P_{MPC54} –YFP- T_{ADH}*	This study
424-SPO74	2µ *SPO74*	This study
424-SPO21-SPO74	2µ *SPO21-SPO74*	M. Nickas
316-SPO74	*CEN SPO74*	This study
316- SPO74-145	*CEN SPO74-145*	This study
316- SPO74-180	*CEN SPO74-180*	This study

Plasmid	Relevant features	Source
316- SPO74-180	*CEN SPO74-180*	This study
316-SPO74-243	*CEN SPO74-243*	This study
316- SPO74-267	*CEN SPO74-267*	This study
426- SPO74	2µ *SPO74*	This study
426- SPO74-145	2µ *SPO74-145*	This study
426- SPO74-180	2µ *SPO74-180*	This study
426- SPO74-243	2µ *SPO74-243*	This study
304- SPO74	integrating *SPO74*	This study
304- SPO74-145	integrating *SPO74-145*	This study
304- SPO74-180	integrating *SPO74-180*	This study
304- SPO74-243	integrating *SPO74-243*	This study
314-MPC54-RFP	*CEN MPC54-RFP*	H. Nakanishi
423-MPC54-RFP	2µ *MPC54-RFP*	H. Nakanishi
316-MPC54-RFP	*CEN MPC54-RFP*	This study
316- MPC54-RFP	*CEN MPC54-RFP*	This study
316- MPC54-40-RFP	*CEN MPC54-40-RFP*	This study
316- MPC54-47-RFP	*CEN MPC54-47-RFP*	This study
316- MPC54-118-RFP	*CEN MPC54-118-RFP*	This study
316- MPC54-123-RFP	*CEN MPC54-123-RFP*	This study
316- MPC54-119-RFP	*CEN MPC54-119-RFP*	This study
316- MPC54-145-RFP	*CEN MPC54-145-RFP*	This study
426- MPC54-RFP	2µ *MPC54-RFP*	This study
426- MPC54-40-RFP	2µ *MPC54-40-RFP*	This study
426- MPC54-47-RFP	2µ *MPC54-47-RFP*	This study
426- MPC54-118-RFP	2µ *MPC54-118-RFP*	This study
426- MPC54-119-RFP	2µ *MPC54-119-RFP*	This study
426- MPC54-145-RFP	2µ *MPC54-145-RFP*	This study
304- MPC54-RFP	integrating *MPC54-RFP*	This study

Plasmid	Relevant features	Source
304- MPC54-40-RFP	integrating *MPC54-40-RFP*	This study
304- MPC54-47-RFP	integrating *MPC54-47-RFP*	This study
304- MPC54-118-RFP	integrating *MPC54-118-RFP*	This study
304- MPC54-119-RFP	integrating *MPC54-119-RFP*	This study
304- MPC54-145-RFP	integrating *MPC54-145-RFP*	This study
424-RFP-SPO20$^{51-91}$	2µ P_{TEF2}-Spo20$^{51-91}$-RFP	(Nakanishi *et al.*, 2006)
424-DTR1-GFP	2µ *DTR1-GFP*	(Nakanishi *et al.*, 2006)
314-SPO21-GFP	*CEN SPO21-GFP*	H. Tachikawa
314-SPO74-GFP	*CEN SPO74-GFP*	(Nickas et al., 2003)
426-SPO14-GFP	2µ *SPO14-GFP*	(Rudge et al., 1998)
pLexA$_{202}$-GLC7	*LexA-GLC7*	(Tu and Carlson, 1994)
pLexA-MPC54	*LexA-MPC54*	M. Nickas
pLexA-SPO21	*LexA-SPO21*	M. Nickas
pSTT91- MPC54^{WT}(1-200)	*LexA- MPC54^{WT}(1-200)*	This study
pSTT91- MPC54-40(1-200)	*LexA- MPC54-40(1-200)*	This study
pSTT91- MPC54-47(1-200)	*LexA- MPC54-47(1-200)*	This study
pSTT91- MPC54-118(1-200)	*LexA- MPC54-118(1-200)*	This study
pSTT91- MPC54-119(1-200)	*LexA- MPC54-119(1-200)*	This study
pSTT91- MPC54-145(1-200)	*LexA- MPC54-145(1-200)*	This study

Table 2-6: Oligonucleotides used in this study

Primer	Sequence	Function
MNO155	gcg gcg TTA ATT AAc cgT Acg cTg cAg gTc gAc ggA	S3 from Knop Series Introduces PacI site
MNO156	gcg gcg ggc gcg ccT ggg ccT ccA TgT cgc Tgg	*KAN* & *HIS* primer from Knop series Introduces AscI site
MNO162	gcg gcg AgA TcTcA cAg gAA AcA GcT ATg Acc	Knf from Huang series Introdues BglII site
MNO163	GCG gcg gttt aaa cgt tgt aaa acg acg gcc agt	Knr from Huang series Introduces PmeI site
MNO146	TCT ACT TGA C TT TGG CTG GTA TTT AAA CAC AAG TAA GAG AAG CAT CAA ACC GGA TCC CCG GGT TAA TTA A	F1 from Longtine series nt -50 to -1 of *DON1*
MNO147	GAG CCC AAA CGC ACT TTG CCG AAA GAG TTA ATA AAC ATT ACC GCT ATA CA GAA TTC GAG CTC GTT TAA AC	R1 from Longtine series nt 1599 to 1648 of *DON1*
MNO226	GCG GCG AGA TCT TTC TTA ACA ATT GCG TAT ATA	nt -300 to-280 of *CNM67* Introduces BglII site
MNO227	gcg gcg gtt aat taa GAT GTA AAG ACC TGT CAC	nt -21 to -1 of *CNM67* Introduces PacI site
MNO228	GCG GCG AGA TCT TTT TCG ATG CTA TTT TGA TAA	nt -300 to -280 of *MPC54* Introduces BglII site
MNO229	gcg gcg gtt aat taa GGC CTT ATA CGA GAA GTT ACA	nt -21 to -1 of *MPC54* Introduces PacI site
MNO224	GcG GCG gTT AAT TAA ATG TCT AAA GGT GAA GAA TTA TTC	nt 4 to 24 of *yEGFP* from pYM12 Introduces START
MNO225	GCG GCG GGG CGC GCC TCA GGC GCC AGC TCC AGC CCC AGC TCC AGC GCC AGC ACC TTT GTA TAG TTC ATC CAT	nt 703 to 720 of *GFP(S65T)* Introduces linker and STOP Introduces AscI site

Primer	Sequence	Function
EMO 1	ATT Tcc AcT gcA ccA gcc AAg gcA cAg Agg ccA	Introduces mutation SxYxG:AxAxA in *SPO74*
EMO 2	Tgg ccT cTg Tgc cTT ggc Tgg Tgc AgT ggA AAT	Introduces mutation SxYxG:AxAxA in *SPO74*
EMO 3	cTA AAA Acc AAc gcg gcT AcA gcc ATT AAA AAA gAg	Introduces mutation LLxY:AAxA in *SPO74*
EMO 4	cTc TTT TTT AAT ggc TgT Agc cgc gTT ggT TTT Tag	Introduces mutation LLxY:AAxA in *SPO74*
EMO 5	AAc TcT TTg cTA gcT gcA gcg cTA gcA gTT cgT	Introduces mutation LNREL:LAAAL in *SPO74*
EMO 6	Acg AAc Tgc TAg cgc Tgc Agc TAg cAA AgA gTT	Introduces mutation LNREL:LAAAL in *SPO74*
EMO 7	Tcc ATT Agg gAT gcT AgA AAT gcA cTT TTg ccA	Introduces mutation FxxP:AxxA in *SPO74*
EMO 8	Tgg cAA AAg Tgc ATT TcT Agc ATc ccT AAT ggA	Introduces mutation FxxP:AxxA in *SPO74*
EMO30	AAg ccA AAT gTA gcT gcA gcA gAT gAT gAT gTT	Introduces mutation RFG:AAA in *MPC54*
EMO31	AAc ATc ATc ATc Tgc Tgc Agc TAc ATT Tgg cTT	Introduces mutation RFG:AAA in *MPC54*
EMO32	gAT gAT gAT gTT gcT gcA gcA gAT cAA AgA AAA	Introduces mutation NIF:AAA in *MPC54*
EMO33	TTT TcT TTg ATc Tgc Tgc Agc AAc ATc ATc ATc	Introduces mutation NIF:AAA in *MPC54*
EMO34	gAc gcg gTT AAc gcT gcA gcA gcg cTT TgT AAc	Introduces mutation RCY:AAA in *MPC54*
EMO35	gTT AcA AAg cgc Tgc Tgc Agc gTT AAc cgc gTc	Introduces mutation RCY:AAA in *MPC54*
EMO36	Tgc TAT gcg cTT gcT gcA gcg gcA AcT AAg cAT gTA	Introduces mutation CNIP:AAAA in *MPC54*

Primer	Sequence	Function
EMO37	TAc ATg cTT AgT Tgc cgc Tgc Agc AAg cgc ATA gcA	Introduces mutation CNIP:AAAA in *MPC54*
EMO38	gcg gTT AAc cgT gcT gcA gcg cTT gcT gcT ATT ccA AcT AAg	Introduces mutation CYxxCN:AAxxAA in *MPC54*
EMO39	cTT AgT Tgg AAT Agc Agc AAg cgc Tgc Agc Acg gTT AAc cgc	Introduces mutation CYxxCN:AAxxAA in *MPC54*
EMO40	Acg TTc gAA Acg gcc gcT gTA gcg gcA Acc cAT gAA Acg	Introduces mutation LxxGI:AxxAA in *MPC54*
EMO41	cgT TTc ATg ggT Tgc cgc TAc Agc ggc cgT TTc gAA cgT	Introduces mutation LxxGI:AxxAA in *MPC54*
EMO64	gcg gcg CTC GAG TcA cAA ATT TTg cTT TgT	Introduces XhoI 600 nt into *MPC54*
EMO 75	gcg gcg ggA Tcc cc Atg ccA gAA	Introduces BamHI before START of *MPC54*

Chapter 3: Membrane assembly modulates the stability of the meiotic spindle pole body

Introduction

Diploid budding yeast cells that are cultured in the absence of nitrogen and the presence of a nonfermentable carbon source are induced to undergo sporulation (Esposito, 1981). During spore formation, prospore membranes capture daughter nuclei at the end of the meiosis, leading to the formation of four autonomous spores within the mother cell (Moens and Rapport, 1971; Neiman, 1998). At the onset of prospore membrane formation, post-Golgi derived vesicles accumulate at the spindle pole bodies where they will coalesce to form the prospore membrane (Neiman, 1998).

During Meiosis II, the prospore membrane associates with the nucleus through its attachment to a spindle pole body (Moens and Rapport, 1971; Rout and Kilmartin, 1990). During mitosis and Meiosis I, the cytoplasmic face, or outer plaque, of the spindle pole body nucleates cytoplasmic microtubules. At the onset of Meiosis II, the MOP undergoes structural and compositional changes, so that the MOP now serves as the initiation site of prospore membrane growth (Moens and Rapport, 1971; Knop and Strasser, 2000).

The MOP is composed primarily of three meiosis-specific proteins: Spo21p, Spo74p, and Mpc54p (Knop and Strasser, 2000; Bajgier *et al.*, 2001; Nickas *et al.*, 2003). These three proteins are required for the formation of the MOP and for prospore membrane initiation (Knop and Strasser, 2000; Bajgier *et al.*, 2001; Nickas *et al.*, 2003). In this thesis, I have shown that Mpc54p is involved in vesicle docking at the MOP, and that this docking is a required prerequisite to vesicle fusion.

Besides Mpc54p, Spo21p, and Spo74p, the constitutive spindle pole body proteins Cnm67p and Nud1p are also found on the cytoplasmic side of the spindle pole body during Meiosis II (Bullitt *et al.*, 1997; Adams and Kilmartin, 1999; Schaerer *et al.*, 2001). Ady4p is a unique meiotically-induced MOP component. Like Spo21p, Spo74p, and Mpc54p, it also promotes wild-type MOP assembly and prospore membrane formation, but, unlike the other three components, Ady4p is not required for either process. Ady4p

is an auxiliary MOP protein whose deletion leads to a variable numbers of prospore membranes with heterogeneous morphologies (Nickas *et al.*, 2003).

In an earlier study (Taxis *et al.*, 2005), fluorescence recovery after photobleaching (FRAP) was used to show that the MOP is a stable structure with little exchange between incorporated and soluble subunits. In this technique a laser is used to bleach the signal from a fluorescently tagged MOP component at a single spindle pole body. The rate of fluorescence recovery, caused by exchange of bleached proteins with unbleached proteins, is then monitored by time-lapse videomicroscopy. In this study, I report that the stability of the MOP requires the formation of an overlying prospore membrane. MOP proteins display elevated rates of fluorescence recovery in mutants where unfused vesicles accumulate on the MOP surface. This requirement for the membrane applies only to the MOP as constitutive spindle pole body components display little exchange under either condition. This effect is not simply due to steric hindrance as fluorescently tagged Ady4p exchanges rapidly into the MOP even in the presence of the prospore membrane. Additionally, I find that Ady4p enhances the stability of different MOP components before and after the fusion of the precursor vesicles. These results suggest a reorganization of this vesicle docking complex coincident with vesicle fusion.

Materials Methods

Yeast strains and media

Standard *S. cerevisiae* genetic methods and media were used (Rose, 1990). The strains used in this study are listed in Table 3-1. All strains used were in the fast-sporulating SK-1 strain background (Kane and Roth, 1974). Gene insertions and replacements were performed using cassettes amplified by PCR (Longtine *et al.*, 1998) and verified by PCR or phenotype. EMD85 (*SPC42-GFP*/*SPC42-GFP*) was constructed by crossing AN117-4B with ESM440, a *MAT**a** SPC42-GFP* haploid obtained from E. Scheibel (Pereira *et al.*, 2001), followed by mating of two of the *SPC42-GFP* segregants. EMD3 (*sso1*Δ*/sso1*Δ *SPC42-GFP*/*SPC42-GFP*) was made by crossing HI1, a *MAT*α *sso1*Δ haploid (Nakanishi *et al.*, 2006), with ESM440, followed by mating of two of the *sso1*Δ *SPC42-GFP* segregants. EMD4 (*CNM67-GFP/CNM67-GFP*) was made by inserting *GFP-HIS3MX6* at the 3' end of the *CNM67* open reading frame (ORF) of AN117-16D and AN117-4B (Neiman *et al.*, 2000) and then mating the resulting haploids. EMD6 (*sso1*Δ*/sso1*Δ *CNM67-GFP/CNM67-GFP*) was constructed by crossing HI1 with the *MAT**a** CNM67-GFP* haploid, followed by mating two of the *sso1*Δ*CNM67-GFP* segregants. To construct EMD10 (*sso1*Δ*/sso1*Δ *ady4*Δ*/ady4*Δ), HI1 was crossed to an *ady4*Δ haploid, AN1119 (Nickas *et al.*, 2003), followed by mating of two of the *sso1*Δ*ady4*Δ segregants. HI60 (*spo14*Δ*/spo14*Δ) was constructed as follows: an XbaI-ClaI DNA fragment from pKR466 (Rose *et al.*, 1995)was used for targeted *SPO14* disruption in two haploid wild-type cells, AN117-4B and AN117-16D. The resulting *MAT*α haploid was then exposed to 5-FOA and a resistant *spo14*Δ:*ura3* haploid was isolated. This haploid was mated to the *MAT**a** spo14*Δ:*URA3* haploid and the resulting diploid was plated on 5-FOA medium to select for *spo14*Δ*:ura3/spo14*Δ*:ura3* convertants. To construct MND46 (*ady4*Δ*/ady4*Δ *MPC54-GFP/MPC54-GFP*), the following chromosomal insertions were made in AN117-16D and AN117-4B, respectively: *HIS3MX6* replacing the *ADY4* ORF and *GFP-HIS3MX6* at the 3' end of the *MPC54* ORF. The resulting haploids were crossed, followed by the mating of two of the *ady4*Δ *MPC54-GFP* segregants. MND48 was constructed similarly, but with *GFP-HISMX6* inserted into the 3' end of the *SPO21* ORF of AN117-4B.

Plasmids

The plasmids used in this study are listed in Table 3-2. pRS426TEF-mRFP was constructed by cloning a HindIII-XhoI fragment carrying the gene for monomeric red fluorescent protein (*RFP*) (Campbell *et al.*, 2002) into similarly digested pRS426TEF (Mumberg *et al.*, 1995). The *RFP* gene was amplified by PCR using pTiKmRFP (Gao *et al.*, 2005) as a template and YSO33 and HNO944 as primers (primer sequences are available upon request). pRS424-DTR1-RFP was constructed by replacing the *GFP* coding region in pRS424-DTR1-GFP (Nakanishi *et al.*, 2006) with the gene for *RFP* using an EcoRI-XhoI fragment carrying the *RFP* of pRS426TEF-mRFP. pRS424-ADY4-DTR1-RFP was constructed by first amplifying *ADY4* by PCR using AN117-16D genomic DNA as template and EMO76 and EMO78 as primers. This PCR product was digested with SacI and NotI and cloned into similarly digested pRS424-DTR1-RFP. To generate pRS426-ADY4-DTR1-RFP, a SacI-KpnI fragment containing *ADY4* and *DTR1-RFP* from pRS424-ADY4-DTR1-RFP was cloned into similarly digested pRS426. pRS314-SPO21-GFP was a gift from H. Tachikawa.

Sporulation assays

Cells were induced to sporulate in liquid medium essentially as described previously (Neiman, 1998). Briefly, cells were cultured to saturation in either rich medium or synthetic medium selective for plasmids, cultured overnight to mid-log phase in yeast extract-peptone-acetate medium, and transferred to 2% potassium acetate at a concentration of 3 X 10^7 cells/ml.

Live cell imaging

Cells were induced to sporulate in liquid medium and were analyzed in early Meiosis II. Glass-bottom tissue culture dishes (MatTek Corporation, Ashland, MA, USA) were prepared with agarose (1% KOAc, 2% agarose, 2 mM $NaHCO_3$). A square of agarose was cut from the agarose plate so that the glass bottom was exposed. 10 ul of cell culture was placed on the face of the agarose square that would be flush with the glass bottom of the dish. The agarose square was then replaced. The time series images for all photobleaching techniques were performed using a Zeiss LSM 510 META NLO two-

photon laser scanning microscope system. The culture plates were mounted on a Zeiss inverted Axiovert 200M microscope. All analyses were performed using a 100X oil objective (Plan-Neofluar, numerical aperture 1.46). GFP was excited with an argon laser at 488 nm, and emission was collected using a 505 nm long pass filter. During Meiosis II, GFP-tagged MOP components localize to the four spindle pole bodies, forming four GFP foci (Knop and Strasser, 2000). For each cell analyzed by FRAP, a single GFP-labeled MOP was bleached with 100% power of an argon laser at 488 nm for 10 s. The recovery of the bleached spindle pole body was measured over a period of five minutes. Images were acquired using LSM 510 Meta version 3.2 imaging software. The images were processed and presented using Adobe Photoshop. The fluorescence intensity of the bleached area was quantified using the mean region of interest (ROI) function of the LSM Imaging software and graphically depicted using Microsoft Excel. The initial fluorescence was normalized to 100% fluorescence. The first time point after bleaching was designated time zero and was normalized to 0% fluorescence. Spindle pole bodies are mobile in the cell and occasionally move outside the focal plane. To prevent these focal anomalies from impacting the results, FRAP values that were less than 35% of the time point preceding them were culled. For Ady4-GFP, fluorescence recovered so rapidly in both wild-type and *sso1*Δ cells that time zero did not achieve baseline fluorescence. Time zero was normalized to 0% nonetheless.

Electron microscopy

Cells were prepared for standard transmission electron microscopy as described elsewhere (Straight *et al.*, 2000). Briefly, cells from sporulating cultures were collected by vacuum filtration to form a yeast paste. Cells were then rapidly frozen by high pressure freezing (BAL-TEC HPM-010, Technotrade International, Manchester, NH) and freeze-substituted at -80C in 2% Osmium Tetraoxide plus 0.1% Uranyl Acetate in acetone for 3 days. The cells were gradually warmed to room temperature then infiltrated with Epon/Araldite resin over a period of 5 days. 300 nm sections of embedded cells were cut for electron tomography.

Electron tomography

10 nm colloidal gold (BBI International, Cardiff, UK) used as fiducials was adsorbed to 300 nm thick sections of sporulating cells, which were imaged using a Tecnai TF30 transmission electron microscope (Philips, Eindhoven, the Netherlands). Tilt-series (+/- 60° with a tilt increment of 1°) were acquired using the automated tilt-series acquisition program, SerialEM (Mastronarde, 2005). Tomographic reconstructions were computed by weighted back projection using IMOD (Kremer *et al.*, 1996). Models were generated using IMOD.

Results

The rate of exchange of MOP components depends on the presence of a prospore membrane

Formation of a properly assembled MOP is necessary for prospore membrane formation (Knop and Strasser, 2000; Bajgier *et al.*, 2001; Nickas *et al.*, 2003). FRAP can be used to examine the stability of the MOP structure based on the rate and the degree of exchange of GFP-tagged MOP components (Taxis *et al.*, 2005). Previous FRAP analysis of the MOP led to the conclusion that the MOP is highly stable (Taxis *et al.*, 2005). Since the prospore membrane is in contact with the surface of the MOP, it is possible that the membrane itself has a role in stabilizing the MOP structure.

To examine this possibility, C-terminal GFP fusions to individual MOP components were introduced into wild-type and *sso1*Δ cells. Each of the C-terminal GFP fusions of spindle pole body components used in this paper was determined to be functional based on rescue of sporulation in the corresponding null mutants (data not shown). In the *sso1*Δ mutant, prospore membrane precursor vesicles dock onto the surface of the MOP, but the fusion of these vesicles to create a larger membrane structure is blocked (Nakanishi *et al.*, 2006). FRAP was used to compare the stability of each MOP protein in the two strains in cells determined to be in mid-Meiosis based on the phenotype of their spindle pole bodies (Figure 3-1B). For all three GFP-tagged MOP components, recovery of fluorescence was very low in the presence of a growing prospore membrane, consistent with earlier studies of Mpc54p (Figure 3-1 A, C, and D) (Knop and Strasser, 2000; Taxis *et al.*, 2005). In contrast, all three GFP-tagged MOP components displayed significant recovery of fluorescence in the absence of a prospore membrane (Figure 3-1 A, C, and D). This increased rate of exchange in the absence of the prospore membrane indicates that the apparent structural stability of the MOP depends upon the presence of an overlying prospore membrane.

Cells lacking the phospholipase D enzyme encoded by *SPO14* also accumulate unfused vesicles on the MOP surface similar to *sso1*Δ cells (Riedel *et al.*, 2005; Nakanishi *et al.*, 2006). To ensure that the changes in Mpc54-GFP dynamics seen by FRAP were caused by the lack of prospore membranes in the *sso1*Δ mutant and not as a

result of the absence of *SSO1* per se, FRAP assays were performed in a *spo14*Δ background. The FRAP values for Mpc54-GFP in the *spo14*Δ mutant were similar to those seen in the *sso1*Δ strain (Figure 3-2A). This result demonstrates that the increased rate of exchange is not caused by the absence of *SSO1* and is likely due to the lack of a prospore membrane.

The behavior of constitutive spindle pole body components is unaffected by the absence of the prospore membrane

The core of the spindle pole body is a central plaque composed of a crystal lattice of Spc42p that is embedded in the nuclear envelope (Adams and Kilmartin, 1999; Jaspersen and Winey, 2004; Muller *et al.*, 2005). Cnm67p is a component of both the vegetative and meiotic outer plaques and connects the central plaque to the MOP (Bajgier *et al.*, 2001; Schaerer *et al.*, 2001). To determine if the absence of the prospore membrane also has a destabilizing effect on these more interior spindle pole body components, FRAP measurements were taken of Spc42-GFP and Cnm67-GFP in sporulating wild-type and *sso1*Δ cells. Exchange of Spc42-GFP remained low in both wild-type and *sso1*Δ (Figure 3-2B), suggesting that the central plaque is stable regardless of the status of the prospore membrane. Similar to Spc42-GFP, Cnm67-GFP displayed little exchange in both conditions (Figure 3-2C). These observations indicate that the central plaque and interior layer of the outer plaque are stable whether or not a prospore membrane is present. Thus, the dependence on the prospore membrane for stability is unique to the MOP.

The prospore membrane is not a barrier to the exchange of cytoplasmic proteins

How does the prospore membrane reduce the exchange of MOP components? One simple possibility is that the membrane acts sterically to inhibit exchange. This could result either from the membrane separating the MOP, which is inside the membrane, from a pool of exchangeable proteins in the mother cell cytoplasm, or from the attachment of the membrane to the surface of the MOP physically restricting the photobleached proteins from leaving the MOP. To test whether the prospore membrane blocks the exchange of contents between the presumptive spore and the mother cell

cytoplasms, I used FRAP analysis to examine the exchange of cytosolic proteins localized within the growing prospore membrane.

Sec7p is a Golgi-associated protein that localizes to the cytoplasmic region captured within the growing prospore membrane during Meiosis II (Reinke *et al.*, 2004; Suda *et al.*, 2007). FRAP analysis was performed on wild-type cells co-transformed with plasmids expressing Sec7-GFP and the prospore membrane marker RFP-Spo20$^{51-91}$ (RFP fused to the lipid binding domain of Spo20p (Nakanishi *et al.*, 2004). RFP-labeled prospore membranes that contained Sec7-GFP signals were identified and the area within the prospore membrane was bleached (Figure 3-3B). I observed that Sec7-GFP fluorescence recovered rapidly (Figure 3-3, A and B), demonstrating that Sec7-GFP is able to exchange between the two cytoplasmic regions of the cell. Similar results have been reported monitoring a different cytoplasmic GFP fusion using a fluoresecence loss in photobleaching assay (Diamond *et al.*, 2009). Taken together these results indicate that the prospore membrane does not prevent the exchange of proteins between the mother cytoplasm and the cytoplasm that is captured within the growing prospore membrane.

The prospore membrane does not sterically prevent the exchange of MOP components

Although cytoplasmic proteins are free to exchange, it may be that the prospore membrane specifically obstructs the exchange of MOP components and thereby blocks recovery from photobleaching. Ady4p is a fourth protein of the MOP, though it appears to be a non-essential component as loss of *ADY4* does not block MOP assembly (Nickas *et al.*, 2003). Ady4-GFP was introduced on a plasmid into both wild-type and *sso1*Δ cells and its exchange was examined. In sharp contrast to the other MOP components, Ady4-GFP displayed rapid recovery of fluorescence at the spindle pole body in both in wild-type and *sso1*Δ cells (Figure 3-3, C and D). The ability of Ady4-GFP to exchange even in the presence of a prospore membrane indicates that the prospore membrane does not create an impermeable barrier to the exchange of all MOP components. Together, the Sec7-GFP and Ady4-GFP FRAP results argue against models in which the prospore membrane impedes fluorescence recovery by acting as a passive diffusion barrier.

Increased MOP stability correlates with membrane assembly

The results described suggest that the change in stability of the MOP correlates with membrane assembly. However, it could be that the MOP becomes progressively more stable as the membrane expands. To look more closely at the timing of the change in stability of the MOP, exchange of components was examined in staged wild-type cells. As seen with a fluorescent marker, the prospore membrane expands in a series of distinct morphological stages (Diamond et al., 2009). An initial dot of fluorescence associated with the MOP resolves into a small horseshoe shape and then subsequently expands into larger structures (Figure 3-4A). The transition from dot to horseshoe is thought to mark the change from clustered vesicles to an assembled membrane cap.

Both a prospore membrane marker (RFP-Spo20$^{51-91}$) and GFP-tagged Mpc54 were transformed into wild-type cells. FRAP was performed on MOPs associated with RFP-labeled dots (operationally defined as having a diameter of 0.4 to 0.65 microns) or horseshoes (0.65 to 1.1 microns at their longest point) (Figure 3-4A). Mpc54-GFP fluorescence recovered very slowly in MOPs associated with horseshoe shaped prospore membranes, indicating that the presence of even a small prospore membrane was sufficient to stabilize the MOP (Figure 3-4B). By contrast, Mpc54-GFP fluorescence recovered significantly in MOPs associated with dots, comparable to the level of recovery seen in *sso1*Δ cells (Figure 3-4B). The range of recovery was somewhat broader in wild-type cells with dots than in *sso1*Δ cells. Presumably this is because the dot-staged wild-type cells represent a mixture of MOPs associated with both unfused and newly fused or fusing vesicles. Together these data indicate that the change in MOP stability corresponds with initial formation of the prospore membrane.

Ady4p reduces the rate of exchange of Spo21p and Spo74p in the absence of a prospore membrane

Ady4p is unique among the MOP components in that it is not essential for MOP assembly (Nickas *et al.*, 2003) and that it exchanges rapidly out of the complex (Figure 3-3C). Earlier work reported that in *ady4*Δ cells, MOPs exhibit variable defects suggesting that Ady4p might play a role in stabilizing the MOP structure (Nickas *et al.*, 2003). To examine the role of Ady4p, FRAP measurements were taken for GFP-tagged MOP

components both when *ADY4* was overexpressed and in the absence of *ADY4*. If Ady4p acts as a stabilizing factor then overexpressing Ady4p might rescue the high exchange of MOP components seen in an *sso1*Δ mutant. To identify the cells containing the Ady4p overexpression plasmid, the prospore membrane marker Dtr1-RFP was co-expressed from the same plasmid (pADY4-DTR1-RFP). *ADY4* in this construct was functional as it rescued the sporulation defect of *ady4*Δ cells (data not shown). Individual GFP-tagged MOP components and pADY4-DTR1-RFP were co-transformed into *sso1*Δ cells and the fluorescence recovery of GFP at the spindle pole body was measured in RFP-expressing cells as the cells progressed through Meiosis II. Overexpression of Ady4p reduced the rate and the degree of fluorescence recovery of both Spo21-GFP and Spo74-GFP, although not to wild-type levels (Figure 3-5, A and B). In contrast, Mpc54-GFP exchange was not altered by the overexpression of Ady4p (Figure 3-5C). This result indicates that, prior to vesicle fusion, Ady4p is able to decrease the rate of exchange of Spo74p and Spo21p and does so in a prospore membrane-independent manner.

Ady4p reduces the exchange of Mpc54p during prospore membrane growth

The effect of *ADY4* overexpression suggests that Ady4p might be important in stabilizing Spo21p and Spo74p at the MOP. To examine if the absence of Ady4p increased the rate of exchange of these proteins, FRAP was measured for GFP-tagged MOP components in an *sso1*Δ *ady4*Δ diploid. For all three MOP components the rate of exchange in the double mutant was comparable to the *sso1* single mutant (Figure 3-6A), demonstrating that the loss of *ADY4* had no additive effect on fluorescence recovery. Since it is possible that the high rate of exchange seen in an *sso1*Δ mutant might mask any modest increase caused by the deletion of *ADY4*, the FRAP of GFP-tagged MOP components was then analyzed in *ady4*Δ *SSO1* cells. An *ady4*Δ strain displays heterogeneous MOP and prospore membrane morphologies within a single cell, including some MOPs that lack prospore membranes (Nickas *et al.*, 2003). To ensure that the MOPs examined in the *ady4*Δ background were associated with prospore membranes, and were therefore functional, RFP-Spo20$^{51\text{-}91}$ was expressed in these cells as a prospore membrane marker and only MOPs with associated RFP fluorescence were photobleached (Figure 3-6C). With the prospore membrane present, the absence of *ADY4* had no effect

on the exchange of Spo21-GFP or Spo74-GFP (Figure 3-6D). Both proteins displayed the same limited recovery seen in wild-type cells. By contrast, modest but significant fluorescence recovery of Mpc54-GFP was seen in the *ady4*Δ cells (Figure 3-6B). These findings suggest that Ady4p assists in retaining Mpc54p in MOPs with associated prospore membranes.

The connection between the MOP and the growing prospore membrane is unstable in ady4 mutants

To examine in more detail the effect of Ady4p on MOP structural integrity, 3D EM tomography was used to generate images of the MOP in both wild-type and *ady4*Δ cells. Consistent with earlier thin-section EM studies (Nickas *et al.*, 2003), heterogeneous MOP defects were seen in the *ady4*Δ cells, including some spindle pole bodies that had largely lost connection to the prospore membrane and others with fragmented MOPs. Importantly, even in those MOPs that appeared more similar to wild-type, defects were seen. In wild-type cells, the prospore membrane was always found in close apposition to the surface of the MOP (Figure 3-7, A and B). In contrast, in *ady4*Δ cells, MOPs frequently harbored regions where this conection between the MOP and the prospore membrane was lost and the prospore membrane appeared to bubble away from the MOP surface (Figure 3-7, C and D). Additionally, the structure of the MOP appeared disorganized opposite these regions where the prospore membrane disconnects from the MOP surface (Figure 3-7, E and F). These disrupted areas could be quite small. In the example in Figure 3-7F, the area of disorganization is ~60 nm in diameter and may be too small to be seen by thin section EM. It is unclear whether the loss of connection leads to MOP disassembly or vice versa, but it is clear that Ady4p plays an integral role in maintaining the connection between the MOP and the prospore membrane.

Discussion: Membrane assembly modulates the stability of the meiotic spindle pole body

The prospore membrane stabilizes the MOP structure

Previous transmission electron microscopy studies have shown that the structure of the MOP appears the same when unfused vesicles are docked and when the prospore membrane is present (Nakanishi *et al.*, 2006). I report here that although the MOP structure appears similar both before and after vesicle fusion, the behavior of individual MOP proteins is altered by fusion of vesicles into the prospore membrane. FRAP analysis reveals that in *sso1Δ* cells, where vesicles never fuse, MOP components are dynamic and exchange freely. In contrast, MOP components do not exchange in wild-type cells where prospore membranes form adjacent to the surface of the MOP. This change is unique to the MOP as the constitutive spindle pole body components Cnm67-GFP and Spc42-GFP are stably localized in both conditions. I determined that in wild-type cells, the change in the stability of the MOP structure corresponds with the timing of the initial fusion of vesicles into a small prospore membrane cap.

How does vesicle fusion confer stability to the MOP structure? I suggest two possibilities. In the first model, the prospore membrane acts as a steric barrier to the exchange between proteins in the plaque and proteins in the soluble cytoplasmic pool. Our data demonstrating that both Sec7-GFP and Ady4-GFP are able to exchange in the presence of a prospore membrane argue against this model.

In the second model, the conversion of vesicles into a membrane stabilizes the MOP. Previous studies have identified proteins involved in the different stages of prospore membrane formation (Neiman *et al.*, 2000; Moreno-Borchart *et al.*, 2001; Riedel *et al.*, 2005; Nakanishi *et al.*, 2006; Diamond *et al.*, 2009). I determined that the initial fusion of vesicles into a prospore membrane cap is sufficient to stabilize the MOP structure. Our data indicates that the MOP structure then remains static and stable throughout prospore membrane formation.

We postulate several ways that the fusion of precursor vesicles may lead to a change in MOP stability. The presence of a continuous sheet of membrane may provide many binding sites for the MOP proteins and therefore may slow the rate of exchange of

those components that bind to the membrane. Each MOP component has been shown to interact with other spindle pole body components by two-hybrid assay (Knop and Strasser, 2000; Nickas *et al.*, 2003). Therefore, proteins involved in and stabilized by binding to the membrane may also stabilize other MOP components surrounding them through their interactions. It should be noted that the MOP protein(s) that interact(s) directly with the membrane has not yet been determined.

An alternative way that the prospore membrane may stabilize the MOP is by subtly altering the organization of the MOP components. Coincident with the fusion of vesicles, proteins may rearrange within the MOP, thereby locking them into a more stable conformation. Though I favor this possibility, to date I have no direct evidence for such an architectural change. Preliminary studies using fluorescence resonance energy transfer between tagged MOP components have not revealed significant differences between wild-type and *sso1Δ* cells (E. M. M., unpublished observations).

Ady4p stabilizes MOP components at specific stages of prospore membrane formation

Our results with *ADY4* also support the idea of a structural change within the MOP coincident with membrane formation. Previously, the heterogeneous loss of MOP structures and disruptions in prospore membrane formation that are observed in *ady4*Δ cells led to the suggestion that Ady4p might be important for the integrity of the MOP structure (Nickas *et al.*, 2003). The results presented here provide evidence that Ady4p is indeed a stabilizing factor for the MOP. Our analysis reveals that Ady4p enhances the binding of different MOP proteins during different stages of prospore membrane formation. Prior to vesicle fusion, *ADY4* overexpression decreases the exchange of Spo21p and Spo74p. Previously, Ady4p was shown to interact with the N-terminus of Spo21p by yeast two-hybrid, and Spo21p and Spo74p were shown to be co-dependent for recruitment to the spindle pole body (Nickas *et al.*, 2003). Perhaps the physical interaction of Ady4p with Spo21p allows Ady4p to directly influence the recruitment of both Spo21p and Spo74p. By contrast, after vesicles fuse into the prospore membrane, the loss of *ADY4* does not have an effect on the exchange of Spo21p or Spo74p. However, the rate at which Mpc54p exchanges is increased in the *ady4*Δ mutant. This

alteration in MOP component sensitivity to *ADY4* dosage before and after vesicle coalescence is consistent with the idea that some rearrangement of the MOP occurs at the time of vesicle fusion into the prospore membrane and that this rearrangement leads to alterations in *ADY4* dependence.

Ady4p maintains the interface between the MOP and the prospore membrane

Seven out of ten 3D reconstructions of MOPs from the *ady4*Δ strain displayed defects in the connection between the MOP and the prospore membrane or more severe structural defects. For those MOPs with attachment defects, the prospore membrane was seen to bubble away from small areas of the MOP surface, as if the connection between the MOP and the prospore membrane was lost in these areas. In the regions of the MOP opposite these prospore membrane bubbles, the regular order of the MOP structure appears to be disrupted. In most cases, this disordered region represented a small fraction of an otherwise intact MOP. It may be that the limited increase in exchange of Mpc54-GFP that is seen by FRAP in the *ady4*Δ mutant represents a rapid exchange of Mpc54p from these small, disordered regions of the MOP.

Cells lacking *ADY4* form asci that frequently contain fewer than four spores due to the failure of a fraction of the prospore membranes to form properly (Nickas *et al.*, 2003). In this study I observed that the majority of MOPs in *ady4*Δ cells analyzed by tomography had structural defects. Therefore it seems likely that most spindle pole bodies in *ady4*Δ cells have at least a modest structural defect. Perhaps if this structural defect remains limited then spore formation is not impaired. However, if these defects expand they may lead to a broader dissociation from the prospore membrane (e.g. supplementary video 1) and a failure to properly form a spore. This interpretation implies that a minor loss of structural integrity within the MOP has the potential to cascade into more severe structural deficiencies in the absence of a stabilizing factor such as Ady4p.

How Ady4 promotes MOP stability remains unknown. Ady4p behaves quite differently than the other MOP components both in that, based on GFP fluorescence intensity, it is present in sub-stoichiometric levels (A. M. N., unpublished observations) and that the protein rapidly exchanges out of the MOP even in wild-type cells. It may be that simply through interactions with other MOP components, Ady4p acts as a glue to

hold the structure together, even if an individual molecule of Ady4p is not tightly associated with the structure. Alternatively, Ady4p may act catalytically to maintain the stability of the MOP, perhaps as a modifier of one of the subunits.

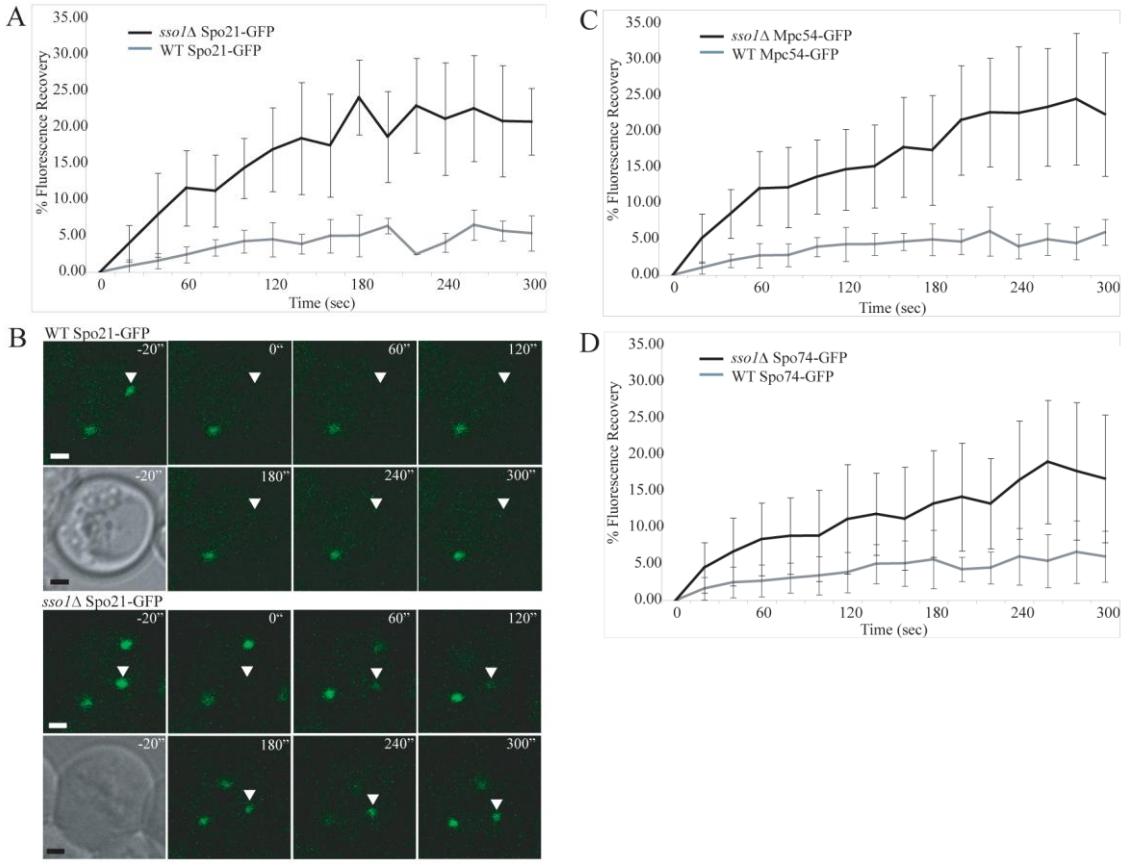

Figure 3-1. The rate of exchange of MOP components depends on the presence of a growing prospore membrane

(A) Fluorescence recovery of Spo21-GFP in wild-type (grey line) and *sso1Δ* (black line) cells during Meiosis II. The plots represent the average of six and ten experiments, respectively. Error bars represent the standard deviation (SD) at each timepoint. (B) Representative images from the Fluorescence recovery of Spo21-GFP. Time points are indicated. Pre-bleach images are shown in both the DIC and GFP channels. The bleached spindle pole body is marked with a white arrow. The scale bar represents one micron. (C) Fluorescence recovery of Mpc54-GFP in wild-type (grey line) and *sso1Δ* (black line) cells during Meiosis II. The plots represent the averages of twelve and seventeen experiments, respectively. (D) Fluorescence recovery of Spo74-GFP in wild-type (grey line) and *sso1Δ* (black line) cells during Meiosis II. The plots represent the averages of thirteen and fourteen experiments, respectively.

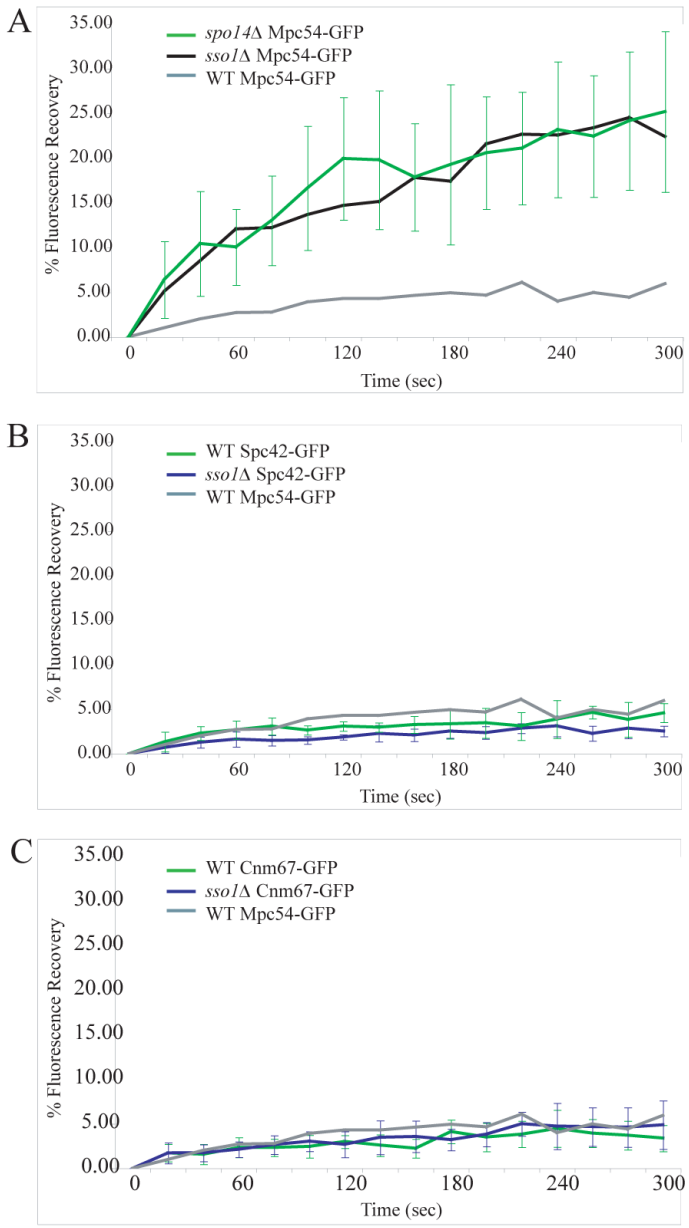

Figure 3-2. The prospore membrane uniquely stabilizes the MOP structure
(A) Fluorescence recovery of Mpc54-GFP in *spo14Δ* cells (green line) during Meiosis II. The plot represents the average of eleven experiments. Error bars represent the SD at each timepoint. Fluorescence recovery of Mpc54-GFP in wild-type (grey line) and *sso1Δ* (black line) cells from Figure 1 are also shown for comparison. (B) Fluorescence recovery of Spc42-GFP in wild-type (green line) and *sso1Δ* (blue line) cells during Meiosis II. The plots represent the average of ten and eight experiments, respectively. Fluorescence recovery of Mpc54-GFP wild-type cells (grey line) from Figure 3-1 is also shown for comparison. (C) Fluorescence recovery of Cnm67-GFP in wild-type (green line) and *sso1Δ* (blue line) cells during Meiosis II. The plots represent the average of eleven experiments each. Fluorescence recovery of Mpc54-GFP wild-type cells (grey line) from Figure 3-1 is also shown for comparison.

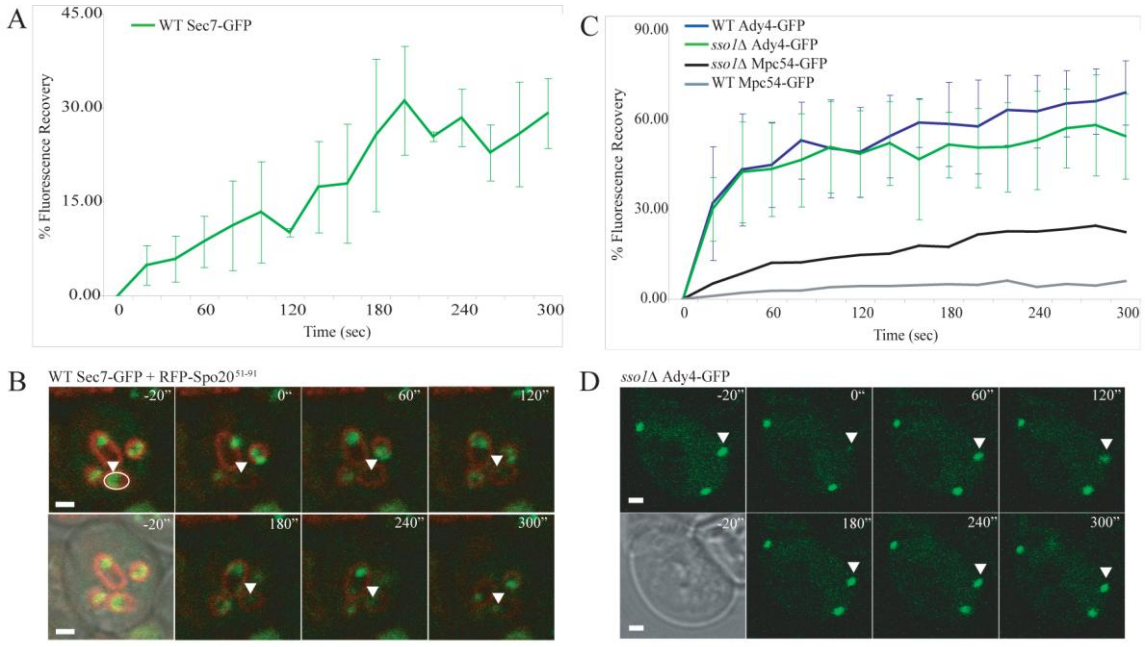

Figure 3-3. The prospore membrane is not a barrier to exchange between cytoplasms
(A) Fluorescence recovery of Sec7-GFP in wild-type cells during Meiosis II. The plot represents the average of five experiments. Error bars represent the SD at each timepoint. (B) Representative images from Fluorescence recovery of Sec7-GFP in wild-type cells. RFP-Spo20$^{51-91}$ labels the prospore membrane. Time points are indicated. Pre-bleach images are shown as both merged DIC/RFP/GFP and merged RFP/GFP. The region that was bleached is marked with a white ellipse in the pre-bleach RFP/GFP image. Fluorescence recovery is marked with a white arrow. The scale bar represents one micron. (C) Fluorescence recovery of Ady4-GFP in wild-type (blue line) and *sso1Δ* (green line) cells during Meiosis II. The plots represent the average of thirteen and ten experiments, respectively. Fluorescence recovery of Mpc54-GFP wild-type (grey line) and *sso1Δ* (black line) cells from Figure 3-1 are also shown for comparison. (D) Representative images from the fluorescence recovery of Ady4-GFP in an *sso1Δ* cell. Time points are indicated. Pre-bleach images are shown in both the DIC and GFP channels. The bleached spindle pole body is marked with a white arrow. The scale bar represents one micron.

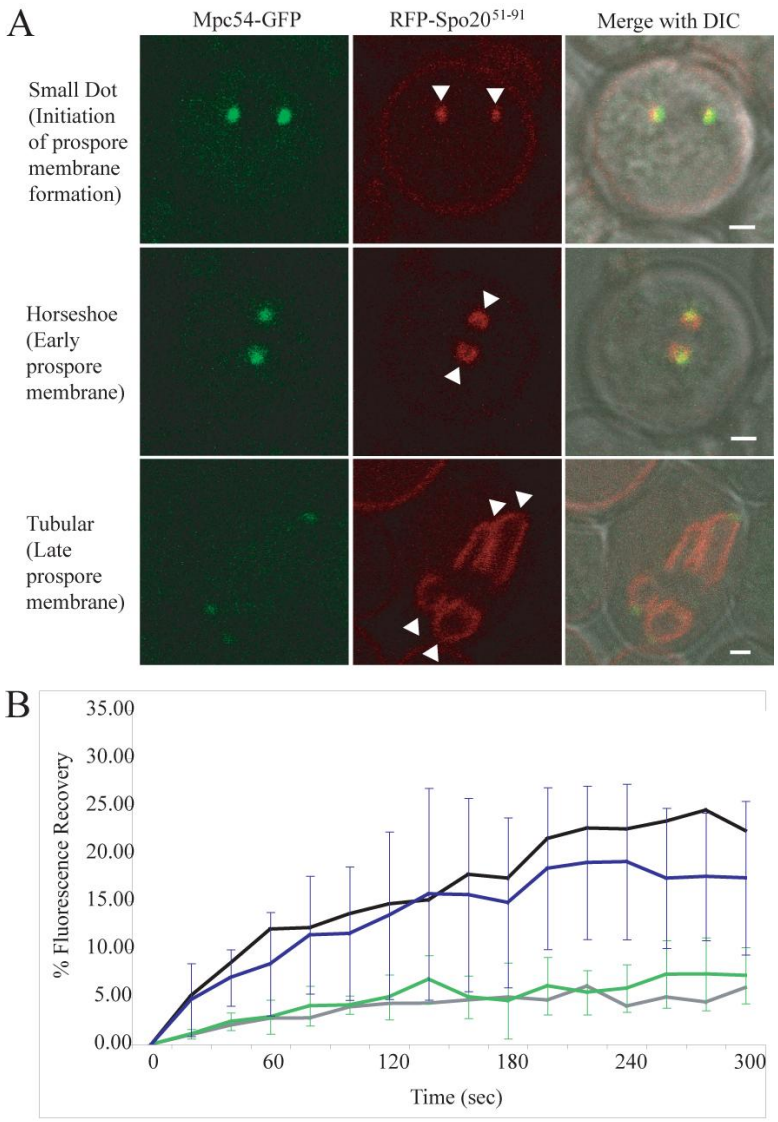

Figure 3-4. Vesicle fusion into a membrane structure reduces the exchange of MOP components

(A) Stages of prospore membrane formation. Images are from wild-type cells coexpressing Mpc54-GFP and RFP-Spo20$^{51-91}$. The scale bar represents one micron. (B) Fluorescence recovery of Mpc54-GFP from cells with RFP dots (blue line) and from cells with RFP horseshoes (green line) during Meiosis II. The plots represent the average of nine and eight experiments, respectively. Fluorescence recovery of Mpc54-GFP wild-type (grey line) and *sso1Δ* (black line) cells from Figure 3-1 are also shown for comparison.

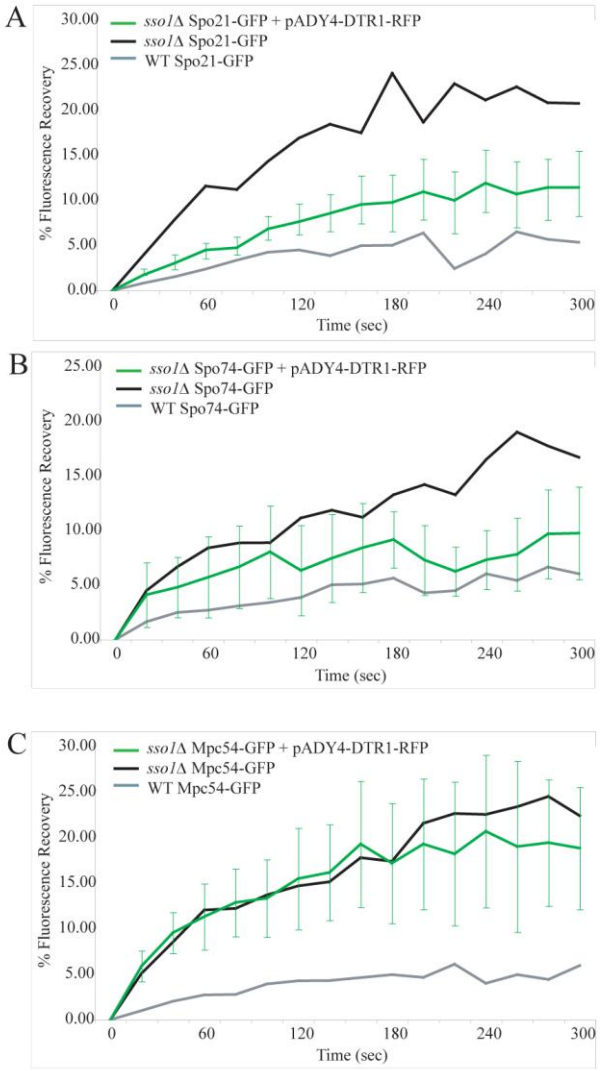

Figure 3-5. Ady4p decreases the rate of exchange of Spo21p and Spo74p in the absence of a prospore membrane

(A) Fluorescence recovery of Spo21-GFP in *sso1Δ* cells overexpressing Ady4p (green line). Cells were analyzed during Meiosis II. The green Spo21-GFP plot represents the average of ten experiments. Fluorescence recovery of Spo21-GFP in wild-type (grey line) and *sso1Δ* (black line) cells from Figure 3-1 are also shown for comparison. Error bars represent the SD at each timepoint. (B) Fluorescence recovery of Spo74-GFP in *sso1Δ* cells overexpressing Ady4p (green line). Cells were analyzed during Meiosis II. The green Spo74-GFP plot represents the average of ten experiments. Fluorescence recovery of Spo74-GFP wild-type (grey line) and *sso1Δ* (black line) cells from Figure 1 are also shown for comparison. (C) Fluorescence recovery of Mpc54-GFP in *sso1Δ* cells overexpressing Ady4p (green line). Cells were analyzed during Meiosis II. The green Mpc54-GFP plot represents the average of eight experiments. Fluorescence recovery of Mpc54-GFP wild-type (grey line) and *sso1Δ* (black line) cells from Figure 3-1 are also shown for comparison.

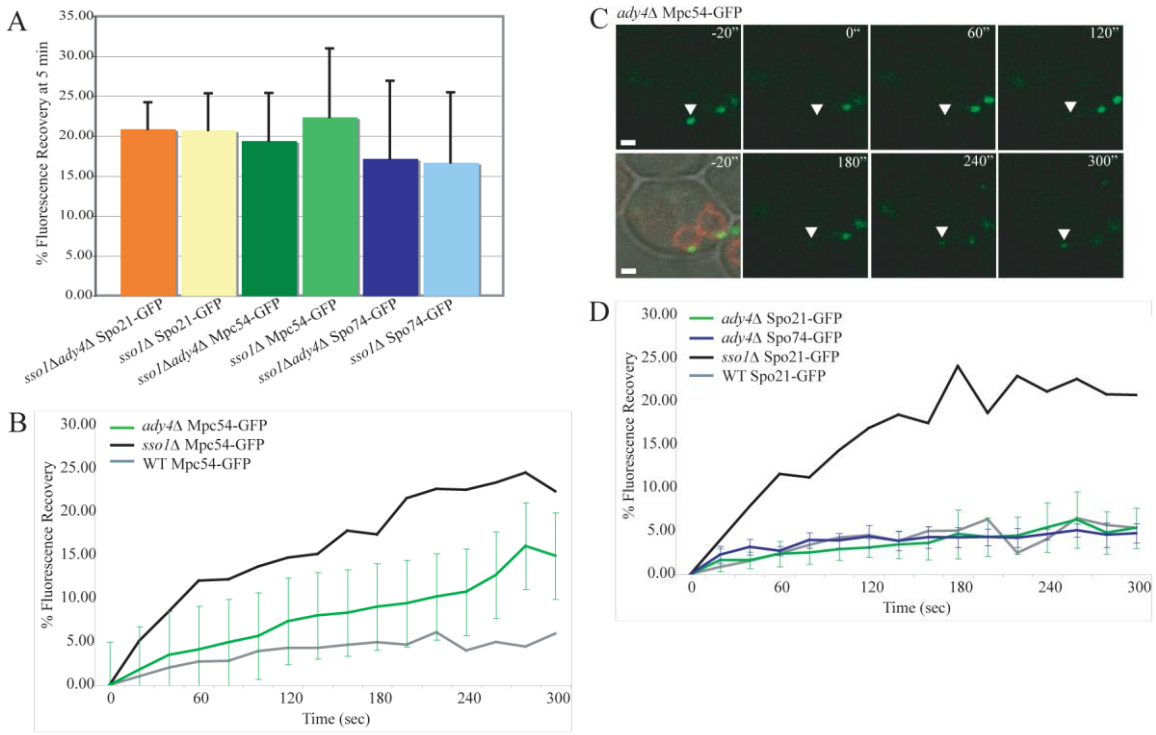

Figure 3-6. Ady4p retains Mpc54p in the MOP during prospore membrane growth
(A) Fluorescence recovery at 5 minutes after photobleaching for Spo21-GFP, Mpc54-GFP, and Spo74-GFP. The graph compares fluorescence recovery in *sso1Δady4Δ* double mutants and *sso1Δ* single mutants. Cells were analyzed during Meiosis II. The *sso1Δady4Δ* bars represent the average of nine, seven, and nine experiments, repectively. Fluorescence recovery values of Spo21-GFP, Mpc54-GFP, and Spo74-GFP in *sso1Δ* cells are from Figure 1. Error bars represent SD. (B) Fluorescence recovery of Mpc54-GFP in *ady4Δ* cells (green line). Cells were analyzed during Meiosis II. The plot represents the average of thirteen experiments. Fluorescence recovery of Mpc54-GFP in wild-type (grey line) and *sso1Δ* (black line) cells from Figure 3-1 are also shown for comparison. (C) Representative images from the Fluorescence recovery of Mpc54-GFP in *ady4Δ* cells. RFP-Spo20$^{51-91}$ labels the prospore membrane. Time points are indicated. Pre-bleach images are shown in merged DIC/RFP/GFP channels and the GFP channel alone. The bleached spindle pole body is marked with a white arrow. The scale bar represents one micron. (D) Fluorescence recovery of Spo21-GFP (green line) and Spo74-GFP (blue line) in *ady4Δ* cells. Cells were analyzed during Meiosis II. The green Spo21-GFP plot represents the average of fourteen experiments. The blue Spo74-GFP plot represents the average of nine experiments. Fluorescence recovery of Spo21-GFP in wild-type (grey line) and *sso1Δ* (black line) cells from Figure 3-1 are also shown for comparison.

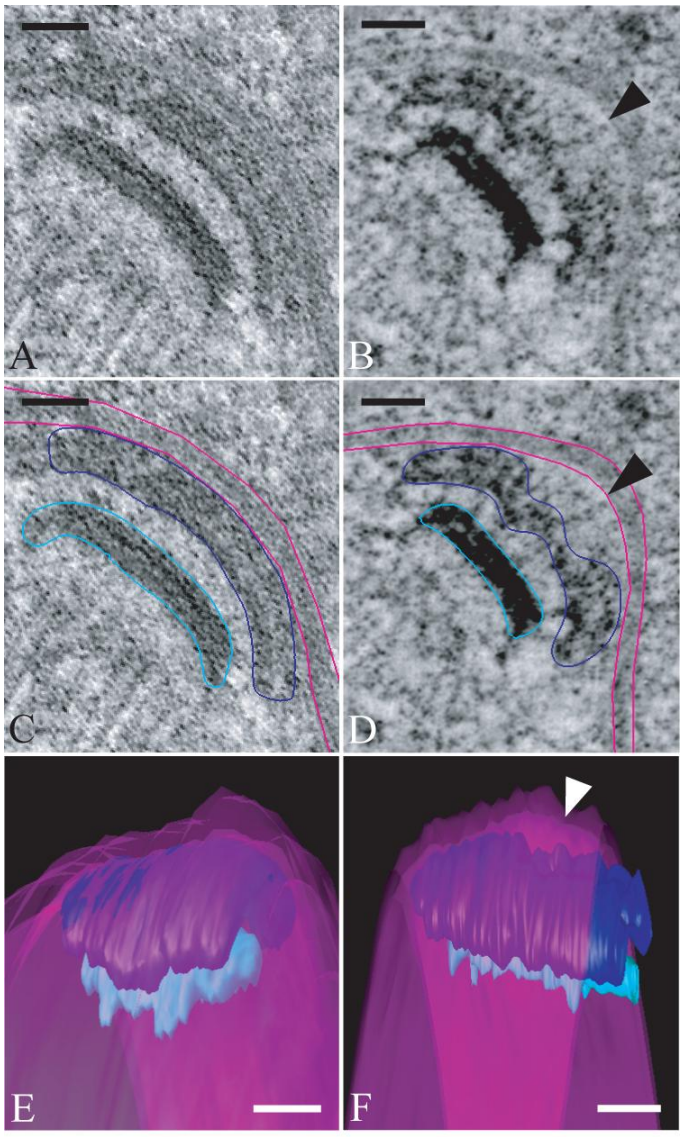

Figure 3-7. Ady4p assists in maintaining the connection between the MOP and the growing PsM

(A) 10 nm tomographic slice of a Meiosis II spindle pole body in a wild-type cell showing the MOP in close association with the prospore membrane. (B) 10 nm tomographic slice of a Meiosis II spindle pole body in an *ady4Δ* cell. Arrow indicates and area where the connection between the prospore membrane and the MOP is lost. (C) Image from (A) with graphic overlay delineating the position of elements shown in the 3D reconstruction. MOP (dark blue), prospore membrane (purple), central plaque (light blue). (D) Image from (B) with graphic overlay delineating the position of elements shown in 3D reconstructrion. Arrow indicates and area where the connection between the prospore membrane and the MOP is lost. Color assignments as in (C). (E) Reconstruction based on the tomogram in (A) demonstrating the close association of the prospore membrane across the entire MOP surface. Color assignments as in (C). (F) Reconstruction based on the tomogram in (B). The area of separation of the prospore membrane from the MOP surface is indicated by an arrow. Color assignments as in (C). Scale bars = 50nm.

Table 3-1. Strains used in this study.

Strain	Genotype	Source
AN117-4B	*MATα arg4-NspI his3SK ho*::*LYS2 leu2 lys2 rme1*::*LEU2 trp1*::*hisG ura3*	(Neiman *et al.*, 2000)
AN117-16D	*MAT***a** *his3/SK ho*::*LYS2 leu2 lys2 trp1*::*hisG ura3*	(Neiman *et al.*, 2000)
AN120	*MAT***a***/MATα ARG4/arg4-NspI his3SK/his3SK ho*::*LYS2/ho*::*LYS2 leu2/leu2 lys2/lys2 RME1/rme1*::*LEU2 trp1*::*hisG/trp1*::*hisG ura3/ura3*	(Neiman *et al.*, 2000)
HI3	*MAT***a**/*MATα ARG4*/*arg4-NspI his3ΔSK*/*his3ΔSK hoΔ::LYS2*/*hoΔ::LYS2 leu2*/*leu2 lys2*/*lys2 RME1*/*rme1Δ::LEU2 trp1::hisG*/*trp1::hisG ura3*/*ura3 sso1Δ::his5+*/*sso1Δ::his5+*	(Nakanishi *et al.*, 2006)
HI60	*MAT***a***/MATα ARG4*/*arg4-NspI his3ΔSK*/*his3ΔSK hoΔ::LYS2*/*hoΔ::LYS2 leu2*/*leu2lys2*/*lys2 RME1*/*rme1Δ::LEU2 trp1::hisG*/*trp1::hisG ura3*/*ura3 spo14Δ::ura3*/*spo14Δ::ura3*	This study
EMD85	*MAT***a**/*MATα ARG4*/*arg4-NspI his3ΔSK*/*his3ΔSK hoΔ::LYS2*/*hoΔ::LYS2 leu2*/*leu2lys2*/*lys2 RME1*/*rme1Δ::LEU2 trp1::hisG*/*trp1::hisG ura3*/*ura3 SPC42-GFP::kanMX4/SPC42-GFP::kanMX4*	This study
EMD3	*MAT***a**/*MATα ARG4*/*arg4-NspI his3ΔSK*/*his3ΔSK hoΔ::LYS2*/*hoΔ::LYS2 leu2*/*leu2 lys2*/*lys2 RME1*/*rme1Δ::LEU2 trp1::hisG*/*trp1::hisG ura3*/*ura3 sso1Δ::his5+*/*sso1Δ::his5+ SPC42-GFP::kanMX4/SPC42-GFP::kanMX4*	This study
EMD4	*MAT***a**/*MATα ARG4*/*arg4-NspI his3ΔSK*/*his3ΔSK hoΔ::LYS2*/*hoΔ::LYS2 leu2*/*leu2 lys2*/*lys2 RME1*/*rme1Δ::LEU2 trp1::hisG*/*trp1::hisG ura3*/*ura3 CNM67-GFP::his5+/CNM67-GFP::his5+*	This study
EMD6	*MAT***a**/*MATα ARG4*/*arg4-NspI his3ΔSK*/*his3ΔSK hoΔ::LYS2*/*hoΔ::LYS2 leu2*/*leu2 lys2*/*lys2 RME1*/*rme1Δ::LEU2 trp1::hisG*/*trp1::hisG ura3*/*ura3 sso1Δ::his5+*/*sso1Δ::his5+ CNM67-GFP::his5+/CNM67-GFP::his5+*	This study

Strain	Genotype	Source
MND57	*MAT***a**/*MAT ARG4/arg4-NspI his3SK/his3SK ho*::*LYS2/ho*::*LYS2 leu2/leu2 lys2/lys2 RME1/rme1*::*LEU2 trp1*::*hisG/trp1*::*hisG ura3/ura3 ady4*Δ::*HIS3MX6/ady4*Δ::*HIS3MX6*	(Nickas *et al.*, 2003)
MND46	*MAT***a**/*MATα ARG4*/*arg4-NspI his3*Δ*SK*/*his3*Δ*SK ho*Δ*::LYS2*/*ho*Δ*::LYS2 leu2*/*leu2 lys2*/*lys2 RME1*/*rme1*Δ*::LEU2 trp1::hisG*/*trp1::hisG ura3*/*ura3 ady4*Δ::*HIS3MX6/ady4*Δ::*HIS3MX6 MPC54-GFP::HIS3MX6/ MPC54-GFP::HIS3MX6*	This study
MND48	*MAT***a**/*MATα ARG4*/*arg4-NspI his3*Δ*SK*/*his3*Δ*SK ho*Δ*::LYS2*/*ho*Δ*::LYS2 leu2*/*leu2 lys2*/*lys2 RME1*/*rme1*Δ*::LEU2 trp1::hisG*/*trp1::hisG ura3*/*ura3 ady4*Δ::*HIS3MX6/ady4*Δ::*HIS3MX6 SPO21-GFP::HIS3MX6/ SPO21-GFP::HIS3MX6*	This study
EMD10	*MAT***a**/*MATα ARG4*/*arg4-NspI his3*Δ*SK*/*his3*Δ*SK ho*Δ*::LYS2*/*ho*Δ*::LYS2 leu2*/*leu2 lys2*/*lys2 RME1*/*rme1*Δ*::LEU2 trp1::hisG*/*trp1::hisG ura3*/*ura3 sso1*Δ*::his5+/sso1*Δ*::his5+ ady4*Δ::*HIS3MX6/ady4*Δ::*HIS3MX6*	This study

Table 3-2. Plasmids used in this study.

Plasmid	Relevant features	Source
314-SPO21-GFP	CEN *SPO21-GFP*	This study
424-MPC54-GFP	2μ *MPC54-GFP*	(Nickas *et al.*, 2003)
424-SPO74-GFP	2μ *SPO74-GFP*	(Nickas *et al.*, 2003)
426-RFP-SPO20$^{51-91}$	2μ P_{TEF2}-Spo20$^{51-91}$-RFP	(Diamond *et al.*, 2009)
pSSEC7-EGFPx3	*SEC7*3' end-*EGFPx3*	(Rossanese and Glick, 2001)
426-ADY4-DTR1-RFP	2μ *ADY4 DTR1-RFP*	This study
424-ADY4-GFP	2μ *ADY4-GFP*	(Nickas *et al.*, 2003)
426-TEF-mRFP	2μ P_{TEF2}-mRFP	This study

Chapter 4: Conclusions and Future experiments

Prospore membrane formation during Meiosis II provides a model for vesicle tethering, docking, and fusion. The MOP serves as a vesicle docking complex during the initiation of prospore membrane growth, and it maintains a connection with the prospore membrane as the membrane grows. Therefore, the MOP structure is critical to initiating prospore membrane formation and to ensuring that the prospore membrane remains associated with the nucleus (Neiman, 1998; Knop and Strasser, 2000; Bajgier *et al.*, 2001; Nickas *et al.*, 2003). An examination of the roles of several MOP proteins during sporulation has revealed that Mpc54p plays a critical role in vesicle docking, and that Ady4p stabilizes the connection between the MOP and the growing prospore membrane. A great deal remains to be studied about prospore membrane initiation and such studies may provide insight into vesicle docking and fusion in general.

What is the role of the MOP during vesicle docking?

The formation of a normal MOP structure is required for vesicle docking and fusion during prospore membrane initiaton (Knop and Strasser, 2000; Bajgier *et al.*, 2001; Nickas *et al.*, 2003). This thesis presents a model for the organization of the MOP structure based on FRET interactions between the MOP components. In this model, the N-termini of Spo21p and Mpc54p are proximal to the outer surface of the MOP. The location of the Spo74p termini within the plaque is difficult to define, but I are not ruling out the possibility that a portion of the globular Spo74p protein also lies at the outer surface of the MOP structure. The remaining MOP proteins appear to be localized more towards the interior of the spindle pole body. Therefore, of the six known MOP components, Spo21p, Mpc54p, and Spo74p are of greatest interest to the study of the role of the MOP during prospore membrane initiation and growth. This is due both to their localization near the outer surface of the MOP structure and to their meiotically-induced expression, which ensures their arrival at the MOP during Meiosis II when the function of the SPB is altered to include acting as the initiation site for prospore membrane formation.

This thesis identifies Mpc54p's involvement in vesicle docking at the MOP. Several *mpc54* mutant alleles have been constructed and characterized. It was demonstrated through fluorescence microscopy that certain Mpc54p mutant proteins promoted normal MOP composition yet disrupted prospore membrane initiation. TEM analysis has revealed that mutations in the N-terminus of Mpc54p disrupt vesicle docking at the MOP. However, for the weaker *mpc54* mutant alleles, vesicle docking is not completely disrupted and prospore membranes are formed at a reduced rate. This could be the result of two possibilities: 1) Mpc54p may play a role in vesicle docking without being essential for this process, or 2) the mutations may not completely block docking. This thesis does not define the details of Mpc54p's role in vesicle docking. Future efforts to describe Mpc54p's role in vesicle docking would be helpful in defining the MOP as a vesicle docking complex.

Spo74p and Spo21p are also critical for the formation of the MOP structure and thus to prospore membrane initiation (Knop and Strasser, 2000; Nickas *et al.*, 2003). Preliminary examinations of point mutant alleles of Spo74p suggest that residues within the central portion of the protein are required for spore formation. Further work should focus on defining the effect of these mutants on the formation of a normal MOP structure and determining the stage of spore formation disrupted by these mutations. Promising alleles could be used as reagents in genetic screens that may identify other proteins critical for prospore membrane formation at the MOP. One preliminary approach to defining the role of Spo21p within the context of the MOP structure would be constructing N-terminal truncations of Spo21p or introducing mutations into the N-terminal portion of the protein. Characterization of these constructs may identify the function of Spo21p.

The MOP as a model for a vesicle docking complex

The study of vesicle trafficking has generated a great deal of scientific interest. The discovery of the SNARE machinery was a breakthrough for the understanding of vesicle fusion at specific membranes (Bonifacino and Glick, 2004). Prospore membrane initiation is a model for vesicle tethering, docking, and fusion. The meiotic SNARE complex at the prospore membrane is an interesting model for the integration of novel

components into an existing SNARE machinery. Many studies have thus used prospore membrane formation as a model for vesicle fusion by SNAREs (Neiman, 1998; Neiman *et al.*, 2000; Jantti *et al.*, 2002; Nakanishi *et al.*, 2004; Nakanishi *et al.*, 2006).

This thesis proposes that the MOP can also be a good model for vesicle docking. During prospore membrane initiation, precursor vesicles must dock to the MOP prior to their SNARE-mediated fusion (Nakanishi *et al.*, 2006). The MOP is therefore analogous to docking complexes that function in other membrane fusion steps (e.g .the exocyst and the TRAPP complex (TerBush *et al.*, 1996; Guo *et al.*, 1999; Barrowman *et al.*, 2000; Sacher *et al.*, 2008)) in that it serves to tether together the two membranes that will fuse, and that the docking of vesicles is a prerequisite to the fusion event.

The exocyst is a multi-subunit complex involved in docking post-Golgi vesicles to the plasma membrane during exocytosis (TerBush *et al.*, 1996; Guo *et al.*, 1999). Docking complexes like the exocyst frequently contain proteins with coiled-coil motifs (Lowe, 2000). This supports our proposal that Mpc54p, which has a coiled-coil motif, is either a component of the MOP docking complex or is the sole docking factor at the MOP. Vesicles accumulate at the plasma membrane in exocyst mutants but do not fuse, as the SNARE complex does not form in the absence of the exocyst. This suggests that the exocyst is required for vesicle docking to the plasma membrane and that this docking is required for the fusion of vesicles with this membrane (Walch-Solimena *et al.*, 1997; Grote *et al.*, 2000). This thesis reports a remarkably similar phenomenon in cells expressing the Mpc54p mutant proteins, in that vesicles accumulate at the MOP, but do not fuse into a membrane. This observation supports the characterization of the MOP as a vesicle docking complex.

The TRAPP (transport protein particle) complex is also a docking complex, and promotes docking specificity at the Golgi (Barrowman *et al.*, 2000; Lowe, 2000). Docking factors are diverse in nature, and can be single proteins or multi-subunit complexes (Rossi *et al.*, 1995; Jiang *et al.*, 1998; Lowe, 2000). TRAPP falls into this last category (Barrowman *et al.*, 2000). Several TRAPP subunits interact with various subunits of the SNARE machinery at the ER-to-Golgi vesicle trafficking step (Rossi *et al.*, 1995; Jiang *et al.*, 1998; Barrowman *et al.*, 2000; Lowe, 2000), suggesting that docking complexes may play a role in recruiting or stabilizing SNAREs during vesicle

fusion. Future attempts to identify proteins that interact with Spo20p, Sec9p, or Sso1p might isolate additional components of the MOP docking complex, if Mpc54p is not acting alone.

One missing player in our understanding of vesicle tethering, docking, and fusion at the MOP is the identification of the guanine nucleotide exchange factor (GEF) involved in prospore membrane initiation. GEFs activate Rab GTPases by exchanging the guanine nucleotide with which the Rab protein is associating. Rabs regulate membrane trafficking between all cellular compartments by assisting in tethering vesicles to the proper site of fusion (Grosshans *et al.*, 2006). Like SNAREs, specific Rabs are involved at particular steps of membrane trafficking (reviewed in (Fukuda, 2008)). The GEF and the Rab that are involved in prospore membrane initiation have yet to be identified. In *S. pombe*, Spo13p is located at the outer surface of the MOP and is required for MOP formation and prospore membrane formation (Nakase *et al.*, 2008). In this way, Spo13p is similar to Mpc54p and Spo21p. Interestingly, work done by Hui-Ju Yang in our lab has shown that Spo13p is not only required for MOP formation, but also acts as a GEF during prospore membrane formation. Thus, the MOP in *S. pombe* may control the tethering of prospore membrane precursor vesicles to its surface by directly activating Rab proteins. If Spo13p also assists in vesicle docking, like Mpc54p, then Spo13p in *S. pombe* may have a dual function as a promoter of vesicle tethering and as a component of the vesicle docking complex. Is there an analogous GEF function for Mpc54p or Spo21p in *S. cerevisiae*?

Is vesicle docking required for Spo14p activation?

The relocation of GFP-Spo20$^{51-91}$ from the plasma membrane to the prospore membrane requires the activity of Spo14p (Nakanishi *et al.*, 2004). Fluorescence microscopy studies reveal that GFP-Spo20$^{51-91}$ relocation is disrupted in cells expressing an Mpc54p mutant protein. However, in this assay the reporter for Spo14p activity is also the reporter for prospore membrane growth. A revised version of this assay in which meiotic progression would be measured by DAPI staining would alleviate this reporter conflict. In this assay, the stage of prospore membrane growth and meiotic progression would be assayed by RFP-tagged Mpc54p proteins and DAPI staining, respectively.

In this assay, the localization of GFP-Spo20$^{51-91}$ at the plasma membrane would therefore be a marker solely for the activation of Spo14p.

Examination of Spo14-GFP in the strain expressing this *mpc54* mutant allele demonstrates that Spo14p localization is not disrupted. Therefore, the *mpc54* mutant allele is not disrupting Spo14p activation by disrupting its localization. I propose that the docking of vesicles, mediated by Mpc54p, is required for Spo14p activation. Therefore, cells in which prospore membranes form at some MOPs while vesicles stall in a tethered state at other MOPs would not activate Spo14p at an optimal level, thus preventing the proper recruitment of Spo20p to all MOPs. However, while this thesis suggests that vesicle docking is required for the activation of Spo14p, direct evidence is not provided to this effect.

An examination of the conversion of PC to PA in cells expressing the *mpc54* mutant alleles would further define the requirement for vesicle docking prior to Spo14p activation. Additionally, future analysis of spore formation in *sec9*Δ mutants expressing the Mpc54p mutant proteins would help to define the effect that the mutant proteins have on Spo20p localization and activity. Sec9p and Spo20p share a partially redundant function. Therefore, Sec9p may be compensating for the lowered activity of Spo20p in cells expressing the Mpc54p mutant proteins. By taking Sec9p out of the equation, I would then be able to determine whether the Spo20p that is recruited to some MOPs is sufficient to promote proper vesicle fusion into a prospore membrane.

A great deal of scientific interest has been focused on the involvement of lipids in vesicle trafficking. Interesting, the local lipid environment during vesicle docking and fusion has been shown to frequently play a role in both the assembly of SNAREs and the recruitment of vesicle docking and fusion machinery (reviewed in (De Matteis and Godi, 2004; van Meer and Sprong, 2004)). This thesis proposes that vesicle docking at the MOP may affect Spo14p activation, so that the docking process itself may prime vesicles for fusion by altering their lipid milieu. Therefore, the lipid environment of the SNARE complex involved in prospore membrane initiation may impact complex's ability to assemble and promote vesicle fusion. Future studies of the role of lipids during vesicle docking and fusion at the MOP might further our understanding of the role of lipids during vesicle trafficking in general.

Regulating the location and timing of prospore membrane formation

Previously it was shown that proper a MOP structure is required for vesicle docking at the MOP (Knop and Strasser, 2000; Bajgier *et al.*, 2001; Nickas *et al.*, 2003). Therefore, by controlling the MOP modification of the SPBs, cells can alter the number of spores that are formed based on nutritional and environmental cues (Nickas *et al.*, 2004). Previous studies demonstrated that vesicle docking is a required prerequisite to vesicle fusion (Nakanishi *et al.*, 2006). This thesis proposes that vesicle docking may regulate Spo14p activation. Our model for Spo14p activation proposes that Spo14p arrives at the SPB in an inactive state, and then is activated through an unknown molecular mechanism when vesicles dock to the MOP. Thus, vesicles only fuse after docking to the MOP. By restricting vesicle fusion events to vesicles docked at the MOP, cells can ensure that each prospore membrane will be attached to a MOP and therefore to the nucleus. Taken together, these findings promote the idea that the cell regulates the location and timing of prospore membrane initiation based on the activation of Spo14p on vesicles docked to the MOP.

Dynamics of the MOP structure

In this thesis, data is presented which supports the proposal that the dynamics of the MOP change at the onset of Meiosis II (Taxis *et al.*, 2005). FRAP analysis of GFP-tagged MOP components in various mutant conditions reveals that the fusion of vesicles into a membrane structure stabilizes the MOP structure. I propose two ways that the fusion of precursor vesicles may lead to a change in MOP stability: 1) The presence of a continuous sheet of membrane may provide many binding sites for the MOP proteins and, therefore, may slow the rate of exchange of those components that bind to the membrane, or 2) The prospore membrane may stabilize the MOP by subtly altering the organization of the MOP components.

Our finding that a change in the stability of the MOP correlates with the vesicle fusion event is quite interesting taken in the context of the MOP serving as a docking complex. Whether the alteration in the dynamics of the MOP is a cause or an effect of vesicle fusion remains to be determined, but I speculate that this change may be important in promoting the SNARE-mediated fusion of the vesicles. That is, the locking

of proteins within the docking complex may be important to promote the transition from tethered to fused vesicles.

What is the role of the MOP during prospore membrane elongation?

In addition to the stabilizing effect of the prospore membrane on the MOP structure, this thesis also demonstrates that Ady4p stabilizes specific components of the MOP structure at particular stages of prospore membrane growth. Previously, the heterogeneous loss of MOP structures and disruptions in prospore membrane formation that are observed in *ady4*Δ cells led to the suggestion that Ady4p might be important for the integrity of the MOP structure (Nickas *et al.*, 2003). The results presented in this thesis provide evidence that Ady4p is indeed a stabilizing factor for the MOP. I have demonstrated that prior to vesicle fusion Ady4p stabilizes the exchange of Spo21p and Spo74p. However, after vesicles fuse into the prospore membrane, Ady4p stabilizes the exchange of Mpc54p. This switch in Ady4p targets may suggest that Spo21p, Spo74p, and Mpc54p play different roles in ensuring the integrity of the MOP structure and in promoting the function of the MOP, and that the localization of these proteins within the MOP is critical at different stages of prospore membrane formation.

3D reconstructions of MOPs from an *ady4*Δ strain displayed defects in the connection between the MOP and the prospore membrane or more severe structural defects. Therefore, Ady4p assists in maintaining the connection between the MOP and the prospore membrane, perhaps by stabilizing the MOP structure. Presumably, if structural defects in portions of the MOP expand they may lead to a broader dissociation from the prospore membrane and a failure to properly form a spore, resulting in the dampened sporulation efficiency observed in *ady4*Δ mutants. How does Ady4 promote MOP stability? I propose two possibilities: 1) Ady4p may act as a glue to hold the structure together, or 2) Ady4p may act catalytically to maintain the stability of the MOP, perhaps as a modifier of one of the subunits.

Prospore membrane formation is a model for membrane formation during cellular differentiation.

The formation of the prospore membrane is a model for the formation of intracellular membrane systems in higher eukaryotes (Moreno-Borchart and Knop, 2003). In spore formation, cell division occurs by the growth of new membranes, and this form of division is similar to cellular division observed in several higher eukaryotes. For example, during the cellularization of the syncytial blastoderm of *Drosophila*, polynucleate cells are divided into mononucleate cells by the formation of new plasma membranes derived from the coalescence of vesicles (Tokuyasu *et al.*, 1972; Loncar and Singer, 1995). Additionally, in higher plants, the cell plate forms initially by the coalescence of vesicles that form a flattened sheet that grows towards the mother plasma membrane, thereby separating the daughter nuclei (Staehelin and Hepler, 1996). The formation of the pollen grain is strikingly similar to the formation of an ascus in yeast (McCormick, 1993). Four haploid products of male meiosis, called microspores, undergo a mitotic division. For each microspore, one daughter nucleus remains in the mother cell cytoplasm and the other daughter nucleus is enclosed in a double membrane within the cytoplasm of the mother cell. This second nucleus undergoes mitotic division to give rise to two small cells within the mother cell. Together, these three cells form a mature pollen grain. Further exploration of prospore membrane initiation and growth may provide insight into cellular division in these systems as well as into cellular differentiation in general.

Adams, I.R., and Kilmartin, J.V. (1999). Localization of core spindle pole body (SPB) components during SPB duplication in *Saccharomyces cerevisiae*. J Cell Biol *145*, 809-823.

Bajgier, B.K., Malzone, M., Nickas, M., and Neiman, A.M. (2001). *SPO21* is required for meiosis-specific modification of the spindle pole body in yeast. Mol Biol Cell *12*, 1611-1621.

Barrowman, J., Sacher, M., and Ferro-Novick, S. (2000). TRAPP stably associates with the Golgi and is required for vesicle docking. EMBO J *19*, 862-869.

Bennett, M.K., and Scheller, R.H. (1993). The molecular machinery for secretion is conserved from yeast to neurons. Proc Natl Acad Sci U S A *90*, 2559-2563.

Bonifacino, J.S., and Glick, B.S. (2004). The mechanisms of vesicle budding and fusion. Cell *116*, 153-166.

Brachat, A., Kilmartin, J.V., Wach, A., and Philippsen, P. (1998). Saccharomyces cerevisiae cells with defective spindle pole body outer plaques accomplish nuclear migration via half-bridge-organized microtubules. Mol Biol Cell *9*, 977-991.

Brennwald, P., and Rossi, G. (2007). Spatial regulation of exocytosis and cell polarity: yeast as a model for animal cells. FEBS Lett *581*, 2119-2124.

Briza, P., Breitenbach, M., Ellinger, A., and Segall, J. (1990). Isolation of two developmentally regulated genes involved in spore wall maturation in Saccharomyces cerevisiae. Genes Dev *4*, 1775-1789.

Bullitt, E., Rout, M.P., Kilmartin, J.V., and Akey, C.W. (1997). The yeast spindle pole body is assembled around a central crystal of Spc42p. Cell *89*, 1077-1086.

Byers, B. (1981). Cytology of the yeast life cycle. In: The molecular biology of the yeast *Saccharomyces*: life cycle and inheritance, ed. E.W.J. J. N. Strathern, and J. R. Broach, Cold Spring Harbor, N.Y.: Cold Spring Harbor Press, 59-96.

Byers, B., and Goetsch, L. (1974). Duplication of spindle plaques and integration of the yeast cell cycle. Cold Spring Harb Symp Quant Biol *38*, 123-131.

Byers, B., and Goetsch, L. (1975). Behavior of spindles and spindle plaques in the cell cycle and conjugation of Saccharomyces cerevisiae. J Bacteriol *124*, 511-523.

Campbell, R.E., Tour, O., Palmer, A.E., Steinbach, P.A., Baird, G.S., Zacharias, D.A., and Tsien, R.Y. (2002). A monomeric red fluorescent protein. Proc Natl Acad Sci U S A *99*, 7877-7882.

Chen, X.P., Yin, H., and Huffaker, T.C. (1998). The yeast spindle pole body component Spc72p interacts with Stu2p and is required for proper microtubule assembly. J Cell Biol *141*, 1169-1179.

Chen, Y.A., and Scheller, R.H. (2001). SNARE-mediated membrane fusion. Nat Rev Mol Cell Biol *2*, 98-106.

Chu, S., DeRisi, J., Eisen, M., Mulholland, J., Botstein, D., Brown, P.O., and Herskowitz, I. (1998). The transcriptional program of sporulation in budding yeast. Science *282*, 699-705.

Chu, S., and Herskowitz, I. (1998). Gametogenesis in yeast is regulated by a transcriptional cascade dependent on Ndt80. Mol Cell *1*, 685-696.

Davidow, L.S., Goetsch, L., and Byers, B. (1980). Preferential occurence of nonsister spores in two-spored asci of *Saccharomyces cerevisiae*: evidence for regulation of spore-wall formation by the spindle pole body. Genetics *94*, 581-595.

De Matteis, M.A., and Godi, A. (2004). PI-loting membrane traffic. Nat Cell Biol *6*, 487-492.

Diamond, A.E., Park, J.S., Inoue, I., Tachikawa, H., and Neiman, A.M. (2009). The anaphase promoting complex targeting subunit *Ama1* links meiotic exit to cytokinesis during sporulation in *Saccharomyces cerevisiae*. Mol Biol Cell *20*, 134-145.

Donaldson, A.D., and Kilmartin, J.V. (1996). Spc42p: a phosphorylated component of the S. cerevisiae spindle pole body (SPD) with an essential function during SPB duplication. J Cell Biol *132*, 887-901.

Elliott, S., Knop, M., Schlenstedt, G., and Schiebel, E. (1999). Spc29p is a component of the Spc110p subcomplex and is essential for spindle pole body duplication. Proc Natl Acad Sci U S A *96*, 6205-6210.

Esposito, R.E., and S. Klapholz. (1981). Meiosis and ascospore development. In: The molecular biology of the yeast *Saccharomyces*: life cycle and inheritance, ed. E.W.J. J. N. Strathern, and J. R. Broach, Cold Spring Harbor: Cold Spring Harbor Press, 211-287.

Fukuda, M. (2008). Regulation of secretory vesicle traffic by Rab small GTPases. Cell Mol Life Sci *65*, 2801-2813.

Gao, X.D., Tachikawa, H., Sato, T., Jigami, Y., and Dean, N. (2005). Alg14 recruits Alg13 to the cytoplasmic face of the endoplasmic reticulum to form a novel bipartite

UDP-N-acetylglucosamine transferase required for the second step of N-linked glycosylation. J Biol Chem *280*, 36254-36262.

Geissler, S., Pereira, G., Spang, A., Knop, M., Soues, S., Kilmartin, J., and Schiebel, E. (1996). The spindle pole body component Spc98p interacts with the gamma-tubulin-like Tub4p of Saccharomyces cerevisiae at the sites of microtubule attachment. EMBO J *15*, 3899-3911.

Grosshans, B.L., Ortiz, D., and Novick, P. (2006). Rabs and their effectors: achieving specificity in membrane traffic. Proc Natl Acad Sci U S A *103*, 11821-11827.

Grote, E., Carr, C.M., and Novick, P.J. (2000). Ordering the final events in yeast exocytosis. J Cell Biol *151*, 439-452.

Gruneberg, U., Campbell, K., Simpson, C., Grindlay, J., and Schiebel, E. (2000). Nud1p links astral microtubule organization and the control of exit from mitosis. EMBO J *19*, 6475-6488.

Guo, W., Roth, D., Walch-Solimena, C., and Novick, P. (1999). The exocyst is an effector for Sec4p, targeting secretory vesicles to sites of exocytosis. EMBO J *18*, 1071-1080.

Hailey, D.W., Davis, T.N., and Muller, E.G. (2002). Fluorescence resonance energy transfer using color variants of green fluorescent protein. Methods Enzymol *351*, 34-49.

Helfant, A.H. (2002). Composition of the spindle pole body of Saccharomyces cerevisiae and the proteins involved in its duplication. Curr Genet *40*, 291-310.

Herskowitz, I. (1988). Life cycle of the budding yeast *Saccharomyces cerevisiae*. Microbiol Rev *52*, 536-553.

Holaway, B.L., Lehman, D.J., Primerano, D.A., Magee, P.T., and Clancy, M.J. (1985). Sporulation-regulated genes of Saccharomyces cerevisiae. Curr Genet *10*, 163-169.

Huh, W.K., Falvo, J.V., Gerke, L.C., Carroll, A.S., Howson, R.W., Weissman, J.S., and O'Shea, E.K. (2003). Global analysis of protein localization in budding yeast. Nature *425*, 686-691.

Jantti, J., Aalto, M.K., Oyen, M., Sundqvist, L., Keranen, S., and Ronne, H. (2002). Characterization of temperature-sensitive mutations in the yeast syntaxin 1 homologues Sso1p and Sso2p, and evidence of a distinct function for Sso1p in sporulation. J Cell Sci *115*, 409-420.

Jaspersen, S.L., and Winey, M. (2004). The budding yeast spindle pole body: structure, duplication, and function. Annu Rev Cell Dev Biol *20*, 1-28.

Jiang, Y., Scarpa, A., Zhang, L., Stone, S., Feliciano, E., and Ferro-Novick, S. (1998). A high copy suppressor screen reveals genetic interactions between BET3 and a new gene. Evidence for a novel complex in ER-to-Golgi transport. Genetics *149*, 833-841.

Jordan, E.G., Severs, N.J., and Williamson, D.H. (1977). Nuclear pore formation and the cell cycle in Saccharomyces cerevisiae. Exp Cell Res *104*, 446-449.

Kane, S.M., and Roth, R. (1974). Carbohydrate metabolism during ascospore development in yeast. J Bacteriol *118*, 8-14.

Kilmartin, J.V., Dyos, S.L., Kershaw, D., and Finch, J.T. (1993). A spacer protein in the *Saccharomyces cerevisiae* spindle poly body whose transcript is cell cycle-regulated. J Cell Biol *123*, 1175-1184.

Kilmartin, J.V., and Goh, P.Y. (1996). Spc110p: assembly properties and role in the connection of nuclear microtubules to the yeast spindle pole body. EMBO J *15*, 4592-4602.

Knop, M., Pereira, G., Geissler, S., Grein, K., and Schiebel, E. (1997). The spindle pole body component Spc97p interacts with the gamma-tubulin of Saccharomyces cerevisiae and functions in microtubule organization and spindle pole body duplication. EMBO J *16*, 1550-1564.

Knop, M., and Schiebel, E. (1997). Spc98p and Spc97p of the yeast gamma-tubulin complex mediate binding to the spindle pole body via their interaction with Spc110p. EMBO J *16*, 6985-6995.

Knop, M., and Schiebel, E. (1998). Receptors determine the cellular localization of a gamma-tubulin complex and thereby the site of microtubule formation. Embo J *17*, 3952-3967.

Knop, M., Siegers, K., Pereira, G., Zachariae, W., Winsor, B., Nasmyth, K., and Schiebel, E. (1999). Epitope tagging of yeast genes using a PCR-based strategy: more tags and improved practical routines. Yeast *15*, 963-972.

Knop, M., and Strasser, K. (2000). Role of the spindle pole body of yeast in mediating assembly of the prospore membrane during meiosis. Embo J *19*, 3657-3667.

Kremer, J.R., Mastronarde, D.N., and McIntosh, J.R. (1996). Computer visualization of three-dimensional image data using IMOD. J Struct Biol *116*, 71-76.

Liu, S., Wilson, K.A., Rice-Stitt, T., Neiman, A.M., and McNew, J.A. (2007). In vitro fusion catalyzed by the sporulation-specific t-SNARE light-chain Spo20p is stimulated by phosphatidic acid. Traffic *8*, 1630-1643.

Loncar, D., and Singer, S.J. (1995). Cell membrane formation during the cellularization of the syncytial blastoderm of *Drosophila*. Proc Natl Acad Sci U S A *92*, 2199-2203.

Longtine, M.S., McKenzie, A., 3rd, Demarini, D.J., Shah, N.G., Wach, A., Brachat, A., Philippsen, P., and Pringle, J.R. (1998). Additional modules for versatile and economical PCR-based gene deletion and modification in Saccharomyces cerevisiae. Yeast *14*, 953-961.

Lowe, M. (2000). Membrane transport: tethers and TRAPPs. Curr Biol *10*, R407-409.

Lynn, R.R., and Magee, P.T. (1970). Development of the spore wall during ascospore formation in Saccharomyces cerevisiae. J Cell Biol *44*, 688-692.

Maier, P., Rathfelder, N., Finkbeiner, M.G., Taxis, C., Mazza, M., Le Panse, S., Haguenauer-Tsapis, R., and Knop, M. (2007). Cytokinesis in yeast meiosis depends on the regulated removal of Ssp1p from the prospore membrane. EMBO J *26*, 1843-1852.

Mastronarde, D.N. (2005). Automated electron microscope tomography using robust prediction of specimen movements. J Struct Biol *152*, 36-51.

McCormick, S. (1993). Male Gametophyte Development. Plant Cell *5*, 1265-1275.

Miller, J.H. (1972). Experiments in Molecular Genetics. Cold Spring Harbor Laboratory Press: Cold Spring Harbor, NY.

Moens, P.B., and Rapport, E. (1971). Spindles, spindle plaques, and meiosis in the yeast *Saccharomyces cerevisiae* (Hansen). J Cell Biol *50*, 344-361.

Moreno-Borchart, A.C., and Knop, M. (2003). Prospore membrane formation: how budding yeast gets shaped in meiosis. Microbiol Res *158*, 83-90.

Moreno-Borchart, A.C., Strasser, K., Finkbeiner, M.G., Shevchenko, A., and Knop, M. (2001). Prospore membrane formation linked to the leading edge protein (LEP) coat assembly. EMBO J *20*, 6946-6957.

Muller, E.G., Snydsman, B.E., Novik, I., Hailey, D.W., Gestaut, D.R., Niemann, C.A., O'Toole, E.T., Giddings, T.H., Jr., Sundin, B.A., and Davis, T.N. (2005). The

organization of the core proteins of the yeast spindle pole body. Mol Biol Cell *16*, 3341-3352.

Mumberg, D., Muller, R., and Funk, M. (1995). Yeast vectors for the controlled expression of heterologous proteins in different genetic backgrounds. Gene *156*, 119-122.

Nakanishi, H., de los Santos, P., and Neiman, A.M. (2004). Positive and negative regulation of a SNARE protein by control of intracellular localization. Mol Biol Cell *15*, 1802-1815.

Nakanishi, H., Morishita, M., Schwartz, C.L., Coluccio, A., Engebrecht, J., and Neiman, A.M. (2006). Phospholipase D and the SNARE Sso1p are necessary for vesicle fusion during sporulation in yeast. J Cell Sci *119*, 1406-1415.

Nakase, Y., Nakamura-Kubo, M., Ye, Y., Hirata, A., Shimoda, C., and Nakamura, T. (2008). Meiotic spindle pole bodies acquire the ability to assemble the spore plasma membrane by sequential recruitment of sporulation-specific components in fission yeast. Mol Biol Cell *19*, 2476-2487.

Neiman, A.M. (1998). Prospore membrane formation defines a developmentally regulated branch of the secretory pathway in yeast. J Cell Biol *140*, 29-37.

Neiman, A.M. (2005). Ascospore formation in the yeast *Saccharomyces cerevisiae*. Microbiol Mol Biol Rev *69*, 565-584.

Neiman, A.M., Katz, L., and Brennwald, P.J. (2000). Identification of domains required for developmentally regulated SNARE function in *Saccharomyces cerevisiae*. Genetics *155*, 1643-1655.

Nickas, M.E., Diamond, A.E., Yang, M.J., and Neiman, A.M. (2004). Regulation of spindle pole function by an intermediary metabolite. Mol Biol Cell *15*, 2606-2616.

Nickas, M.E., and Neiman, A.M. (2002). Ady3p links spindle pole body function to spore wall synthesis in Saccharomyces cerevisiae. Genetics *160*, 1439-1450.

Nickas, M.E., Schwartz, C., and Neiman, A.M. (2003). Ady4p and Spo74p are components of the meiotic spindle pole body that promote growth of the prospore membrane in *Saccharomyces cerevisiae*. Eukaryot Cell *2*, 431-445.

Novick, P., Field, C., and Schekman, R. (1980). Identification of 23 complementation groups required for post-translational events in the yeast secretory pathway. Cell *21*, 205-215.

O'Toole, E.T., Winey, M., and McIntosh, J.R. (1999). High-voltage electron tomography of spindle pole bodies and early mitotic spindles in the yeast *Saccharomyces cerevisiae*. Mol Biol Cell *10*, 2017-2031.

Pak, J., and Segall, J. (2002). Regulation of the premiddle and middle phases of expression of the NDT80 gene during sporulation of Saccharomyces cerevisiae. Mol Cell Biol *22*, 6417-6429.

Palade, G. (1975). Intracellular Aspects of the Process of Protein Synthesis. Science *189*, 867.

Percival-Smith, A., and Segall, J. (1984). Isolation of DNA sequences preferentially expressed during sporulation in Saccharomyces cerevisiae. Mol Cell Biol *4*, 142-150.

Pereira, G., Tanaka, T.U., Nasmyth, K., and Schiebel, E. (2001). Modes of spindle pole body inheritance and segregation of the Bfa1p-Bub2p checkpoint protein complex. EMBO J *20*, 6359-6370.

Primig, M., Williams, R.M., Winzeler, E.A., Tevzadze, G.G., Conway, A.R., Hwang, S.Y., Davis, R.W., and Esposito, R.E. (2000). The core meiotic transcriptome in budding yeasts. Nat Genet *26*, 415-423.

Reinke, C.A., Kozik, P., and Glick, B.S. (2004). Golgi inheritance in small buds of *Saccharomyces cerevisiae* is linked to endoplasmic reticulum inheritance. Proc Natl Acad Sci U S A *101*, 18018-18023.

Riedel, C.G., Mazza, M., Maier, P., Korner, R., and Knop, M. (2005). Differential requirement for phospholipase D/Spo14 and its novel interactor Sma1 for regulation of exocytotic vesicle fusion in yeast meiosis. J Biol Chem *280*, 37846-37852.

Robinow, C.F., and Marak, J. (1966). A fiber apparatus in the nucleus of the yeast cell. J Cell Biol *29*, 129-151.

Rose, K., Rudge, S.A., Frohman, M.A., Morris, A.J., and Engebrecht, J. (1995). Phospholipase D signaling is essential for meiosis. Proc Natl Acad Sci U S A *92*, 12151-12155.

Rose, M.D., G.R. Fink. (1990). Methods in Yeast Genetics. Cold Spring Harbor Laboratory Press: Cold Spring Harbor, NY.

Rossanese, O.W., and Glick, B.S. (2001). Deconstructing Golgi inheritance. Traffic *2*, 589-596.

Rossi, G., Kolstad, K., Stone, S., Palluault, F., and Ferro-Novick, S. (1995). BET3 encodes a novel hydrophilic protein that acts in conjunction with yeast SNAREs. Mol Biol Cell *6*, 1769-1780.

Rothman, J.E. (1994). Mechanisms of intracellular protein transport. Nature *372*, 55-63.

Rout, M.P., and Kilmartin, J.V. (1990). Components of the yeast spindle and spindle pole body. J Cell Biol *111*, 1913-1927.

Rudge, S.A., Morris, A.J., and Engebrecht, J. (1998). Relocalization of phospholipase D activity mediates membrane formation during meiosis. J Cell Biol *140*, 81-90.

Rudge, S.A., Pettitt, T.R., Zhou, C., Wakelam, M.J., and Engebrecht, J.A. (2001). *SPO14* separation-of-function mutations define unique roles for phospholipase D in secretion and cellular differentiation in *Saccharomyces cerevisiae*. Genetics *158*, 1431-1444.

Sacher, M., Kim, Y.G., Lavie, A., Oh, B.H., and Segev, N. (2008). The TRAPP complex: insights into its architecture and function. Traffic *9*, 2032-2042.

Schaerer, F., Morgan, G., Winey, M., and Philippsen, P. (2001). Cnm67p is a spacer protein of the *Saccharomyces cerevisiae* spindle pole body outer plaque. Mol Biol Cell *12*, 2519-2533.

Shafaatian, R., Payton, M.A., and Reid, J.D. (1996). PWP2, a member of the WD-repeat family of proteins, is an essential Saccharomyces cerevisiae gene involved in cell separation. Mol Gen Genet *252*, 101-114.

Sobel, S.G., and Snyder, M. (1995). A highly divergent gamma-tubulin gene is essential for cell growth and proper microtubule organization in Saccharomyces cerevisiae. J Cell Biol *131*, 1775-1788.

Sogaard, M., Tani, K., Ye, R.R., Geromanos, S., Tempst, P., Kirchhausen, T., Rothman, J.E., and Sollner, T. (1994). A rab protein is required for the assembly of SNARE complexes in the docking of transport vesicles. Cell *78*, 937-948.

Sollner, T., Whiteheart, S.W., Brunner, M., Erdjument-Bromage, H., Geromanos, S., Tempst, P., and Rothman, J.E. (1993). SNAP receptors implicated in vesicle targeting and fusion. Nature *362*, 318-324.

Soues, S., and Adams, I.R. (1998). SPC72: a spindle pole component required for spindle orientation in the yeast Saccharomyces cerevisiae. J Cell Sci *111 (Pt 18)*, 2809-2818.

Stade, K., Ford, C.S., Guthrie, C., and Weis, K. (1997). Exportin 1 (Crm1p) is an essential nuclear export factor. Cell *90*, 1041-1050.

Staehelin, L.A., and Hepler, P.K. (1996). Cytokinesis in higher plants. Cell *84*, 821-824.

Straight, P.D., Giddings, T.H., Jr., and Winey, M. (2000). Mps1p regulates meiotic spindle pole body duplication in addition to having novel roles during sporulation. Mol Biol Cell *11*, 3525-3537.

Suda, Y., Nakanishi, H., Mathieson, E.M., and Neiman, A.M. (2007). Alternative modes of organellar segregation during sporulation in *Saccharomyces cerevisiae*. Eukaryot Cell *6*, 2009-2017.

Sun, G.H., Hirata, A., Ohya, Y., and Anraku, Y. (1992). Mutations in yeast calmodulin cause defects in spindle pole body functions and nuclear integrity. J Cell Biol *119*, 1625-1639.

Sundin, B.A., Chiu, C.H., Riffle, M., Davis, T.N., and Muller, E.G. (2004). Localization of proteins that are coordinately expressed with Cln2 during the cell cycle. Yeast *21*, 793-800.

Taxis, C., Keller, P., Kavagiou, Z., Jensen, L.J., Colombelli, J., Bork, P., Stelzer, E.H., and Knop, M. (2005). Spore number control and breeding in *Saccharomyces cerevisiae*: a key role for a self-organizing system. J Cell Biol *171*, 627-640.

TerBush, D.R., Maurice, T., Roth, D., and Novick, P. (1996). The Exocyst is a multiprotein complex required for exocytosis in *Saccharomyces cerevisiae*. EMBO J *15*, 6483-6494.

Tokuyasu, K.T., Peacock, W.J., and Hardy, R.W. (1972). Dynamics of spermiogenesis in *Drosophila melanogaster*. II. Coiling process. Z Zellforsch Mikrosk Anat *127*, 492-525.

Tu, J., and Carlson, M. (1994). The GLC7 type 1 protein phosphatase is required for glucose repression in Saccharomyces cerevisiae. Mol Cell Biol *14*, 6789-6796.

van Meer, G., and Sprong, H. (2004). Membrane lipids and vesicular traffic. Curr Opin Cell Biol *16*, 373-378.

Verhage, M., and Sorensen, J.B. (2008). Vesicle docking in regulated exocytosis. Traffic *9*, 1414-1424.

Vershon, A.K., and Pierce, M. (2000). Transcriptional regulation of meiosis in yeast. Curr Opin Cell Biol *12*, 334-339.

Vojtek, A.B., Hollenberg, S.M., and Cooper, J.A. (1993). Mammalian Ras interacts directly with the serine/threonine kinase Raf. Cell *74*, 205-214.

Wach, A., Brachat, A., Alberti-Segui, C., Rebischung, C., and Philippsen, P. (1997). Heterologous HIS3 marker and GFP reporter modules for PCR-targeting in Saccharomyces cerevisiae. Yeast *13*, 1065-1075.

Walch-Solimena, C., Collins, R.N., and Novick, P.J. (1997). Sec2p mediates nucleotide exchange on Sec4p and is involved in polarized delivery of post-Golgi vesicles. J Cell Biol *137*, 1495-1509.

Weimbs, T., Mostov, K., Low, S.H., and Hofmann, K. (1998). A model for structural similarity between different SNARE complexes based on sequence relationships. Trends Cell Biol *8*, 260-262.

Wickner, W., and Schekman, R. (2008). Membrane fusion. Nat Struct Mol Biol *15*, 658-664.

Wigge, P.A., Jensen, O.N., Holmes, S., Soues, S., Mann, M., and Kilmartin, J.V. (1998). Analysis of the *Saccharomyces* spindle pole by matrix-assisted laser desorption/ionization (MALDI) mass spectrometry. J Cell Biol *141*, 967-977.

Yang, H.J., Nakanishi, H., Liu, S., McNew, J.A., and Neiman, A.M. (2008). Binding interactions control SNARE specificity in vivo. J Cell Biol *183*, 1089-1100.

Appendix I: Yeast Strains

Strain	Genotype	Source Grandparents
EMD1	*MAT**a**/MATα ARG4/arg4-NspI his3SK/his3SK ho::LYS2/ho::LYS2 leu2/leu2 lys2/lys2 RME1/rme1::LEU2 trp1::hisG/trp1::hisG ura3/ura3 MPC54/mpc54Δ::his5*	AN117-4B x NY51
EMD3	*MAT**a**/MATα ARG4/arg4-NspI his3ΔSK/his3ΔSK hoΔ::LYS2/hoΔ::LYS2 leu2/leu2 lys2/lys2 RME1/rme1Δ::LEU2 trp1::hisG/trp1::hisG ura3/ura3 sso1Δ::his5+/sso1Δ::his5+ SPC42-GFP::kanMX4/SPC42-GFP::kanMX4*	Chapter 3 ESM440 x HI1
EMD4	*MAT**a**/MATα ARG4/arg4-NspI his3ΔSK/his3ΔSK hoΔ::LYS2/hoΔ::LYS2 leu2/leu2 lys2/lys2 RME1/rme1Δ::LEU2 trp1::hisG/trp1::hisG ura3/ura3 CNM67-GFP::his5+/CNM67-GFP::his5+*	Chapter 3 ADY138 x ADY135
EMD5	*MAT**a**/MATα ARG4/arg4-NspI his3ΔSK/his3ΔSK hoΔ::LYS2/hoΔ::LYS2 leu2/leu2 lys2/lys2 RME1/rme1Δ::LEU2 trp1::hisG/trp1::hisG ura3/ura3 sso1Δ::his5+/sso1Δ::his5+ NUD1-YFP/NUD1-YFP*	AN1122 x HI1
EMD6	*MAT**a**/MATα ARG4/arg4-NspI his3ΔSK/his3ΔSK hoΔ::LYS2/hoΔ::LYS2 leu2/leu2 lys2/lys2 RME1/rme1Δ::LEU2 trp1::hisG/trp1::hisG ura3/ura3 sso1Δ::his5+/sso1Δ::his5+ CNM67-GFP::his5+/CNM67-GFP::his5+*	Chapter 3 ADY138 x HI1
EMD7	*MAT**a**/MATα ARG4/arg4-NspI his3ΔSK/his3ΔSK hoΔ::LYS2/hoΔ::LYS2 leu2/leu2 lys2/lys2 RME1/rme1Δ::LEU2 trp1::hisG/trp1::hisG ura3/ura3 mso1Δ::his5+ /mso1Δ::his5+ MPC54-GFP::his5+ / MPC54-GFP::his5+*	HI31 x NY76
EMD9	*MAT**a**/MATα ARG4/arg4-NspI his3ΔSK/his3ΔSK hoΔ::LYS2/hoΔ::LYS2 leu2/leu2 lys2/lys2 RME1/rme1Δ::LEU2 trp1::hisG/trp1::hisG ura3/ura3 gip1Δ::HIS3 / gip1Δ::HIS3 cyhR canR MPC54-GFP::his5+ / MPC54-GFP::his5+*	AN104-1D x NY76

Strain	Genotype	Source Grandparents
EMD10	*MAT***a**/*MATα ARG4/arg4-NspI his3ΔSK/his3ΔSK ho::LYS2/ho::LYS2 leu2/leu2 lys2/lys2 RME1/rme1::LEU2 trp1::hisG/trp1::hisG ura3/ura3 sso1::his5+/sso1::his5+ ady4::HIS3MX6/ady4::HIS3MX6*	Chapter 3 AN1119 x HI1
EMD11	*MAT***a**/*MATα ARG4/arg4-NspI his3ΔSK/his3ΔSK ho::LYS2/ho::LYS2 leu2/leu2 lys2/lys2 RME1/rme1::LEU2 trp1::hisG/trp1::hisG ura3/ura3 sso1::his5+/sso1::his5+ mpc54-RFP^{145}::TRP1/ mpc54-RFP^{145}::TRP1*	NY66 x EMH6
EMD12	*MAT***a**/*MATα ARG4/arg4-NspI his3ΔSK/his3ΔSK ho::LYS2/ho::LYS2 leu2/leu2 lys2/lys2 RME1/rme1::LEU2 trp1::hisG/trp1::hisG ura3/ura3 ady4::HIS3MX6/ady4::HIS3MX6 mpc54-RFP^{145}::TRP1/ mpc54-RFP^{145}::TRP1*	AN1069 x EMH6
EMD13	*MAT***a**/*MATα ARG4/arg4-NspI his3SK/his3SK ho::LYS2/ho::LYS2 leu2/leu2 lys2/lys2 RME1/rme1::LEU2 trp1::hisG/trp1::hisG ura3/ura3 MPC54 / MPC54-RFP::TRP1*	AN117-4B x EMH7 no dissection
EMD15	*MAT***a**/*MATα ARG4/arg4-NspI his3SK/his3SK ho::LYS2/ho::LYS2 leu2/leu2 lys2/lys2 RME1/rme1::LEU2 trp1::hisG/trp1::hisG ura3/ura3 MPC54 / mpc54-47-RFP::TRP1*	AN117-4B x EMH8 no dissection
EMD17	*MAT***a**/*MATα ARG4/arg4-NspI his3SK/his3SK ho::LYS2/ho::LYS2 leu2/leu2 lys2/lys2 RME1/rme1::LEU2 trp1::hisG/trp1::hisG ura3/ura3 MPC54 / mpc54-119-RFP::TRP1*	AN117-4B x EMH26 no dissection
EMD19	*MAT***a**/*MATα ARG4/arg4-NspI his3SK/his3SK ho::LYS2/ho::LYS2 leu2/leu2 lys2/lys2 RME1/rme1::LEU2 trp1::hisG/trp1::hisG ura3/ura3 MPC54-GFP::his5+ / MPC54-RFP::TRP1*	NY77 x EMH7 no dissection

Strain	Genotype	Source Grandparents
EMD20	*MAT**a**/MATα ARG4/arg4-NspI his3SK/his3SK ho::LYS2/ho::LYS2 leu2/leu2 lys2/lys2 RME1/rme1::LEU2 trp1::hisG/trp1::hisG ura3/ura3 MPC54-GFP::his5+ / mpc54-40-RFP::TRP1*	AN117-4B x EMH24 no dissection
EMD21	*MAT**a**/MATα ARG4/arg4-NspI his3SK/his3SK ho::LYS2/ho::LYS2 leu2/leu2 lys2/lys2 RME1/rme1::LEU2 trp1::hisG/trp1::hisG ura3/ura3 MPC54-GFP::his5+ / mpc54-47-RFP::TRP1*	AN117-4B x EMH8 no dissection
EMD22	*MAT**a**/MATα ARG4/arg4-NspI his3SK/his3SK ho::LYS2/ho::LYS2 leu2/leu2 lys2/lys2 RME1/rme1::LEU2 trp1::hisG/trp1::hisG ura3/ura3 MPC54-GFP::his5+ / mpc54-118-RFP::TRP1*	AN117-4B x EMH25 no dissection
EMD23	*MAT**a**/MATα ARG4/arg4-NspI his3SK/his3SK ho::LYS2/ho::LYS2 leu2/leu2 lys2/lys2 RME1/rme1::LEU2 trp1::hisG/trp1::hisG ura3/ura3 MPC54-GFP::his5+ / mpc54-119-RFP::TRP1*	AN117-4B x EMH26 no dissection
EMD24	*MAT**a**/MATα ARG4/arg4-NspI his3SK/his3SK ho::LYS2/ho::LYS2 leu2/leu2 lys2/lys2 RME1/rme1::LEU2 trp1::hisG/trp1::hisG ura3/ura3 MPC54-GFP::his5+ / mpc54-145-RFP::TRP1*	AN117-4B x EMH27 no dissection
EMD25	*MAT**a**/MATα ARG4/arg4-NspI his3SK/his3SK ho::LYS2/ho::LYS2 leu2/leu2 lys2/lys2 RME1/rme1::LEU2 trp1::hisG/trp1::hisG ura3/ura3 mpc54-118::TRP1 / mpc54-118::TRP1*	AN117-4B x EMH25 no dissection
EMD26	*MAT**a**/MATα ARG4/arg4-NspI his3SK/his3SK ho::LYS2/ho::LYS2 leu2/leu2lys2/lys2 RME1/rme1::LEU2 trp1::hisG/trp1::hisG ura3/ura3 mpc54Δ::his5/ mpc54Δ::his5 MPC54-RFP::TRP1/ MPC54-RFP::TRP1*	Chapter 2 EMH1 x EMH7
EMD27	*MAT**a**/MATα ARG4/arg4-NspI his3SK/his3SK ho::LYS2/ho::LYS2 leu2/leu2lys2/lys2 RME1/rme1::LEU2 trp1::hisG/trp1::hisG ura3/ura3 mpc54Δ::his5/ mpc54Δ::his5 mpc54-RFP^{40}::TRP1/ mpc54-RFP^{40}::TRP1*	Chapter 2 EMH2 x EMH24

Strain	Genotype	Source Grandparents
EMD28	*MAT***a**/*MATα ARG4/arg4-NspI his3SK/his3SK ho::LYS2/ho::LYS2 leu2/leu2lys2/lys2 RME1/rme1::LEU2 trp1::hisG/trp1::hisG ura3/ura3 mpc54Δ::his5/ mpc54Δ::his5 mpc54-RFP^{47}::TRP1/ mpc54-RFP^{47}::TRP1*	Chapter 2 EMH3 x EMH8
EMD29	*MAT***a**/*MATα ARG4/arg4-NspI his3SK/his3SK ho::LYS2/ho::LYS2 leu2/leu2lys2/lys2 RME1/rme1::LEU2 trp1::hisG/trp1::hisG ura3/ura3 mpc54Δ::his5/ mpc54Δ::his5 mpc54-RFP^{118}::TRP1/ mpc54-RFP^{118}::TRP1*	Chapter 2 EMH4 x EMH25
EMD31	*MAT***a**/*MATα ARG4/arg4-NspI his3SK/his3SK ho::LYS2/ho::LYS2 leu2/leu2lys2/lys2 RME1/rme1::LEU2 trp1::hisG/trp1::hisG ura3/ura3 mpc54Δ::his5/ mpc54Δ::his5 mpc54-RFP^{145}::TRP1/ mpc54-RFP^{145}::TRP1*	Chapter 2 EMH6 x EMH27
EMD32	*MAT***a**/*MATα ARG4/arg4-NspI his3SK/his3SK ho::LYS2/ho::LYS2 leu2/leu2lys2/lys2 RME1/rme1::LEU2 trp1::hisG/trp1::hisG ura3/ura3 mpc54Δ::his5/ mpc54Δ::his5 spo74Δ::HIS3MX6/ spo74Δ::HIS3MX6*	NY51 x MNH39
EMD33	*MAT***a**/*MATα ARG4/arg4-NspI his3SK/his3SK ho::LYS2/ho::LYS2 leu2/leu2 lys2/lys2 RME1/rme1::LEU2 trp1::hisG/trp1::hisG ura3/ura3 mpc54Δ::his5/ mpc54Δ::his5 spo74Δ::HIS3MX6/ spo74Δ::HIS3MX6 spo21Δ::TRP1 / spo21Δ::TRP1*	(NY51 x MNH39) x AN1064
EMD34	*MAT***a**/*MATα ARG4/arg4-NspI his3SK/his3SK ho::LYS2/ho::LYS2 leu2/leu2 lys2/lys2 RME1/rme1::LEU2 trp1::hisG/trp1::hisG ura3/ura3 spo74Δ::HIS3MX6/ spo74Δ::HIS3MX6 spo21Δ::TRP1 / spo21Δ::TRP1*	AN1120 x AN1064
EMD35	*MAT***a**/*MATα ARG4/arg4-NspI his3SK/his3SK ho::LYS2/ho::LYS2 leu2/leu2 lys2/lys2 RME1/rme1::LEU2 trp1::hisG/trp1::hisG ura3/ura3 mpc54Δ::his5/ mpc54Δ::his5 spo21Δ::TRP1 / spo21Δ::TRP1*	NY51 x AN1064

Strain	Genotype	Source Grandparents
EMD50	*MAT***a**/*MATα ARG4/arg4-NspI his3SK/his3SK ho::LYS2/ho::LYS2 leu2/leu2lys2/lys2 RME1/rme1::LEU2 trp1::hisG/trp1::hisG ura3/ura3 spo74Δ::HIS3MX6/ spo74Δ::HIS3MX6 SPO74::TRP1/ SPO74::TRP1*	Chapter 2
EMD51	*MAT***a**/*MATα ARG4/arg4-NspI his3SK/his3SK ho::LYS2/ho::LYS2 leu2/leu2lys2/lys2 RME1/rme1::LEU2 trp1::hisG/trp1::hisG ura3/ura3 spo74Δ::HIS3MX6/ spo74Δ::HIS3MX6 spo74-243::TRP1/ spo74-243::TRP1*	Chapter 2
EMD52	*MAT***a**/*MATα ARG4/arg4-NspI his3SK/his3SK ho::LYS2/ho::LYS2 leu2/leu2lys2/lys2 RME1/rme1::LEU2 trp1::hisG/trp1::hisG ura3/ura3 KlURA3-*P_{MPC54}*-YFP::SPO21/ KlURA3-*P_{MPC54}*-YFP::SPO21 CgTRP1-*P_{MPC54}*-CFP::MPC54/ CgTRP1-*P_{MPC54}*-CFP::MPC54*	Chapter 2
EMD53	*MAT***a**/*MATα ARG4/arg4-NspI his3SK/his3SK ho::LYS2/ho::LYS2 leu2/leu2lys2/lys2 RME1/rme1::LEU2 trp1::hisG/trp1::hisG ura3/ura3 KlURA3-*P_{MPC54}*-YFP::SPO74/ KlURA3-*P_{MPC54}*-YFP::SPO74 CgTRP1-*P_{MPC54}*-CFP::MPC54/ CgTRP1-*P_{MPC54}*-CFP::MPC54*	Chapter 2
EMD56	*MAT***a**/*MATα ARG4/arg4-NspI his3SK/his3SK ho::LYS2/ho::LYS2 leu2/leu2lys2/lys2 RME1/rme1::LEU2 trp1::hisG/trp1::hisG ura3/ura3 spo74Δ::HIS3MX6/ spo74Δ::HIS3MX6 spo74-145::TRP1/ spo74-145::TRP1*	Chapter 2
EMD57	*MAT***a**/*MATα ARG4/arg4-NspI his3SK/his3SK ho::LYS2/ho::LYS2 leu2/leu2lys2/lys2 RME1/rme1::LEU2 trp1::hisG/trp1::hisG ura3/ura3 spo74Δ::HIS3MX6/ spo74Δ::HIS3MX6 spo74-180::TRP1/ spo74-180::TRP1*	Chapter 2

Strain	Genotype	Source Grandparents
EMD58	*MAT***a**/*MATα ARG4/arg4-NspI his3SK/his3SK ho*::*LYS2/ho*::*LYS2 leu2/leu2 lys2/lys2 RME1/rme1*::*LEU2 trp1*::*hisG/trp1*::*hisG ura3/ura3 sec2-41::HIS / sec2-41::HIS*	AN117-4B x AN60-5B
EMD60	*MAT***a**/*MATα ARG4*/*arg4-NspI his3ΔSK*/*his3ΔSK hoΔ::LYS2*/*hoΔ::LYS2 leu2*/*leu2 lys2*/*lys2 RME1*/*rme1Δ::LEU2 trp1::hisG*/*trp1::hisG ura3*/*ura3 sso1Δ::his5+/sso1Δ::his5+ CgTRP1- P $_{MPC54}$-CFP::SPO74/ CgTRP1- P $_{MPC54}$-CFP::SPO74 KlURA3-P$_{MPC54}$-YFP::SPO21/ KlURA3-P$_{MPC54}$-YFP::SPO21*	YS392 x HI2
EMD62	*MAT***a**/*MATα ARG4*/*arg4-NspI his3ΔSK*/*his3ΔSK hoΔ::LYS2*/*hoΔ::LYS2 leu2*/*leu2 lys2*/*lys2 RME1*/*rme1Δ::LEU2 trp1::hisG*/*trp1::hisG ura3*/*ura3 sso1Δ::his5+/sso1Δ::his5+ KlURA3-P$_{MPC54}$-YFP::SPO74/ KlURA3-P$_{MPC54}$-YFP::SPO74 SPO21-CFP::his5/ SPO21-CFP::his5*	YS145 x HI2
EMD63	*MAT***a**/*MATα ARG4*/*arg4-NspI his3ΔSK*/*his3ΔSK hoΔ::LYS2*/*hoΔ::LYS2 leu2*/*leu2 lys2*/*lys2 RME1*/*rme1Δ::LEU2 trp1::hisG*/*trp1::hisG ura3*/*ura3 sso1Δ::his5+/sso1Δ::his5+ CgTRP1-P$_{MPC54}$-CFP::MPC54/ CgTRP1-P$_{MPC54}$-CFP::MPC54 SPO74::YFP-HIS3MX6 /SPO74::YFP-HIS3MX6*	YS320 x HI2
EMD64	*MAT***a**/*MATα ARG4*/*arg4-NspI his3ΔSK*/*his3ΔSK hoΔ::LYS2*/*hoΔ::LYS2 leu2*/*leu2 lys2*/*lys2 RME1*/*rme1Δ::LEU2 trp1::hisG*/*trp1::hisG ura3*/*ura3 sso1Δ::his5+/sso1Δ::his5+ CgTRP1-P$_{MPC54}$-CFP::SPO21/ CgTRP1-P$_{MPC54}$-CFP::SPO21 SPO74::YFP-HIS3MX6 /SPO74::YFP-HIS3MX6*	YS348 x HI2

Strain	Genotype	Source Grandparents
EMD65	*MAT***a**/*MAT*α *ARG4*/*arg4-NspI his3ΔSK*/*his3ΔSK ho*Δ*::LYS2*/*ho*Δ*::LYS2 leu2*/*leu2 lys2*/*lys2 RME1*/*rme1*Δ*::LEU2 trp1::hisG*/*trp1::hisG ura3*/*ura3 sso1*Δ*::his5+*/*sso1*Δ*::his5+ CgTRP1-*P_{CNM67}*-CFP::CNM67*/ *CgTRP1-*P_{CNM67}*-CFP::CNM67 KlURA3-*P_{MPC54}*-YFP::SPO74*/ *KlURA3-*P_{MPC54}*-YFP::SPO74*	YS183 x HI2
EMD66	*MAT***a**/*MAT*α *ARG4*/*arg4-NspI his3ΔSK*/*his3ΔSK ho*Δ*::LYS2*/*ho*Δ*::LYS2 leu2*/*leu2 lys2*/*lys2 RME1*/*rme1*Δ*::LEU2 trp1::hisG*/*trp1::hisG ura3*/*ura3 sso1*Δ*::his5+*/*sso1*Δ*::his5+ CgTRP1-*P_{CNM67}*-CFP::CNM67*/ *CgTRP1-*P_{CNM67}*-CFP::CNM67 MPC54-YFP::his5+*/ *MPC54-YFP::his5+*	YS162 x HI2
EMD67	*MAT***a**/*MAT*α *ARG4*/*arg4-NspI his3ΔSK*/*his3ΔSK ho*Δ*::LYS2*/*ho*Δ*::LYS2 leu2*/*leu2 lys2*/*lys2 RME1*/*rme1*Δ*::LEU2 trp1::hisG*/*trp1::hisG ura3*/*ura3 sso1*Δ*::his5+*/*sso1*Δ*::his5+ CgTRP1-*P_{CNM67}*-CFP::CNM67*/ *CgTRP1-*P_{CNM67}*-CFP::CNM67 SPO21::YFP-CgTRP*/ *SPO21::YFP-CgTRP1*	YS168 x HI2
EMD68	*MAT***a**/*MAT*α *ARG4*/*arg4-NspI his3ΔSK*/*his3ΔSK ho*Δ*::LYS2*/*ho*Δ*::LYS2 leu2*/*leu2 lys2*/*lys2 RME1*/*rme1*Δ*::LEU2 trp1::hisG*/*trp1::hisG ura3*/*ura3 spo74*Δ*::his5+*/*spo74*Δ*::his5+ MPC54-GFP::his5+* / *MPC54-GFP:: his5+*	NY76 x AN1120
EMD69	*MAT***a**/*MAT*α *ARG4*/*arg4-NspI his3ΔSK*/*his3ΔSK ho*Δ*::LYS2*/*ho*Δ*::LYS2 leu2*/*leu2 lys2*/*lys2 RME1*/*rme1*Δ*::LEU2 trp1::hisG*/*trp1::hisG ura3*/*ura3 ady4*Δ*::HIS3MX6/ady4*Δ*::HIS3MX6 sec2ts::his+* / *sec2ts::his+*	AN1119 x EMH51
EMD70	*MAT***a**/*MAT*α *ARG4*/*arg4-NspI ho*Δ*::LYS2*/*ho*Δ*::LYS2 leu2*/*leu2 lys2*/*lys2 RME1*/*rme1*Δ*::LEU2 trp1::hisG*/*trp1::hisG ura3*/*ura3 his3ΔSK*/*his3ΔSK ady4*Δ*::his5+*/*ady4*Δ*::his5+ mpc54*Δ*::his5+*/*mpc54*Δ*::his5+*	AN117-4B x AN300-2A

Strain	Genotype	Source Grandparents
EMD71	*MAT***a**/*MAT*α *ARG4/arg4-NspI his3SK/his3SK ho::LYS2/ho::LYS2 leu2/leu2lys2/lys2 RME1/rme1::LEU2 trp1::hisG/trp1::hisG ura3/ura3 ylr301wΔ:: TRP1/ ylr301wΔ::TRP1*	Chapter 2
EMD72	*MAT***a**/*MAT*α *ARG4*/*arg4-NspI his3ΔSK/his3ΔSK hoΔ::LYS2*/*hoΔ::LYS2 leu2*/*leu2 lys2*/*lys2 RME1*/*rme1Δ::LEU2 trp1::hisG*/*trp1::hisG ura3*/*ura3 sso1Δ::his5+/sso1Δ::his5+ CgTRP1-P_{CNM67}-CFP::CNM67/ CgTRP1-P_{CNM67}-CFP::CNM67 SPO74::YFP-HIS3MX6 /SPO74::YFP-HIS3MX6*	YS171 x HI2
EMD73	*MAT***a**/*MAT*α *ARG4/arg4-NspI his3SK/his3SK ho::LYS2/ho::LYS2 leu2/leu2lys2/lys2 RME1/rme1::LEU2 trp1::hisG/trp1::hisG ura3/ura3 ylr301wΔ:: TRP1/ ylr301wΔ::TRP1 ady4Δ::HIS3MX6/ady4Δ::HIS3MX6*	AN1119 x EMH77
EMD74	*MAT***a**/*MAT*α *ARG4/arg4-NspI his3SK/his3SK ho::LYS2/ho::LYS2 leu2/leu2lys2/lys2 RME1/rme1::LEU2 trp1::hisG/trp1::hisG ura3/ura3 ylr301wΔ:: TRP1/ ylr301wΔ::TRP1 mpc54-RFP^{118}::TRP1/ mpc54-RFP^{118}::TRP1*	EMH4 x EMH77
EMD75	*MAT***a**/*MAT*α *ARG4*/*arg4-NspI his3ΔSK/his3ΔSK hoΔ::LYS2*/*hoΔ::LYS2 leu2*/*leu2 lys2*/*lys2 RME1*/*rme1Δ::LEU2 trp1::hisG*/*trp1::hisG ura3*/*ura3 ady4Δ::his5+ / ady4Δ::his5+ CgTRP1-P_{MPC54}-CFP::SPO21/ CgTRP1-P_{MPC54}-CFP::SPO21 SPO74::YFP-HIS3MX6 /SPO74::YFP-HIS3MX6*	YS348 x AN1119
EMD76	*MAT***a**/*MAT*α *ARG4*/*arg4-NspI his3ΔSK/his3ΔSK hoΔ::LYS2*/*hoΔ::LYS2 leu2*/*leu2 lys2*/*lys2 RME1*/*rme1Δ::LEU2 trp1::hisG*/*trp1::hisG ura3*/*ura3 sma1Δ::his5+ / sma1Δ::his5+ CgTRP1-P_{MPC54}-CFP::SPO21/ CgTRP1-P_{MPC54}-CFP::SPO21 SPO74::YFP-HIS3MX6 /SPO74::YFP-HIS3MX6*	YS348 x HI40

Strain	Genotype	Source Grandparents
EMD77	*MAT***a**/*MATα ARG4/arg4-NspI his3ΔSK/his3ΔSK ho*Δ*::LYS2/ho*Δ*::LYS2 leu2/leu2 lys2/lys2 RME1/rme1*Δ*::LEU2 trp1::hisG/trp1::hisG ura3/ura3 spo14::URA3 / spo14::URA3 CgTRP1-P$_{MPC54}$-CFP::SPO21/ CgTRP1-P$_{MPC54}$-CFP::SPO21 SPO74::YFP-HIS3MX6 /SPO74::YFP-HIS3MX6*	YS348 x HI5
EMD79	*MAT***a**/*MATα ARG4/arg4-NspI his3SK/his3SK ho::LYS2/ho::LYS2 leu2/leu2lys2/lys2 RME1/rme1::LEU2 trp1::hisG/trp1::hisG ura3/ura3 SPO74::*YFP-*HIS3MX6* / *CgTRP1-P$_{MPC54}$-CFP::SPO74*	Chapter 2
EMD80	*MAT***a**/*MATα ARG4/arg4-NspI his3SK/his3SK ho::LYS2/ho::LYS2 leu2/leu2lys2/lys2 RME1/rme1::LEU2 trp1::hisG/trp1::hisG ura3/ura3 SPO74::*YFP-*HIS3MX6* / *SPO74::CFP::HIS3MX6*	YS114 x AN1124
EMD81	*MAT***a**/*MATα ARG4/arg4-NspI his3SK/his3SK ho::LYS2/ho::LYS2 leu2/leu2lys2/lys2 RME1/rme1::LEU2 trp1::hisG/trp1::hisG ura3/ura3 KlURA3-P$_{MPC54}$-YFP::SPO74/ CgTRP1-P$_{MPC54}$-CFP::SPO74*	YS323 x YS132
EMD82	*MAT***a**/*MATα ARG4/arg4-NspI his3SK/his3SK ho::LYS2/ho::LYS2 leu2/leu2lys2/lys2 RME1/rme1::LEU2 trp1::hisG/trp1::hisG ura3/ura3 KlURA3-P$_{MPC54}$-YFP::SPO74/ CgTRP1-P$_{MPC54}$-CFP::SPO74 sso1*Δ*::his5+/sso1*Δ*::his5+*	(YS323 x HI1) x (YS132xHI2)
EMD83	*MAT***a**/*MATα ARG4/arg4-NspI his3SK/his3SK ho::LYS2/ho::LYS2 leu2/leu2lys2/lys2 RME1/rme1::LEU2 trp1::hisG/trp1::hisG ura3/ura3 SPO74::*YFP-*HIS3MX6* / *SPO74::CFP::HIS3MX6 sso1*Δ*::his5+/sso1*Δ*::his5+*	(YS114 x HI2) x (MNH50 xHI1)

Strain	Genotype	Source Grandparents
EMD84	*MAT***a**/*MAT*α *ARG4/arg4-NspI his3SK/his3SK ho::LYS2/ho::LYS2 leu2/leu2lys2/lys2 RME1/rme1::LEU2 trp1::hisG/trp1::hisG ura3/ura3 SPO74::*YFP-*HIS3MX6 CgTRP1-*P_{MPC54}*-CFP::SPO74*	(YS323xHI1) x (MNH50xHI1)
EMD85	*MAT***a**/*MAT*α *ARG4/arg4-NspI his3ΔSK/his3ΔSK hoΔ::LYS2/hoΔ::LYS2 leu2/leu2lys2/lys2 RME1/rme1Δ::LEU2 trp1::hisG/trp1::hisG ura3/ura3 SPC42-GFP::kanMX4/SPC42-GFP::kanMX4*	Chapter 3
EMD86	*MAT***a**/*MATα ARG4/arg4-NspI his3ΔSK/his3ΔSK hoΔ::LYS2/hoΔ::LYS2 leu2/leu2lys2/lys2 RME1/rme1Δ::LEU2 trp1::hisG/trp1::hisG ura3/ura3 spo14Δ::ura3/spo14Δ::ura3 Tubulin-GFP::URA3 (p306AfS91)*	HI60 integrated
EMD87	*MAT***a**/*MAT*α *ARG4/arg4-NspI his3ΔSK/his3ΔSK hoΔ::LYS2/hoΔ::LYS2 leu2/leu2 lys2/lys2 RME1/rme1Δ::LEU2 trp1::hisG/trp1::hisG ura3/ura3 sso1Δ::his5+/sso1Δ::his5+ Tubulin-GFP::URA3 (p306AfS91)*	HI3 integrated
EMD88	*MAT***a**/*MAT*α *ARG4/arg4-NspI his3SK/his3SK hoΔ::LYS2/hoΔ::LYS2 leu2/leu2 lys2/lys2 ho::LYS2/ho::LYS2 leu2/leu2lys2/lys2 RME1/rme1::LEU2 trp1::hisG/trp1::hisG ura3/ura3 mpc54Δ::his5/ mpc54Δ::his5 Tubulin-GFP::URA3 (p306AfS91)*	NY541 integrated
EMD89	*MAT***a**/*MATα ARG4/arg4-NspI his3SK/his3SK ho::LYS2/ho::LYS2 leu2/leu2 lys2/lys2 RME1/rme1::LEU2 trp1::hisG/trp1::hisG ura3/ura3 Tubulin-GFP::URA3 (p306AfS91)*	AN120 integrated
EMD90	*MAT***a**/*MAT*α *ARG4/arg4-NspI his3SK/his3SK ho::LYS2/ho::LYS2 leu2/leu2lys2/lys2 RME1/rme1::LEU2 trp1::hisG/trp1::hisG ura3/ura3 NUD1::YFP::his5+/ NUD1-CFP::his5+*	Chapter 2

Strain	Genotype	Source Grandparents
EMD91	*MAT***a**/*MAT*α *ARG4/arg4-NspI his3SK/his3SK ho::LYS2/ho::LYS2 leu2/leu2lys2/lys2 RME1/rme1::LEU2 trp1::hisG/trp1::hisG ura3/ura3 KlURA3-*P_{CNM67}*-YFP::NUD1/ CgTRP1-*P_{CNM67}*-CFP::NUD1*	Chapter 2
EMD92	*MAT***a**/*MAT*α *ARG4/arg4-NspI his3SK/his3SK ho::LYS2/ho::LYS2 leu2/leu2lys2/lys2 RME1/rme1::LEU2 trp1::hisG/trp1::hisG ura3/ura3 KlURA3-*P_{CNM67}*-YFP::NUD1/ NUD1-CFP::his5*	Chapter 2
EMD93	*MAT***a**/*MAT*α *ARG4/arg4-NspI his3SK/his3SK ho::LYS2/ho::LYS2 leu2/leu2lys2/lys2 RME1/rme1::LEU2 trp1::hisG/trp1::hisG ura3/ura3 NUD1::YFP::his5/ CgTRP1-*P_{CNM67}*-CFP::NUD1*	Chapter 2
EMD94	*MAT***a**/*MAT*α *ARG4/arg4-NspI his3SK/his3SK ho::LYS2/ho::LYS2 leu2/leu2lys2/lys2 RME1/rme1::LEU2 trp1::hisG/trp1::hisG ura3/ura3 CNM67-YFP::his5/ CNM67::CFP-CgTRP1*	Chapter 2
EMD95	*MAT***a**/*MAT*α *ARG4/arg4-NspI his3SK/his3SK ho::LYS2/ho::LYS2 leu2/leu2lys2/lys2 RME1/rme1::LEU2 trp1::hisG/trp1::hisG ura3/ura3 KlURA3-* P_{CNM67}*-YFP::CNM67/ CgTRP1-*P_{CNM67}*-CFP::CNM67*	Chapter 2
EMD96	*MAT***a**/*MAT*α *ARG4/arg4-NspI his3SK/his3SK ho::LYS2/ho::LYS2 leu2/leu2lys2/lys2 RME1/rme1::LEU2 trp1::hisG/trp1::hisG ura3/ura3 KlURA3-* P_{CNM67}*-YFP::CNM67// CNM67::CFP-CgTRP1*	Chapter 2
EMD97	*MAT***a**/*MAT*α *ARG4/arg4-NspI his3SK/his3SK ho::LYS2/ho::LYS2 leu2/leu2lys2/lys2 RME1/rme1::LEU2 trp1::hisG/trp1::hisG ura3/ura3 CNM67-YFP::his5/ CgTRP1-*P_{CNM67}*-CFP::CNM67*	Chapter 2

Strain	Genotype	Source Grandparents
EMD98	*MAT***a**/*MATα ARG4/arg4-NspI his3SK/his3SK ho::LYS2/ho::LYS2 leu2/leu2lys2/lys2 RME1/rme1::LEU2 trp1::hisG/trp1::hisG ura3/ura3 SPO21::YFP-CgTRP/ SPO21-CFP::his5*	Chapter 2
EMD99	*MAT***a**/*MATα ARG4/arg4-NspI his3SK/his3SK ho::LYS2/ho::LYS2 leu2/leu2lys2/lys2 RME1/rme1::LEU2 trp1::hisG/trp1::hisG ura3/ura3 KlURA3-*P_{MPC54}*-YFP::SPO21/ CgTRP1-*P_{MPC54}*-CFP::SPO21*	Chapter 2
EMD100	*MAT***a**/*MATα ARG4/arg4-NspI his3SK/his3SK ho::LYS2/ho::LYS2 leu2/leu2lys2/lys2 RME1/rme1::LEU2 trp1::hisG/trp1::hisG ura3/ura3 KlURA3-*P_{MPC54}*-YFP::SPO21/ SPO21-CFP::his5*	Chapter 2
EMD101	*MAT***a**/*MATα ARG4/arg4-NspI his3SK/his3SK ho::LYS2/ho::LYS2 leu2/leu2lys2/lys2 RME1/rme1::LEU2 trp1::hisG/trp1::hisG ura3/ura3 SPO21::YFP-CgTRP/ CgTRP1-*P_{MPC54}*-CFP::SPO21*	Chapter 2
EMD102	*MAT***a**/*MATα ARG4/arg4-NspI his3SK/his3SK ho::LYS2/ho::LYS2 leu2/leu2lys2/lys2 RME1/rme1::LEU2 trp1::hisG/trp1::hisG ura3/ura3 SPO74::*YFP-*HIS3MX6* / *SPO74::linkerCFP ::his5+*	Chapter 2
EMD103	*MAT***a**/*MATα ARG4/arg4-NspI his3SK/his3SK ho::LYS2/ho::LYS2 leu2/leu2lys2/lys2 RME1/rme1::LEU2 trp1::hisG/trp1::hisG ura3/ura3 KlURA3-*P_{MPC54}*-YFP::SPO74/ CgTRP1-*P_{MPC54}*-CFP::SPO74*	Chapter 2
EMD104	*MAT***a**/*MATα ARG4/arg4-NspI his3SK/his3SK ho::LYS2/ho::LYS2 leu2/leu2lys2/lys2 RME1/rme1::LEU2 trp1::hisG/trp1::hisG ura3/ura3 MPC54-YFP::his5+/ MPC54::CFP-CgTRP1*	Chapter 2
EMD105	*MAT***a**/*MATα ARG4/arg4-NspI his3SK/his3SK ho::LYS2/ho::LYS2 leu2/leu2lys2/lys2 RME1/rme1::LEU2 trp1::hisG/trp1::hisG ura3/ura3 MPC54::KlURA3-*P_{MPC54}*-YFP/MPC54::CFP-CgTRP1*	Chapter 2

Strain	Genotype	Source Grandparents
EMD106	*MAT***a**/*MATα ARG4/arg4-NspI his3SK/his3SK ho::LYS2/ho::LYS2 leu2/leu2lys2/lys2 RME1/rme1::LEU2 trp1::hisG/trp1::hisG ura3/ura3 mpc54Δ::his5 / mpc54Δ::his5 mpc54-RFP^{119}::TRP1 / mpc54-RFP^{119}::TRP1*	EMH102 x EMH103
EMD107	*MAT***a**/*MATα ARG4/arg4-NspI his3SK/his3SK ho::LYS2/ho::LYS2 leu2/leu2lys2/lys2 RME1/rme1::LEU2 trp1::hisG/trp1::hisG ura3/ura3 MPC54::KlURA3-P$_{MPC54}$-YFP/ CgTRP1-P$_{MPC54}$-CFP::MPC54*	Chapter 2
EMD108	*MAT***a**/*MATα ARG4/arg4-NspI his3SK/his3SK ho::LYS2/ho::LYS2 leu2/leu2lys2/lys2 RME1/rme1::LEU2 trp1::hisG/trp1::hisG ura3/ura3 mpc54Δ::his5/ mpc54-RFP::TRP1*	NY51xEMH7
EMD109	*MAT***a**/*MATα ARG4/arg4-NspI his3SK/his3SK ho::LYS2/ho::LYS2 leu2/leu2lys2/lys2 RME1/rme1::LEU2 trp1::hisG/trp1::hisG ura3/ura3 mpc54Δ::his5/ mpc54-RFP^{40}::TRP1*	NY50xEMH2
EMD110	*MAT***a**/*MATα ARG4/arg4-NspI his3SK/his3SK ho::LYS2/ho::LYS2 leu2/leu2lys2/lys2 RME1/rme1::LEU2 trp1::hisG/trp1::hisG ura3/ura3 mpc54Δ::his5/ mpc54-RFP^{47}::TRP1*	NY50xEMH3
EMD111	*MAT***a**/*MATα ARG4/arg4-NspI his3SK/his3SK ho::LYS2/ho::LYS2 leu2/leu2lys2/lys2 RME1/rme1::LEU2 trp1::hisG/trp1::hisG ura3/ura3 mpc54Δ::his5/ mpc54-RFP^{118}::TRP1*	NY50xEMH4
EMD112	*MAT***a**/*MATα ARG4/arg4-NspI his3SK/his3SK ho::LYS2/ho::LYS2 leu2/leu2lys2/lys2 RME1/rme1::LEU2 trp1::hisG/trp1::hisG ura3/ura3 mpc54Δ::his5/ mpc54-RFP^{119}::TRP1*	Chapter 2 NY50xEMH5
EMD113	*MAT***a**/*MATα ARG4/arg4-NspI his3SK/his3SK ho::LYS2/ho::LYS2 leu2/leu2lys2/lys2 RME1/rme1::LEU2 trp1::hisG/trp1::hisG ura3/ura3 mpc54Δ::his5/ mpc54-RFP^{145}::TRP1*	NY50xEMH6

Strain	Genotype	Source Grandparents
EMD118	*MAT***a**/*MAT*α *ARG4/arg4-NspI his3SK/his3SK* *ho*::*LYS2/ho*::*LYS2 leu2/leu2 lys2/lys2* *RME1/rme1*::*LEU2 trp1*::*hisG/trp1*::*hisG ura3/ura3* P_{TEF}*-GFP-SPO20*$^{51-91}$*::TRP1 /* P_{TEF}*-GFP-SPO20*$^{51-91}$*::TRP1*	AN117-4B integrated AN117-16Dintegrated
EMD119	*MAT***a**/*MAT*α *ARG4/arg4-NspI his3SK/his3SK* *ho::LYS2/ho::LYS2 leu2/leu2lys2/lys2* *RME1/rme1::LEU2 trp1::hisG/trp1::hisG ura3/ura3* *mpc54*Δ*::his5/ mpc54*Δ*::his5* P_{TEF}*-GFP-SPO20*$^{51-91}$*::TRP1 /* P_{TEF}*-GFP-SPO20*$^{51-91}$*::TRP1*	NY51 integrated NY50 integrated
EMD120	*MAT***a**/*MAT*α *ARG4*/*arg4-NspI his3*Δ*SK*/*his3*Δ*SK* *ho*Δ*::LYS2*/*ho*Δ*::LYS2 leu2*/*leu2lys2*/*lys2* *RME1*/*rme1*Δ*::LEU2 trp1::hisG*/*trp1::hisG* *ura3*/*ura3 spo14*Δ*::ura3/spo14*Δ*::URA3* P_{TEF}*-GFP-SPO20*$^{51-91}$*::TRP1 /* P_{TEF}*-GFP-SPO20*$^{51-91}$*::TRP1*	HI61 integrated HI5 integrated
EMD121	*MAT***a**/*MAT*α *ARG4*/*arg4-NspI his3*Δ*SK*/*his3*Δ*SK* *ho*Δ*::LYS2*/*ho*Δ*::LYS2 leu2*/*leu2 lys2*/*lys2* *RME1*/*rme1*Δ*::LEU2 trp1::hisG*/*trp1::hisG ura3*/*ura3* *sso1*Δ*::his5+/sso1*Δ*::his5+* P_{TEF}*-GFP-SPO20*$^{51-91}$*::TRP1 /* P_{TEF}*-GFP-SPO20*$^{51-91}$*::TRP1*	HI1 integrated HI2 integrated
TC534	*MAT***a**/*MAT*α *ARG4/arg4-NspI his3SK/his3SK* *ho*::*LYS2/ho*::*LYS2 leu2/leu2 lys2/lys2* *RME1/rme1*::*LEU2 trp1*::*hisG/trp1*::*hisG ura3/ura3* *ssp1-GFP::his5+ / ssp1-GFP::his5+*	H. Tachi

Appendix II: Oligonucleotides

Primer	Sequence	Function
EMO 1	ATT Tcc AcT gcA ccA gcc AAg gcA cAg Agg ccA	Introduces mutation SxYxG:AxAxA in *SPO74*
EMO 2	Tgg ccT cTg Tgc cTT ggc Tgg Tgc AgT ggA AAT	Introduces mutation SxYxG:AxAxA in *SPO74*
EMO 3	cTA AAA Acc AAc gcg gcT AcA gcc ATT AAA AAA gAg	Introduces mutation LLxY:AAxA in *SPO74*
EMO 4	cTc TTT TTT AAT ggc TgT Agc cgc gTT ggT TTT Tag	Introduces mutation LLxY:AAxA in *SPO74*
EMO 5	AAc TcT TTg cTA gcT gcA gcg cTA gcA gTT cgT	Introduces mutation LNREL:LAAAL in *SPO74*
EMO 6	Acg AAc Tgc TAg cgc Tgc Agc TAg cAA AgA gTT	Introduces mutation LNREL:LAAAL in *SPO74*
EMO 7	Tcc ATT Agg gAT gcT AgA AAT gcA cTT TTg ccA	Introduces mutation FxxP:AxxA in *SPO74*
EMO 8	Tgg cAA AAg Tgc ATT TcT Agc ATc ccT AAT ggA	Introduces mutation FxxP:AxxA in *SPO74*
EMO 9	AAT Tgg gAA AgT TTT Tgg	*SPO74* nt 312-331; sense
EMO10	gAc TTg gAT gAA gAA TAT	*SPO74* nt 643-660; sense
EMO11	ATA AcT ggT ggA AcA ccc	*SPO74* nt 943-960; sense
EMO12	TTT AgT TTT gTA Acc TTc	*SPO74* nt 357-340; antisense
EMO13	TTg cAT ATg AAA gAA gTT	*SPO74* nt 714-697; antisense
EMO14	TAg TTc Tgc TTT TTc Tcc	*SPO74* nt 932-925; antisense
EMO15	gcggcgccgcggTAAggccAAA AgAAgAcgTcAAcA	Introduce SacII 200bp past STOP of *SPO74*
EMO16	ATT Tcc AcT gcA ccA TAc AAg ggA cAg	Single mutation Sxxxx:Axxxx *SPO74* bp 424-454; sense
EMO17	cTg Tcc cTT gTA Tgg Tgc AgT ggA AAT	Single mutation Sxxxx:Axxxx *SPO74* bp 424-454; antisense

Primer	Sequence	Function
EMO18	Tcc AcT TcA ccA gcc AAg ggA cAg Agg	Single mutation xxYxx:xxAxx *SPO74* bp 424-454; sense
EMO19	cTg Tcc cTT ggc Tgg TgA AgT ggA	Single mutation xxYxx:xxAxx *SPO74* bp 424-454; antisense
EMO20	AcT TcA ccA TAc AAg gcA cAg Agg ccA	Single mutation xxxxG:xxxxA *SPO74* bp 424-454; sense
EMO21	Tgg ccT cTg Tgc cTT gTA Tgg TgA AgT	Single mutation xxxxG:xxxxA *SPO74* bp 424-454; antisense
EMO22	cTA AAA Acc AAc gcg cTT AcA TAc ATT	Single mutation Lxxx:Axxx *SPO74* bp 526-556; sense
EMO23	AAT gTA TgT AAg cgc gTT ggT TTT Tag	Single mutation Lxxx:Axxx *SPO74* bp 526-556; antisense
EMO24	AAA Acc AAc TTg gcT AcA TAc ATT AAA	Single mutation xLxx:xAxx *SPO74* bp 526-556; sense
EMO25	TTT AAT gTA TgT Agc cAA gTT ggT TTT	Single mutation xLxx:xAxx *SPO74* bp 526-556; antisense
EMO26	AAc TTg cTT AcA gcc ATT AAA AAA gAg	Single mutation xxxY:xxxA *SPO74* bp 526-556; sense
EMO27	cTT TTT TTT AAT ggc TgT AAg cAA gTT	Single mutation xxxY:xxxA *SPO74* bp 526-556; antisense
EMO28	AAc TcT TTg gcA gcT gcA gcg gcA gcA gTT cgT	Mutation LNREL:AAAA *SPO74* bp 721-751; sense
EMO29	Acg AAc Tgc Tgc cgc Tgc Agc Tgc cAA AgA gTT	Mutation LNREL:AAAA *SPO74* bp 721-751; antisense
EMO30	AAg ccA AAT gTA gcT gcA gcA gAT gAT gAT gTT	Introduces mutation RFG:AAA in *MPC54*
EMO31	AAc ATc ATc ATc Tgc Tgc Agc TAc ATT Tgg cTT	Introduces mutation RFG:AAA in *MPC54*
EMO32	gAT gAT gAT gTT gcT gcA gcA gAT cAA AgA AAA	Introduces mutation NIF:AAA in *MPC54*

Primer	Sequence	Function
EMO33	TTT TcT TTg ATc Tgc Tgc Agc AAc ATc ATc ATc	Introduces mutation NIF:AAA in *MPC54*
EMO34	gAc gcg gTT AAc gcT gcA gcA gcg cTT TgT AAc	Introduces mutation RCY:AAA in *MPC54*
EMO35	gTT AcA AAg cgc Tgc Tgc Agc gTT AAc cgc gTc	Introduces mutation RCY:AAA in *MPC54*
EMO36	Tgc TAT gcg cTT gcT gcA gcg gcA AcT AAg cAT gTA	Introduces mutation CNIP:AAAA in *MPC54*
EMO37	TAc ATg cTT AgT Tgc cgc Tgc Agc AAg cgc ATA gcA	Introduces mutation CNIP:AAAA in *MPC54*
EMO38	gcg gTT AAc cgT gcT gcA gcg cTT gcT gcT ATT ccA AcT AAg	Introduces mutation CYxxCN:AAxxAA in *MPC54*
EMO39	cTT AgT Tgg AAT Agc Agc AAg cgc Tgc Agc Acg gTT AAc cgc	Introduces mutation CYxxCN:AAxxAA in *MPC54*
EMO40	Acg TTc gAA Acg gcc gcT gTA gcg gcA Acc cAT gAA Acg	Introduces mutation LxxGI:AxxAA in *MPC54*
EMO41	cgT TTc ATg ggT Tgc cgc TAc Agc ggc cgT TTc gAA cgT	Introduces mutation LxxGI:AxxAA in MPC54
EMO42	Tcg AAA AAT gAA AcT cTg	*MPC54* nt 310-328; sense
EMO43	cTT cAA ATg gcA ATc gAT	*MPC54* nt 553-570; sense
EMO44	TTT gTT Tcc ATc gTc Agc	*MPC54* nt 610-628; antisense
EMO45	Agg cgT TTA TgT cAc gAg	*MPC54* nt 781-799; sense
EMO46	gAg TTT TTg cAc cTc ATA	*MPC54* nt 847-865; antisense
EMO47	AAA TTg AgT cTg AAg cgA	*MPC54* nt 1081-1109; antisense
EMO48	gTT cTT ccg cgg TgA TcA ATg AAA gTA AAT AAA	Introduces SacII before *SPO74* START
EMO49	gTT cTT cTc gAg TgA TcA ATg AAA gTA AAT AAA	Introduces XhoI before *SPO74* START

Primer	Sequence	Function
EMO50	gTT cTT ggT Acc TAA ggc cAA AAg AAg Acg TcA	Introduce KpnI 240bp downstream of STOP in *SPO74*. Want to see if having 3'UTR in plasmid increases the stability of Spo74
EMO51	gTT cTT gTg cTc TAA ggc cAA AAg AAg Acg TcA	Introduce SacI 240bp downstream of STOP in *SPO74*. Want to see if having 3'UTR in plasmid increases the stability of Spo74
EMO52	GAC AAG AGG AAA GAG CAA ACT	*CNM67* nt 575-595; sense
EMO53	gcg gcg ggA Tcc Atg ccA gAA gAT AcA Agc	Introduce BamHI at *MPC54* START sense
EMO54	gcg gcg Tcc ggA gg TcA ATT TgT Aac gTg TTc	Introduce StuI after *MPC54* STOP antisense
EMO55	gcg gcg Tcc ggA gg TcA cAA ATT TTg cTT TgT	Introduce StuI & STOP 200aa into *MPC54;* antisense
EMO56	gcg gcg ggA Tcc Atg gAT AAT ATT TTA AAg gc	Introduce BamHI at *SPO21* START sense
EMO57	gcg gcg cTc gAg g TcA cTT gAT ggA gTg cgg	Introduce XhoI after *SPO21* STOP antisense
EMO58	gcg gcg cTc gAg g TcA Acc ATT Tgg Atc gAA	Introduce XhoI & STOP 240aa into *SPO21;* antisense
EMO59	gcg gcg ggA Tcc Atg ggA gcT ggc AcT cTT	Introduce BamHI at *SPO74* START sense
EMO60	gcg gcg Tcc ggA gg TcA ATT Acg TgA ccA gcT	Introduce StuI after *SPO74* STOP antisense
EMO61	AAG CGC GCA ATT AAC CTT	pRS426; sense
EMO62	GCG GCG GCG GCC GCT TAA CTA GTC TAA GTG GCG	Introduce STOP and NotI in *SPO20* at nt 258-273; antisense
EMO63	gcg gcg AAG CTT Atg ccA gAA gAT AcA Agc	Introduce HindIII at *MPC54* START sense

Primer	Sequence	Function
EMO64	gcg gcg CTC GAG TcA cAA ATT TTg cTT TgT	Introduces XhoI 200aa into *MPC54* antisense
EMO65	gcg gcg AAG CTT Atg gAT AAT ATT TTA AAg gc	Introduces HindIII at *SPO21* START sense
EMO66	GGC CGG AAT TCG GGT TCG AAT CCC TTA GC	Introduces EcoRI 500bp upstream of *ADY4* START; sense
EMO66II	gcg gcg gaa ttc ATG cca gaa gat aca agc	Introduce EcoRI at *MPC54* START in frame with pGEX-5x-1; sense
EMO67	gcg gcg gaa ttc ATG gat aat att tta aag gc	Introduce EcoRI at *SPO21* START in frame with pGEX-5x-1; sense
EMO68	gcg gcg gga tcc cc ATG gat aat att tta aag gc	Introduce BamHI at *SPO21* START in frame with pGEX-5x-1; sense
EMO71	tta acg cgt ttt gac aac ggc tgg gac aac aac gac aac aac aac gac tag aat tcg agc tcg ttt aaa c	R1 for *SSO1*
EMO72	atg agt tat aat aat ccg tac cag ttg gaa acc cct ttt gaa gag tca tac gga tcc ccg ggt taa tta a	F1 for *SSO1*
EMO73	gga tca tat gca tag tac cga	pHR81 reverse primer for sequencing
EMO74	GTA AAA CGA CGG CCA G	pHR81 M13 forward primer for sequencing
EMO 75	gcg gcg ggA Tcc cc Atg ccA gAA	Introduces BamHI before START of *MPC54;* sense
EMO76	GGC CGg agc tcG GGT TCG AAT CCC TTA GC	Introduces SacI 500bp upstream of *ADY4* START; sense
EMO77	gcg gcg tct aga *TTA ATT GGA GGG ATC AGT AAA*	Introduces XbaI 15bp downstream of *ADY4* STOP; antisense
EMO78	gcg gcg gcggccgc *TTA ATT GGA GGG ATC AGT AAA*	Introduces NotI 15bp downstream of *ADY4* STOP; antisense

Primer	Sequence	Function
EMO79	GTG GTA TTA CCC AAA CAG	100nt downstream of *SPO21* STOP antisense
EMO80	GTT TGT TTT AAA AAA CG	150bp upstream of *GST* STOP; sense
EMO81	gcggcg ggatcc TCACTTGATG GAGTGCGG	Introduces BamHI after *SPO21* STOP; antisense
EMO82	AAAAGAACTTAAACAACA ACAAACAAAAAATTAAGT TACA cgg atc ccc ggg tta att aa	F1 to delete *YLR301W*
EMO83	TAGCAGCAGAAGAAAGTA GAAAACGATTTATTCTCCT TTA gaa ttc gag ctc gtt taa ac	R1 to delete *YLR301W*
EMO84	ATG CCA GCA TTA TTA AAA	START of *YLR301W*; sense
EMO85	TTA AGC GTG ATA TTC AAT	STOP of *YLR301W*; antisense
EMO86	gcg ggg TTA ATT AAg ATg ccA gAA gAT Ac	Introduces PacI at MPC54 START in frame with Pringle C-term marker; sense
EMO87	ctc act ata ggg cga att ggg	Sikorsky vector just upstream of SacI site and polylinker; Reads into polylinker (1974 bp into pRS306 Strider Sequence); sense
EMO88	gcg gcg cgg ATc ccc ATG GAT AAT ATT TTA	Introduce BamHI at SPO21 START in frame with Pringle C-term marker; sense
EMO89	cgc cgc cgg ATc ccc TTG ATG GAG TGC GG	Introduces BamHI and removes STOP of *SPO21* all in frame with Pringle C-terminal marker addition
EMO90	gcc gcc gaa ttc AGCTGAA TTTTCTA	Introduce EcoRI 500bp upstream of *YLR301W* START; sense
EMO91	cgg cgg atc gat TGTAACTTA ATTTTT	Introduces ClaI just before *YLR301W* START; -1 to -19; antisense
EMO92	ggc ggc ccg cgg TAAAGGA GAATAAATCG	Introduces SacII just past *YLR301W* STOP; sense

Primer	Sequence	Function
EMO93	cgg cgg tct aga TCT ATT ATA GCA TTA AAT	Introduces XbaI 500bp past *YLR301W* STOP; antisense
EMO94	ggc ggc ccg cgg GCA CCT ATG GGA TCT ATA	Introduces SacII just past *YLR301W* STOP; sense
EMO95	cgg cgg tct aga CGA ACC CTT GCA TCC GAA	Introduces XbaI 561bp past *YLR301W* STOP
EMO96	cggcgg gga tcc cc ATGCCAGA AGATACAAGC	Introduces BamHI at *MPC54* START in frame for pFA6; sense
EMO97	cggcggttaattaaATTTGTAAC GTGTTC	Introduce PacI at *MPC54* STOP; removes STOP; in frame for pFA6; antisense
EMO98	GACGTTATGTGGAGGCAC	700bp upstream of *YLR301W;* sense
EMO99	ccc ggg gcg gcc gcg gAT TGG AGG GAT CAG TAA AGG	Introduce NotI at *ADY4* STOP; STOP removed; antisense
EMO100	ccc tca cta aag gga aca	Sikorsky vector just downstream of KpnI site and polylinker Reads into polylinker (2108 bp into pRS306 Strider Sequence); antisense
EMO101	ggcggcctcgagGATCCCAT AGGTGCT	Introduces XhoI just downstream of *YLR301W* STOP; antisense

Appendix III: Plasmids

Plasmid	Relevant features	Source
316-SPO74	*CEN SPO74*	Chapter 2
316- SPO74-145	*CEN SPO74-145*	Chapter 2
316- SPO74-180	*CEN SPO74-180*	Chapter 2
316- SPO74-180	*CEN SPO74-180*	Chapter 2
316-SPO74-243	*CEN SPO74-243*	Chapter 2
316- SPO74-267	*CEN SPO74-267*	Chapter 2
426- SPO74	2µ *SPO74*	Chapter 2
426- SPO74-145	2µ *SPO74-145*	Chapter 2
426- SPO74-180	2µ *SPO74-180*	Chapter 2
426- SPO74-243	2µ *SPO74-243*	Chapter 2
304- SPO74	integrating *SPO74*	Chapter 2
304- SPO74-145	integrating *SPO74-145*	Chapter 2
304- SPO74-180	integrating *SPO74-180*	Chapter 2
304- SPO74-243	integrating *SPO74-243*	Chapter 2
314-MPC54-RFP	*CEN MPC54-RFP*	H. Nakanishi
316-MPC54-RFP	*CEN MPC54-RFP*	Chapter 2
316- MPC54-RFP	*CEN MPC54-RFP*	Chapter 2
316- MPC54-40-RFP	*CEN MPC54-40-RFP*	Chapter 2
316- MPC54-47-RFP	*CEN MPC54-47-RFP*	Chapter 2
316- MPC54-118-RFP	*CEN MPC54-118-RFP*	Chapter 2
316- MPC54-123-RFP	*CEN MPC54-123-RFP*	Chapter 2
316- MPC54-119-RFP	*CEN MPC54-119-RFP*	Chapter 2
316- MPC54-145-RFP	*CEN MPC54-145-RFP*	Chapter 2
426- MPC54-RFP	2µ *MPC54-RFP*	Chapter 2
426- MPC54-40-RFP	2µ *MPC54-40-RFP*	Chapter 2
426- MPC54-47-RFP	2µ *MPC54-47-RFP*	Chapter 2
426- MPC54-118-RFP	2µ *MPC54-118-RFP*	Chapter 2
426- MPC54-119-RFP	2µ *MPC54-119-RFP*	Chapter 2

Plasmid	Relevant features	Source
426- MPC54-145-RFP	2µ *MPC54-145-RFP*	Chapter 2
304- MPC54-RFP	integrating *MPC54-RFP*	Chapter 2
304- MPC54-40-RFP	integrating *MPC54-40-RFP*	Chapter 2
304- MPC54-47-RFP	integrating *MPC54-47-RFP*	Chapter 2
304- MPC54-118-RFP	integrating *MPC54-118-RFP*	Chapter 2
304- MPC54-119-RFP	integrating *MPC54-119-RFP*	Chapter 2
304- MPC54-145-RFP	integrating *MPC54-145-RFP*	Chapter 2
pSTT91- MPC54(1-200)	*LexA- MPC54(1-200)*	Chapter 2
pSTT91- MPC54-40(1-200)	*LexA- MPC54-40(1-200)*	Chapter 2
pSTT91- MPC54-47(1-200)	*LexA- MPC54-47(1-200)*	Chapter 2
pSTT91- MPC54-118(1-200)	*LexA- MPC54-118(1-200)*	Chapter 2
pSTT91- MPC54-119(1-200)	*LexA- MPC54-119(1-200)*	Chapter 2
pSTT91- MPC54-145(1-200)	*LexA- MPC54-145(1-200)*	Chapter 2
pRS426-ADY4-DTR1-RFP	2µ *ADY4 DTR1-RFP*	Chapter 3
pRS314-SSP1-GFP	*CEN SSP1-GFP*	H. Tachi
pRS306-MPC54-GFP	integrating *MPC54-GFP*	
pRS426-ADY4	2µ *ADY4*	
pGEX-5x-1 MPC54(1-200aa)	*GST-MPC54(1-200aa)*	
pGEX-5x-1 MPC54	*GST-MPC54*	
pGEX-5x-1 SPO74	*GST-SPO74*	
pRS426-MPC54(1-200aa)	2µ *MPC54(1-200aa)*	
pRS426-SPO21(1-200aa)	2µ *SPO21(1-200aa)*	
pRS424-CNM67-TEV-HA	2µ *CNM67-TEV-HA*	
pRS424-CNM67-TEV	2µ *CNM67-TEV*	
pRS314-ADY4-GFP	2µ *ADY4-GFP*	
pRS303-MPC54	integrating *MPC54*	
pRS304-GFP-SPO20$^{51-91}$	integrating *GFP-SPO20-51-91*	

Appendix IV: High-Copy Suppression of the *mpc54* mutants

A. High copy suppressor screen: Overexpressing proteins does not rescue the sporulation defect of the *mpc54* mutant alleles. The high-copy suppression screen failed: sporulation was not rescued to significant levels. Final candidates were: HSL1, **YKL00-C**, YPL062W, **TUL1**, **ALD6**, **PPS1**, **YBR277C**, DPB3, RGS2, VAM3 (in bold are genes that have been shown to affect sporulation in other screens).

Concept: Does the overexpression of proteins rescue the sporulation defect of the Mpc54 mutant alleles? A means of identifying proteins important to the vesicle docking function of MOP components is to examine whether the defect in prospore membrane formation observed in Spo74p and Mpc54p site directed mutant alleles can be rescued by the overexpression of an unknown protein. I performed a suppression assay by overexpresssing a library of yeast proteins in *mpc54*Δ cells transformed with the *mpc54* mutant alleles. Transformants were replica plated to sporulation medium and then screened by exposure to ether vapor, which is lethal to vegetative cells but not to spores. Viable candidates were assayed for sporulation efficiency by light microscopy. If spores were formed then the protein that was overexpressed was able to rescue prospore membrane formation. The localization and expression pattern of the candidate protein would then be examined *in silico* to determine the feasibility of it having a role in prospore membrane formation.

High Copy Suppression Screen: Two yeast libraries (PuvI and pHR81) were introduced into strains which were integrated with single *mpc54* mutant alleles (used alleles 47 and 118). If the overexpression of a particular gene rescues the *mpc54* mutant phenotype, then sporulation would be rescued. The recovery of sporulation was assayed by ether testing.

B. Directed high copy suppression: No known pre-PsM vesicular membrane component was able to rescue sporulation in the mpc54 mutant alleles. There was no rescue of sporulation for any candidates tested (induced on two-micron plasmid: Sec1, Sec3, Sec9, Snc1, Sso2, Ady3, Exo70, Sso1, Ypt1).

Concept: Presumably, the target of the MOP's vesicle docking complex would either be protein(s) associated with post-Golgi vesicles or the lipids that comprise the vesicles. Previous studies have identified several genes important to the early stages of prospore membrane formation at the Meiosis II SPB. These genes include MOP components, members of the secretory pathway, and a phospholipase D enzyme. However, the interactions necessary for vesicle docking remain unknown. A directed high-copy suppression assay using the proteins known to be involved in prospore membrane formation might identify proteins involved in vesicle docking. Determining the protein-protein interactions or protein-lipid interactions necessary for prospore membrane formation is important to the understanding of the initiation of prospore membrane formation. Of particular interest to my project are the interactions and regulations of the MOP components.

Directed examinations**:** Add 2u plasmid containing a known pre-PsM vesicle membrane component. Does it rescue sporulation in the Mpc54 mutants? NO RESCUE: Sec1, Sec3, Sec9, Snc1, Sso2, Ady3, Exo70, Sso1, Ypt1. Interesting: Sec4 did not rescue Mutant 32 or 34, but 2 triads were seen in Mutant 40 (which normally only forms monads and dyads) and while this is hardly a robust rescue, it is still worth noting.

Appendix V: TEM images

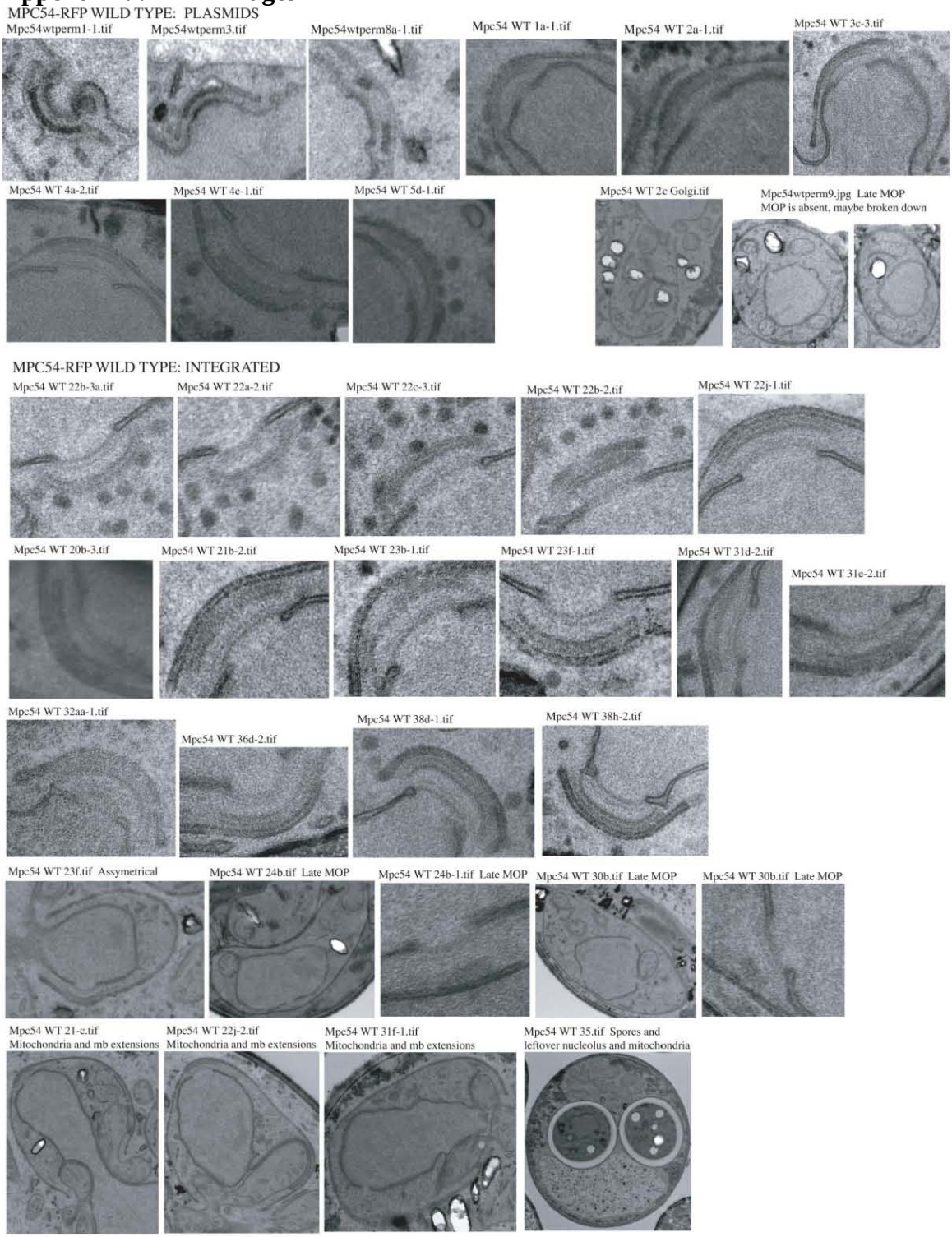

***MPC54-RFP* Wild Type. Images represent one section from each MOP. Image titles are file names, files found in "TEM compilation" folder.**

PLASMID

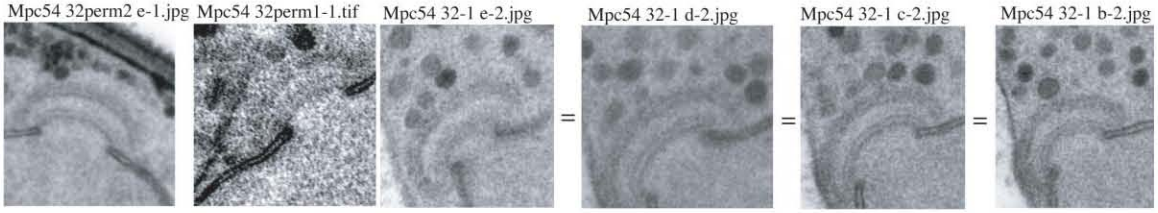

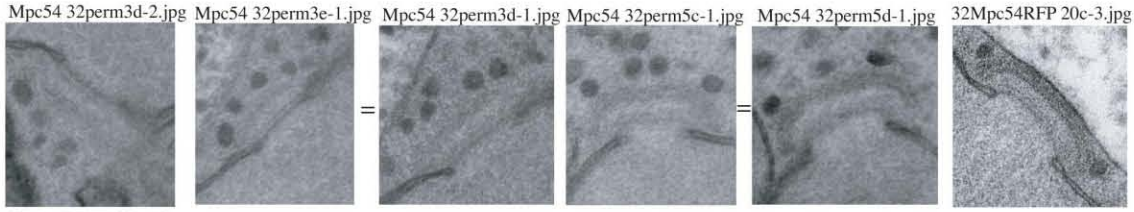

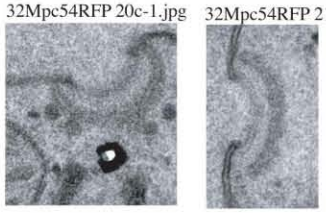

INTEGRATED

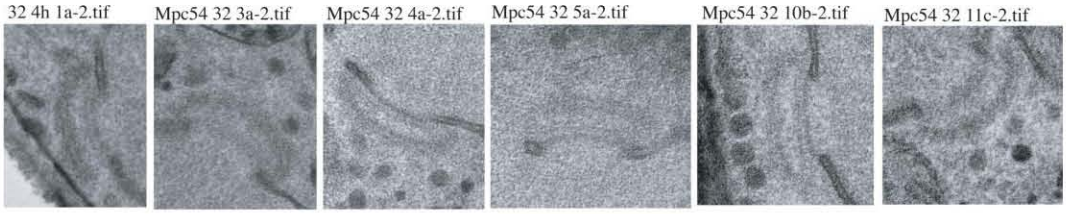

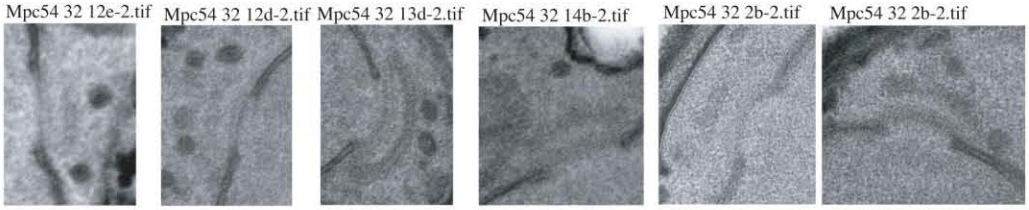

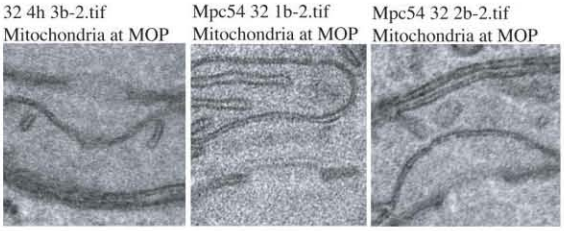

mpc54-47-RFP. **Images represent one section from each MOP. Image titles are file names, files found in "TEM compilation" folder.**

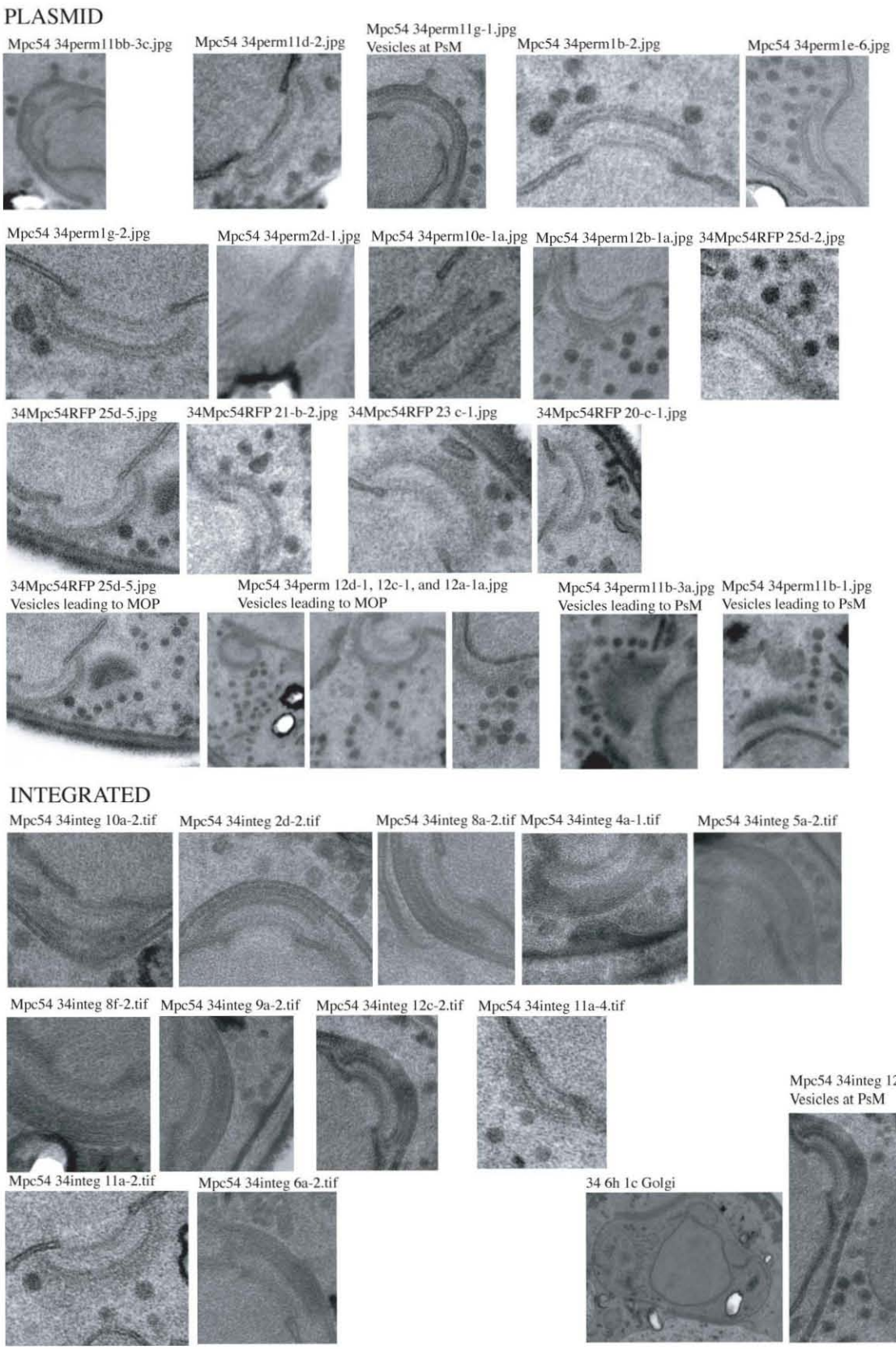

***mpc54-118-RFP*. Images represent one section from each MOP.**

PLASMID

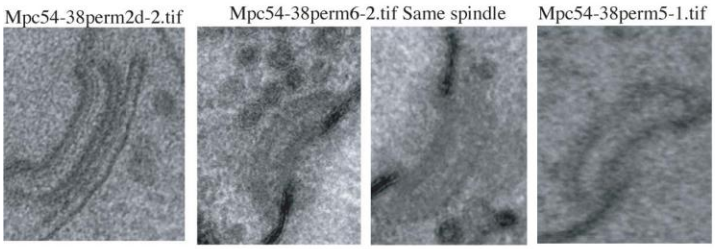

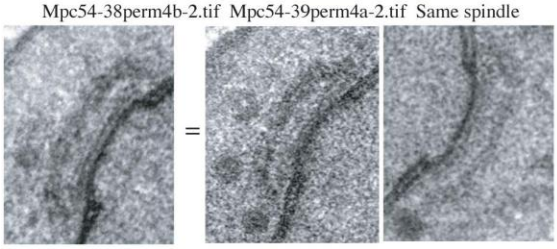

INTEGRATED: Heterozygous Mpc54.38+/-

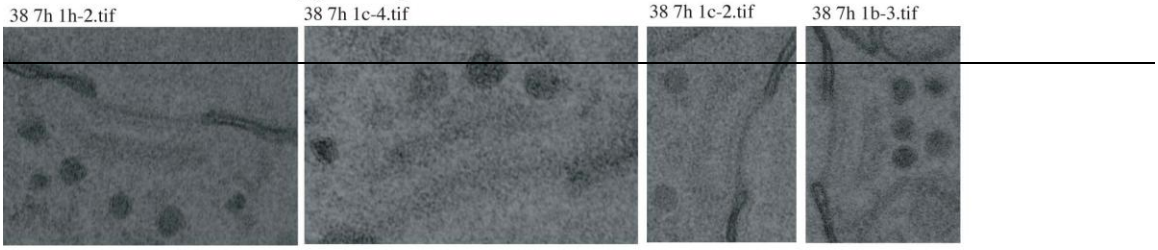

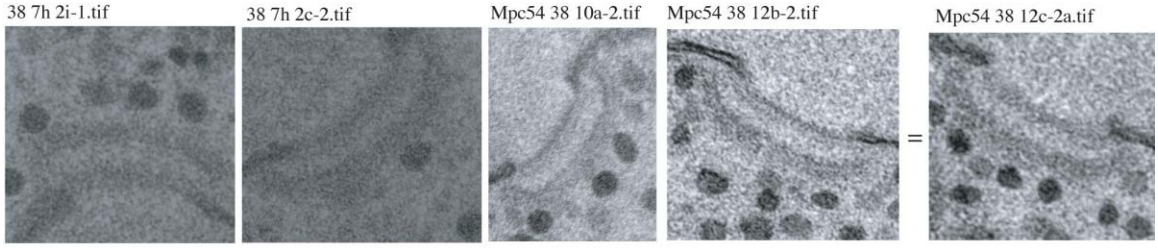

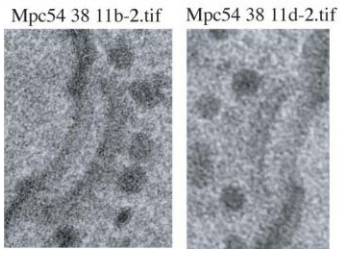

***mpc54-119-RFP*. Images represent one section from each MOP. Image titles are file names, files found in "TEM compilation" folder.**

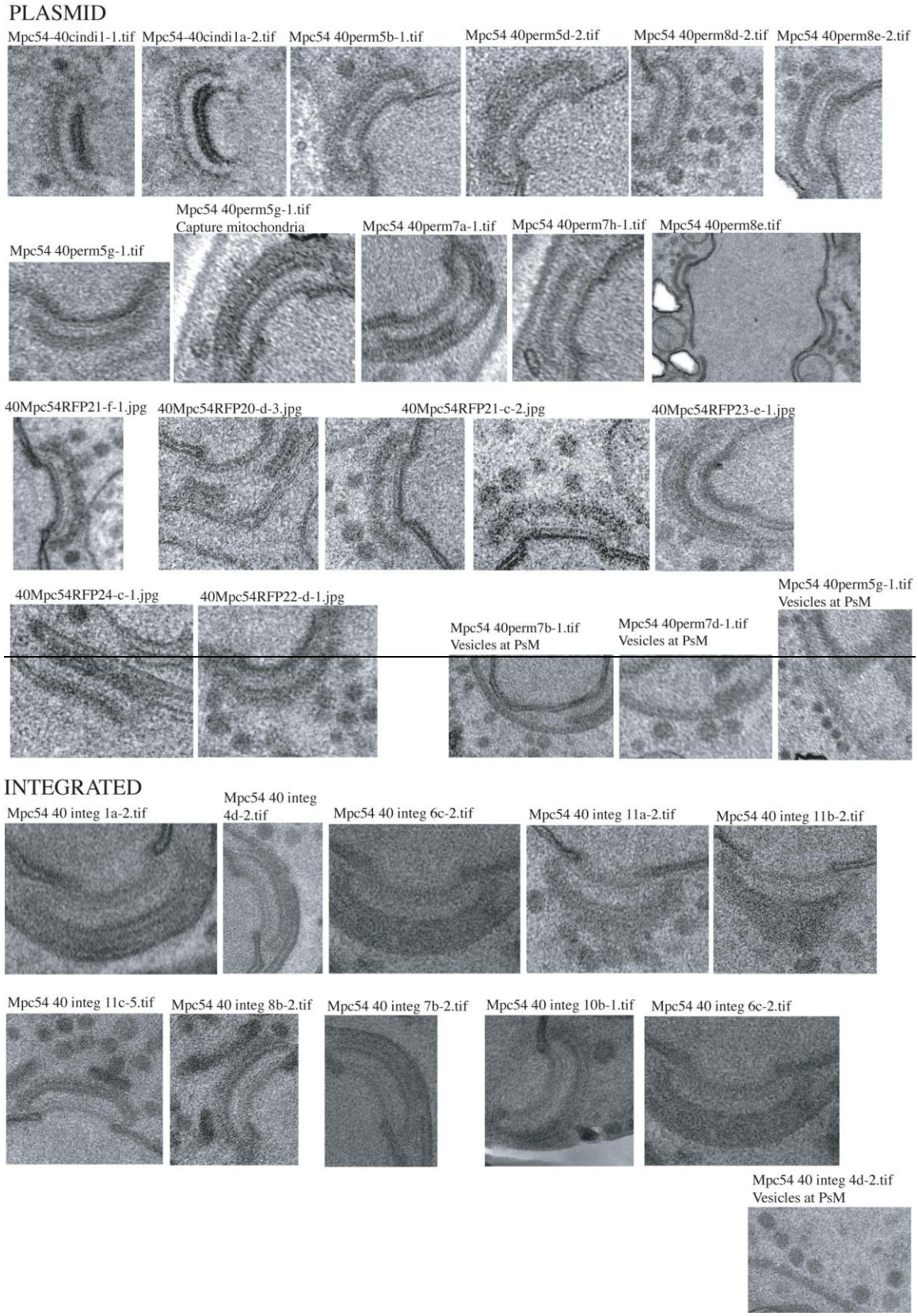

***mpc54-145-RFP*. Images represent one section from each MOP.**

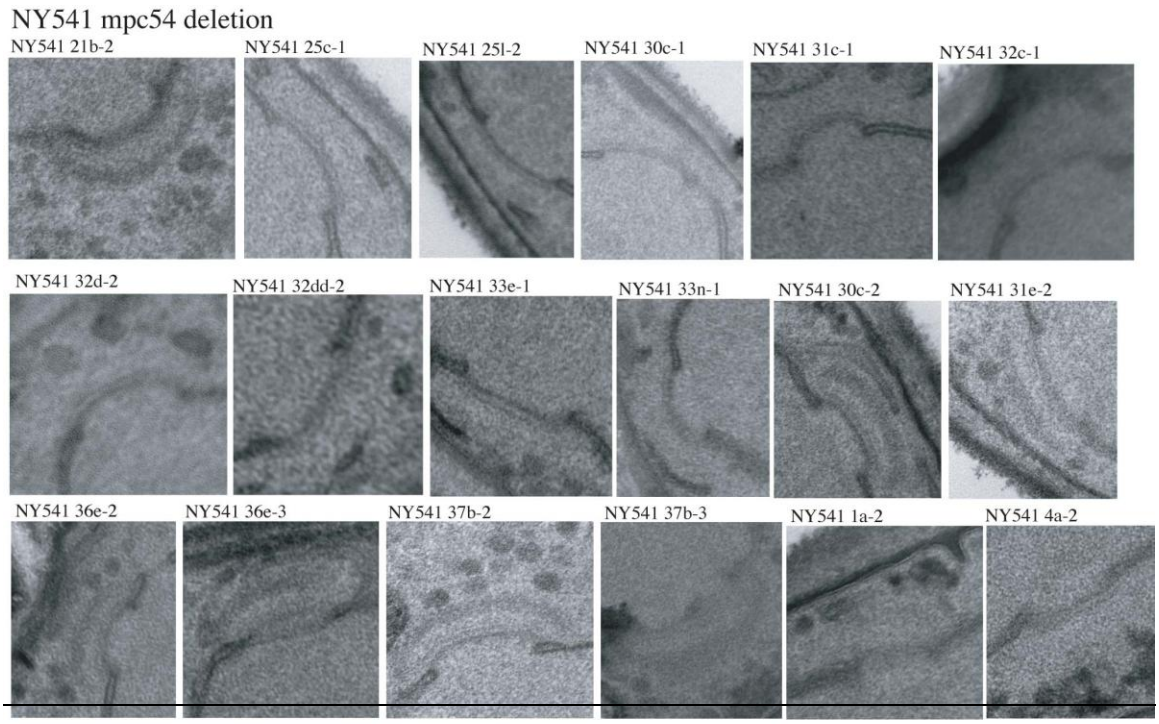

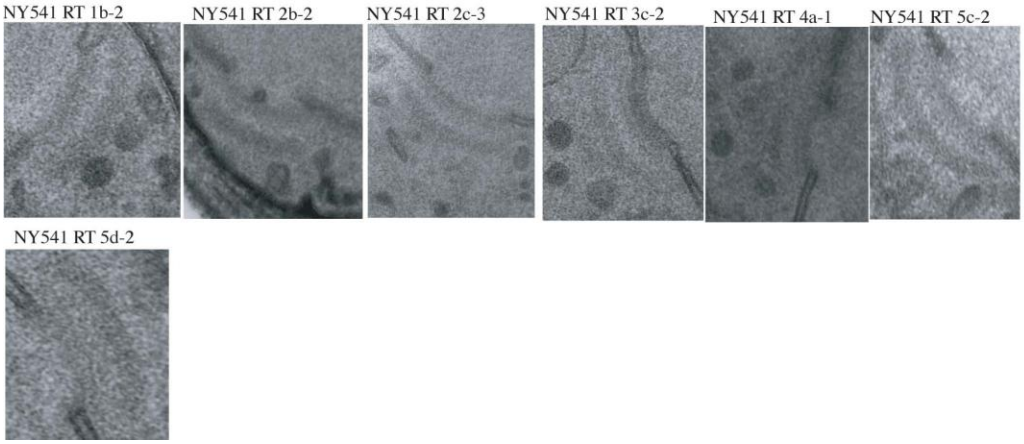

***mpc54*Δ. Images represent one section from each MOP. Image titles are file names, files found in "TEM compilation" folder.**

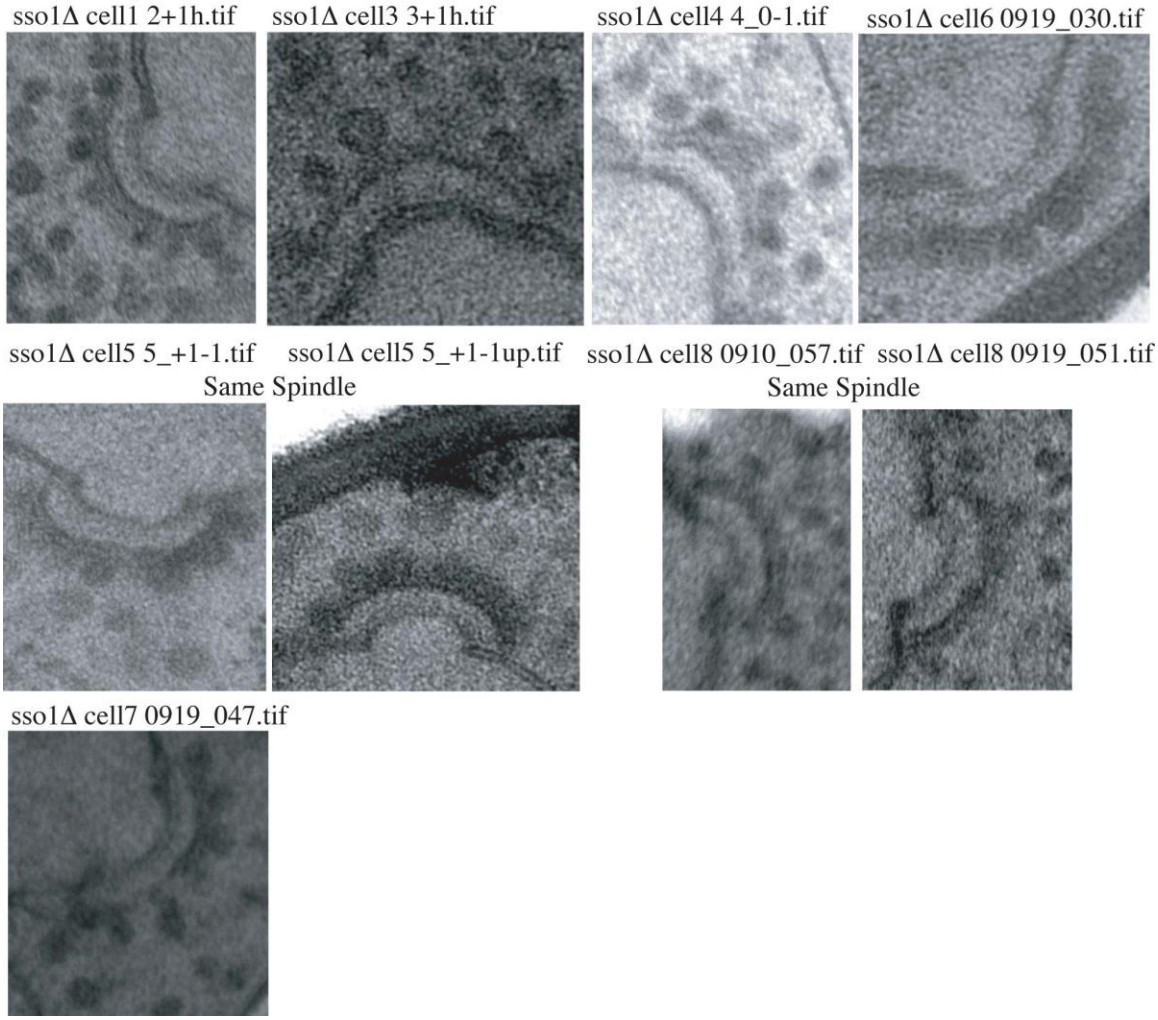

***sso1*Δ. Images represent one section from each MOP. Image titles are file names, files found in "TEM compilation" folder.**